UNIVERSITEIT VAN PRETORIA
UNIVERSITY OF PRETORIA
YUNIBESITHI YA PRETORIA

Denkleiers • Leading Minds • Dikgopolo tša Dihlalefi

Design, construction and commissioning of a counter-flow rotary pyrolyser

William Peter Baasch

CVD 800

2024-09-25

Design, construction and commissioning of a counter-flow rotary pyrolyser

William Peter Baasch
u16041268

A dissertation submitted in the partial fulfilment of the requirements of the degree

Masters of Engineering (Chemical Engineering)

Supervisor: Dr Ryan David Merckel

Department of Chemical Engineering
Faculty of Engineering, the Built
Environment and Information Technology

University of Pretoria

CVD 800

2024-09-25

Design, construction and commissioning of a counter-flow rotary pyrolyser

Abstract

Biochar is a sustainable carbon sequestrate and a strong contender for renewable carbon-based materials. Biomass is a key commodity which should be exploited in the pursuit of the energy transition due to the wide variety of fossil fuel-like derivatives it can produce. The conversion of biomass to value-added products usually focuses on pyrolysis vapour and noncondensable gases because of their properties and possible use cases. In general, biochar is typically consumed in the process, via combustion, to improve the energy efficiency of these processes. Biochar has a variety of uses that are often disregarded/sacrificed in favour of the aforementioned pyrolysis products, and therefore further analysis and research into biochar would not only benefit the biochar value chain but also aid in understanding the technical and economic uses of the solid pyrolysis product.

Extensive research has been done on biochar and its potential usage, but further practical research into biochar reactor design, construction, and commissioning allows the exploration of biochar generation and the quality of the final product. This will also allow the evaluation of the commissioned experimental apparatus and what further may be modified to produce increased product generation rates and higher product quality. Ignoring biochar as a value-adding product could result in research that develops a suboptimal solution to the energy transition. While biochar may not pose immediate benefits to the pyrolysis process besides additional energy-generating capacity via combustion the resulting product has potential in various areas of great value and therefore additional research into the manufacturing of this value-adding product would be of great benefit.

For the investigation of biochar as a value-adding product, the requirement to produce a potentially large amount of repeatable samples was identified and therefore the requirement for a biochar-focused pyrolysis reactor was identified. The Rotary Kiln Pyrolyser (RKP) In-*situ* Activation (ISA) was designed, constructed, commissioned and operated.

Throughout the exploration of this research topic the design, construction, commissioning and operation of a biochar-focused reactor was a major objective. This objective was much more difficult to achieve due to the complexities of the processing material and the products produced. Therefore, three prototype versions of the reactor (RKP-ISA) were constructed. The first rendition was prototype 1 where areas of improvement were identified and the lessons learnt from the execution of the first prototype were implemented

on the second prototype. Thereafter the second prototype was analysed and further modifications were made to improve the operation and quality of the products produced.

An investigation of the reactor performance was completed via the analysis of the produced biochar samples. Experimental runs were completed utilising the prototype 2 reactor and the quality of the resulting biochar was determined through thermogravimetric and elemental analyses. The biochar analysis indicated that further improvement to the prototype 2 reactor could be implemented to produce improved samples. The modifications made to the reactor resulted in improved biochar stability and quality. The body of work completed demonstrates the advancement of the reactor design and operation, but further investigation can still be completed regarding the modification of biochar for specific use cases and the scaling up of the established process for industrial application.

Keywords: Bioprocessing; Pyrolysis; Biochar Stability; In-*situ* Activation; *Macadamia tetraphylla*; Thermogravimetric Analysis; Elemental Analysis

Acknowledgements

I would like to acknowledge the invaluable support and encouragement I've received throughout my journey toward completing my master's degree in chemical engineering brings me a profound sense of gratitude. Many people have been instrumental in this achievement, and I would like to express my sincere appreciation to each of them.

First and foremost, I would like to thank my beloved partner, whose support and understanding have been invaluable. I certainly tried my very best to quit but thanks to you and your belief in my abilities I have managed to push through and to strive for excellence. Thank you for standing by my side and for being a constant source of motivation.

Thank you to my family for their unwavering love and support. Thank you for always believing in me and encouraging me to do my very best. Your sacrifices and dedication have provided me with the foundation and motivation to succeed.

To my friends, I am deeply grateful for your encouragement and friendship throughout this challenging time. You have offered me a listening ear, wise advice, and many moments of laughter, helping me to navigate the ups and downs of this journey. Your presence has been a source of strength and inspiration.

Finally, I would like to extend my thanks to my supervisors and employer for their guidance and support. Your expertise and insight have been instrumental in shaping my academic and professional journey.

"Success is not final, failure is not fatal: It is the courage to continue that counts." - Winston Churchill

Contents

List of Figures

List of Tables

Nomenclature

α	Thermal Diffusivity	$m^2.s^{-1}$
ρ	Density	$kg.m^{-3}$
C_p	Thermal Conductivity	$W.m^{-1}.K^{-1}$
L	Half length of heating element	m
L_t	Half the total length of apparatus	m
m_{O_2}	Mass of oxygen required for complete combustion	kg
$\Delta_c h_{HHV}$	Higher heating value	$MJ\,kg^{-1}$
t	Time	s
$T_{element}$	Heating element temperature	°C
A	Area of heat transfer	m^2
h	Convective heat transfer coefficient	$W.m^{-2}.K^{-1}$
k	conductive heat transfer coefficient	$W.m^{-1}\ K^{-1}$
L	Length	m
Q_{cond}	Heat due to conduction	W
Q_{conv}	Heat due to convection	W

Chapter 1

Introduction

1.1 Overview

Prehistoric civilisations have successfully used biochar to modify tropical forest soils for at least 45 millennia. The artificially altered soils exhibit improved soil quality and fertility to this day (Roberts *et al*, 2017). The technology of pyrolysis has been around throughout the development of civilisations and has played an integral part in chemical and petrochemical refinery processes. Pyrolysis is the process through which biomass is converted into gases, pyrolysis vapours and solid biochar (Palamanit *et al*, 2019).

Biochar has the potential to be used in a multitude of industries to great effect. These areas include environmental remediation, energy storage materials, composite material production, porous catalytic media and electrochemical measurement devices (Bartoli *et al*, 2020). This project will focus primarily on the biochar product due to its potential as a beneficial soil adjunct.

Biochar is a sustainable carbon sequestrate and a strong contender for renewable carbon-based materials. Therefore, biomass has the potential to replace current technology in many of the areas listed above, provided that it demonstrates feasibility. Biochar produced from one type of biomass feedstock and process conditions can exhibit vastly different properties and it is therefore important to develop and demonstrate its reliability for the intended application (Dhyani & Bhaskar, 2018).

For the investigation of biochar as a value-adding product, the requirement to produce a potentially large amount of repeatable samples is identified and therefore the requirement for a biochar-focused pyrolysis reactor is identified.

1.2 Background

The University of Pretoria has been conducting bioprocessing research for the last couple of years. In that time, they have focused specifically on the study of pyrolysis vapour as a potential renewable fuel. The Generation and upgradation of the Pyrolysis Vapour using either method during generation or post-processing have been studied. In this pursuit, a bench-scale conical reactor and a pilot-scale fluidized bed reactor have been constructed. These reactor technologies are localised around fast pyrolysis which generates the highest yield fraction of pyrolysis vapour and non-condensable gases. Therefore, the solid products of pyrolysis were considered as a byproduct and utilised as a supplement to the heating requirements of the processes. The generation of the solid pyrolysis product and its ability to be a value-added product has been overlooked.

This created an opportunity to explore the generation, characterisation, and utilisation of biochar as a solid product from the pyrolysis process. This opportunity is pursued in this master's dissertation through the design, construction and commissioning of a counter-flow rotary kiln pyrolyser.

1.3 Problem Statement and Research Motivation

Biomass is a key commodity which should be exploited in the pursuit of the energy transition due to the wide variety of fossil fuel-like derivatives it can produce. The conversion of biomass to value-added products usually focuses on pyrolysis vapour and noncondensable gases because of their properties and possible use cases. In general, biochar is typically consumed in the process, via combustion, to improve the energy efficiency of these processes. Biochar has a variety of uses that are often disregarded/sacrificed in favour of the aforementioned pyrolysis products, and therefore further analysis and research into biochar would not only benefit the biochar value chain but also aid in understanding the technical and economic uses of the solid pyrolysis product.

Extensive research has been done on biochar and its potential usage, but further practical research into biochar reactor design, construction, and commissioning allows the exploration of biochar generation and the quality of the final product. This will also allow the evaluation of the commissioned experimental apparatus and what further may be modified to produce increased product generation rates and higher product quality. Ignoring biochar as a value-adding product could result in research that develops a suboptimal solution to the energy transition. While biochar may not pose immediate benefits to

the pyrolysis process besides additional energy-generating capacity via combustion the resulting product has potential in various areas of great value and therefore additional research into the manufacturing of this value-adding product would be of great benefit.

1.4 Research Aim and Objectives

This study aims to demonstrate the design, construction, and commissioning of a pyrolysis reactor capable of performing at a wide array of pyrolysis conditions to generate the required pyrolysis products. A secondary aim is to optimize the design of the pyrolysis reactor to provide quality products as determined through analysis, the modifications and the subsequent improvements will be demonstrated. A tertiary aim is to provide a simple and accessible platform on which further pyrolysis work specifically biochar can be completed. The main objective of this study was to design, commission and operate a rotary kiln pyrolyser, to have an operating unit that could be used for further biochar synthesis studies, and to be able to explore the possibility of in situ activation as well as auto-thermal pyrolysis in future studies.

The step wise objectives of this study are enumerated below:

1. Investigate bioprocessing and demonstrate knowledge of this key area of the energy transition.
2. Utilise a technology comparison to choose the correct reactor technology.
3. Explore the design and development of a suitable design for the pyrolysis reactor.
4. Construct the Pyrolysis Reactor Design.
5. Commission the Pyrolysis Reactor.
6. Generate Pyrolysis products.
7. Determine the quality of the products.
8. Identify areas of improvement.

1.5 Research Scope

The scope of research in this dissertation includes reactor design, construction, commissioning, and operation. Biochar is the specific focus of this work, and, therefore, the

pyrolysis vapour and noncondensable gases are excluded. This dissertation intends to further develop the conversion of renewable feedstocks to value-added products. The study will be completed in the bioprocessing laboratories at the University of Pretoria.

1.6 Dissertation Outline

This dissertation is presented in a total of 5 chapters.

- **Chapter 1** - The introduction to this dissertation explores the motivation for the exploration of the topic as well as a problem statement which defines the requirement for the commencement of this study.
- **Chapter 2** - The literature review provides the fundamentals of bioprocessing. Focus is afforded to pyrolysis as a process, pyrolysis products, applications of biochar, pyrolysis reactor technologies, influencing factors on pyrolysis products, biochar characterisation and biochar modifications techniques which could be made to products to improve their properties for specific use cases.
- **Chapter 3** - The experimental methods chapter outlines the experimental work surrounding the design, construction and commissioning of the pyrolysis reactors. This includes construction, commissioning, experimental analysis, modifications, challenges, and successes.
- **Chapter 4** - Results and Discussion.
- **Chapter 5** - Final Research Conclusions and Future Recommendations.

Chapter 2

Literature Review

2.1 Bioprocessing

Bioprocess engineering is a specialisation within chemical engineering that focuses on processes that require biological feedstock and/or biological systems to produce valuable products. Due to the continuous drive for sustainability, there is already a wide range of processes and products in which a bioprocess engineer would be able to provide valuable input and thus bioprocess engineering can be found in many industries from biopharmaceuticals to conventional oil, gas, and chemicals. A bioprocess engineer combines principles from traditional chemical engineering, biology, chemistry and physics to design, develop and optimise energy-efficient and scalable bioprocessing facilities. Bioprocess engineering plays a pivotal role in the biotechnology industry, enabling the large-scale production of bioproducts with applications in energy, agriculture, healthcare, and environmental sustainability. Advances and research into bioprocess engineering continue to drive innovation and the development of solutions for addressing global challenges (Igbokwe *et al*, 2022).

The design, development, operation and optimisation of a bioprocessing facility are greatly aided by a fundamental understanding of the biological feedstock provided to the process and biological systems which govern the conversion of the feedstock to the value-added products. Bioprocessing is focused on the conversion of these biological feedstocks to value-added products but bioprocess is not restricted to only biological systems. Alternative conversion routes exist via chemical, barometric and thermal methods which are viable for the reaction step of biological processing facilities. Generally, a combination of these conversion routes is utilised to produce final products (Mitchell, Berovic & Krieger, 2002).

Examples of biological processes are; fermentation, enzyme technology, bioconversion and bioremediation. These biological methods form the foundation of bioprocess engineering, enabling the sustainable production of a wide range of bioproducts and contributing to advancements in biotechnology, environmental science, and healthcare. By integrating biological principles with engineering principles, bioprocess engineers develop innovative solutions for addressing global challenges and improving industrial processes (Guajardo & Schrebler, 2024).

An example of a chemical process chemical hydrolysis system in the context of bioprocessing engineering involves the use of chemical reactions to break down complex organic substrates into simpler compounds. Chemical hydrolysis systems play a critical role in the bio-based economy, enabling the conversion of renewable biomass resources into value-added products. Through advancements in bioprocessing engineering, these systems contribute to the development of sustainable and environmentally friendly alternatives to conventional fossil fuels and petrochemicals (Binder & Raines, 2010).

Hydrothermal processing involves the use of high-temperature and high-pressure water to convert biomass into various valuable products, including biofuels, biochemicals, and bioproducts. This technique utilizes the unique properties of water under supercritical or near-critical conditions to enhance the breakdown and conversion of biomass constituents. Hydrothermal processing offers several advantages in bioprocess engineering, including high product yields, minimal waste generation, and versatility in feedstock utilization. However, challenges such as reactor design, process optimization, and product upgrading need to be addressed to realize the full potential of this technology for sustainable biomass conversion. Ongoing research and development efforts aim to enhance the efficiency, scalability, and economic viability of hydrothermal processing for biorefinery applications (Williams *et al*, 2022).

Thermal processing systems in bioprocessing engineering involve the application of heat to convert biomass into valuable products or to treat waste materials for energy recovery or environmental remediation. These systems utilize various thermal processes, including pyrolysis, gasification, combustion, and torrefaction, to thermally decompose biomass constituents into biofuels, biochemicals, or biochar.

These conversion routes all play critical roles in bioprocessing engineering, enabling the conversion of biomass resources into renewable energy, fuels, chemicals, and other value-added products. Through advancements in process design, reactor technology, and feedstock utilization, the conversion routes contribute to the development of sustainable biorefinery concepts and the transition towards a bio-based economy. The focus of this study is afforded to pyrolysis and its solid products due to its accessible reaction conditions and

potential benefits.

2.2 Pyrolysis principles

Pyrolysis is defined as the thermochemical decomposition of organic matter into three broad products; pyrolysis vapours, non-condensable gasses (NCG) and biochar (Brassard, Godbout & Raghavan, 2017). Pyrolysis occurs when organic matter is subjected to high temperatures in an anoxic environment.

Pyrolysis requires organic matter as a feed material. This can include any organic matter since the decomposition of these materials at high temperatures in an anoxic environment produces the pyrolysis products. Biomass is an abundant and popular feed material and can create pyrolysis products that have various uses and properties. Woody biomass is used in pyrolysis because thermochemical decomposition creates the pyrolysis products. The use of woody biomass is attractive since it helps to reduce the carbon footprint of the products, as the carbon in the woody biomass comes from the atmosphere. Thus any renewable fuel created from biomass would be recycled carbon and other products can assist in carbon sequestration (Woolf *et al*, 2010; Q Hu *et al*, 2021; T Xie *et al*, 2015).

Pyrolysis has had a significant impact on humanity throughout history and can be considered an ancient technology with modern applications. Archaeological evidence indicates that homo sapiens used biochar to proactively improve the food production capacity of their environment (Roberts *et al*, 2017). Figure 2.1 shows typical soil profiles where one can notice the impact of anthropogenic modification on the soil. "*Terra Preta*" has notably improved properties for cultivation and is the result of the introduction of biochar and other materials to the soil. The unmodified soil, known as "Oxisoil" is also given for comparison (Glaser *et al*, 2001). Today, interest has primarily been focused on pyrolysis vapour as an alternative and renewable source of energy. This approach has been successful but has also changed the focus away from the other products of pyrolysis (Prussi *et al*, 2020).

A few key process conditions must be considered when discussing pyrolysis. The pyrolysis temperature, the heat transfer parameters, the heating rate of the biomass in the reactor, and the residence time. The residence time has a great effect not only on the final properties of the pyrolysis products but also on their respective yields. Pyrolysis can be divided into three regimes; slow, intermediate, and fast. Table 2.1 indicates how the different pyrolysis regimes' process conditions differ, resulting in differing mass yields.

Figure 2.1: Evidence of anthropogenic modification to soil shown as typical soil profiles of Terra Preta (a) and Oxisoil (b) (Glaser *et al*, 2001).

Due to the nature of pyrolysis, these regimes all require a high-temperature anoxic environment. Reaction temperatures over 900°C approach gasification and can no longer be classified as pyrolysis (Yaashikaa *et al*, 2020).

Table 2.1: Process conditions and resulting % mass yield ranges associated with pyrolysis regimes (Sakhiya, Anand & Kaushal, 2020).

Regime	Slow	Intermediate	Fast
Heating rate ($°C\,s^{-1}$)	0.1-0.8	3-5	10-1000
Temperature low (°C)	300	300	300
Temperature high (°C)	550	450	1000
Biochar Yield (% mass)	25-35	25-40	10-30
Pyrolysis vapour Yield (% mass)	20-50	35-50	50-70
NCG Yield(% mass)	20-50	20-30	15-20

For this study, particular interest should be given to the appropriateness of the heating rate, the temperature ranges of the system, and the biochar yield as indicated in Table 2.1. The NCG yield and pyrolysis oil yield are not vital at this point of the study but will

be essential for auto-fueled systems. Due to our identified goals slow pyrolysis seems to provide the best option concerning the objectives. Slow Pyrolysis has an effective heating rate of 0.1-0.8 $^{\circ}\mathrm{C\,s^{-1}}$ which in reality can only be achieved by preheating the biomass before entering the reaction zone. The reaction zone should be between 300-500 °C. The parameters noted in this section have a profound effect on the final characteristics of the pyrolysis products. Therefore, careful consideration must be made to ensure that the correct regime is chosen so that the final product and the associated yield match the use case.

2.3 Pyrolysis products

2.3.1 Pyrolysis Vapour

Pyrolysis vapour is a co-product formed by the depolymerisation of cellulose, hemicellulose and lignin. This process forms hundreds of complex organic compounds.

The produced vapour can be condensed into an unstable oil at room temperature. The instability observed in pyrolysis vapour is created by oligomers forming aerosols, which indicates that pyrolysis vapours are a multiphase microemulsion. This instability leads to aging which chemically and physically changes the final product (Brassard, Godbout & Raghavan, 2017). Although pyrolysis vapours have a multitude of reactive components and therefore have the potential to be used as an alternative fuel source, the high water content and instability of the product must be reduced by upgrading before the product can be used as engine oil/fuel (X Hu & Gholizadeh, 2019). The properties of pyrolysis vapour are compared to the properties of typical diesel fuel in Table 2.2. The moisture content, pH, Higher Heating Value (HHV), solid percentages and pour points are especially important for the use of the hydrocarbon mixtures as a diesel fuel replacement. Table 2.2 demonstrates how different the produced Pyrolysis vapour condensate is to the commonly used fuel. For renewable fuels to gain wide acceptance and utilisation they should be a replacement for the existing fossil fuels and from this comparison due to the wide ranges in values and the large differences from that of diesel fuel the pyrolysis vapour condensate requires a myriad of additional processing to be utilised as a typical fossil fuel replacement. The processing required to upgrade pyrolysis oils to be suitable to replace typical fossil fuels is highlighted to indicate that a pyrolysis reactor system would only fulfil part of a biomass conversion facility and that the co-products (pyrolysis vapour, biochar and NCG) would need to be handled as per their final required use case as a product or as a combustion product.

Table 2.2: Generalized properties of pyrolysis vapour condensate and Diesel Fuel (15 PPM Sulphur) (Mohan, Pittman & Steele, 2006; ASTM, 2022).

Properties	Pyrolysis Vapour Condensate	Diesel Fuel	Unit
Moisture content	15.0-30.0	0.05	%
pH	2.5-6.0	5.5-8.0	-
Higher heating value	16.0-19.0	45.0	$MJ\,kg^{-1}$
Solids	0.2-1.0	0.01	%
Pour point	-33.0	52.0	°C

The properties of the pyrolysis vapour vary greatly with the given pyrolysis conditions, the regime, and the properties of the feed material (A Ahmed *et al*, 2020). Therefore, creating a consistent pyrolysis vapour is an arduous task, because of the variety of influencing conditions.

The term "pyrolysis oil", also known as "bio-oil", refers to the dark brown, freely flowing liquid produced by the decomposition of biomass. The vapour products are quickly cooled or quenched to create this liquid. Additionally, the liquid is made up of a few fragments of lignin, hemicellulose, and cellulose that have not been able to volatilise in the pyrolysis environment and/or are small enough to be removed from the reactor *via liquid entrainment* (Oasmaa *et al*, 2010). The liquid byproduct of biomass pyrolysis frequently represents two distinct phases(aqueous phase and organic phase) due to the moist raw material and the water produced as a result of the secondary reactions during storage. Direct use of the organic phase as fuels or upgrading to high-grade chemical or fuel products is both possible (Wright *et al*, 2010).

Pyrolysis hydrocarbons have physiochemical characteristics that are very different from those of regular mineral oils. Feedstock, feed moisture content, process parameters (vapour phase residence time, temperature, pressure), reactor type, recovery design unit and operating scale are just a few of the variables that affect the properties and content of oil(Dhyani & Bhaskar, 2018). Significant amounts of moisture, suspended solids, charcoal, oxygen, and corrosive compounds are found in pyrolysis oils. Poor heating and calorific values are present in these components. Pyrolysis oil contains 35-40 % oxygen, which is present in many organic functional groups, while mineral oils have a ppm oxygen content. These functional groups are also responsible for the extremely polar character of the resulting oil (Roggero *et al*, 2011).

2.3.2 Biochar

Biochar is a major product of the pyrolysis of biomass feedstock and can be utilised in a variety of applications for example biochar can be used to supplement energy requirements of the reactor, as a platform material in the production of specialised products such as catalysts, to improve the efficacy of soil or in water treatment (Sakhiya, Anand & Kaushal, 2020; H Li *et al*, 2017; Zhang *et al*, 2018; Ahmad *et al*, 2014; Sohi *et al*, 2010; Beesley *et al*, 2011). The provided list is not exhaustive but it assists in highlighting the potential of this underutilised product. Optimised manufacturing and modification of biochar to value-adding products can further its economic potential and socioeconomic impact. An example of *Eucalyptus Grandis* biomass and the final converted biochar is

given in Figure 2.2. It can be noted that the final produced biochar is reminiscent of the originating biomass.

Figure 2.2: *Eucalyptus Grandis* biomass (a) vs biochar (b).

The variety of feedstock used, the amount of moisture (trapped and surface) in the feedstock, and the operating pressure and temperature points at which the experiments were performed have a significant impact on the performance outcomes of biochar production, which are achieved using various production technologies (Bartoli *et al*, 2020). Cellulose, hemicellulose, and lignin are the three main components of biomass, each of which contains traces of minerals and extractives. The feedstock components greatly affect the final mass yields of the different pyrolysis products. The high lignin and mineral content increases biochar yield because the majority of the fixed carbon is sourced from lignin from the biomass and the mineral content is known to catalyse the conversion of lignin into biochar. Therefore high lignin biomass should be identified as a key source for the specific production of biochar (Kazemi Shariat Panahi *et al*, 2020). Another element that influences biochar properties and biochar yield is moisture content. The biochar reaction is influenced by the moisture content, which is often used to create activated carbon. According to reports, the feedstock contains 15 to 20% moisture that can be carbonised, making fast pyrolysis processes relatively desirable for 10 % moisture content (Kazemi Shariat Panahi *et al*, 2020; Ippolito *et al*, 2020).

Temperature has a significant impact on the characteristics of biochar but it is known that biochar's yield is greatly affected by pyrolysis temperature. The decrease in yield can be attributed to a combination of fixed carbon cracking and volatile removal. This process is an illustrative example of the increase in the stability of biochar. The additional thermal degradation of the biochar can also affect its chemical and surface characteristics. To achieve "biochar", a minimum process temperature of 300 °C must be achieved, as this will ensure that the desired carbon structure will be developed(Y Xie *et al*, 2022). Table

2.3 illustrates the simple correlations that can be developed between the pyrolysis temperature and the elemental composition of the final biochar produced. As the pyrolysis temperature increases the carbon content is somewhat positively correlated and increases whereas the hydrogen and oxygen contents of the final product are negatively correlated and decrease. The nitrogen concentration is strongly uncorrelated with the pyrolysis temperature. This follows the expected regime of thermal degradation as the effect of cracking is not the prevailing mechanism but rather the pyrolysis of the hydrocarbon substances.

Table 2.3: Biochar pyrolysis temperature elemental composition impact (Ahmad *et al*, 2014; Panwar, Pawar & Salvi, 2019; T Xie *et al*, 2015).

	Temperature (°C)	C (%)	H (%)	O (%)	N (%)
Temperature (°C)	1.00	0.43	-0.86	-0.65	0.08
C (%)	0.43	1.00	-0.25	-0.28	-0.11
H (%)	-0.86	-0.25	1.00	0.71	-0.11
O (%)	-0.65	-0.28	0.71	1.00	-0.35
N (%)	0.08	-0.11	-0.11	-0.35	1.00

The identified behaviour can be more easily identified by utilising the given pair plot in Figure 2.3. A pair plot allows for each of the measured variables to be compared to each other thereby allowing for quick identification of potential relationships between variables. Figure 2.3 shows the elemental compositions of produced biochar at different pyrolysis temperatures to understand the product envelope from multiple biomass sources. The positive and negative correlations between the elemental compositions and pyrolysis temperatures (Ahmad *et al*, 2014; Panwar, Pawar & Salvi, 2019; T Xie *et al*, 2015) can be identified in the first column of the plot. It should be noted that from Figure 2.3 the differences due to the presence of nitrogen in the original biomass greatly impacts the final biochar composition. This behaviour is clearly demonstrated by the "pink" group of feedstocks in Figure 2.3.

"High-quality" biochar requires minimal postprocessing to achieve desirable properties but can be achieved more reliably at higher process temperatures; therefore, the mass yield of the biochar product and process conditions must be carefully managed to meet the final product specifications required for the application. Biochar has been the focus of numerous research papers in recent years because of its diverse applications. To serve as references for upcoming biochar application studies, the following section provides a summary of the current applications and systems. Despite its well-known and favourable properties, biochar is not widely utilised to its full potential (Kazemi Shariat Panahi *et al*, 2020).

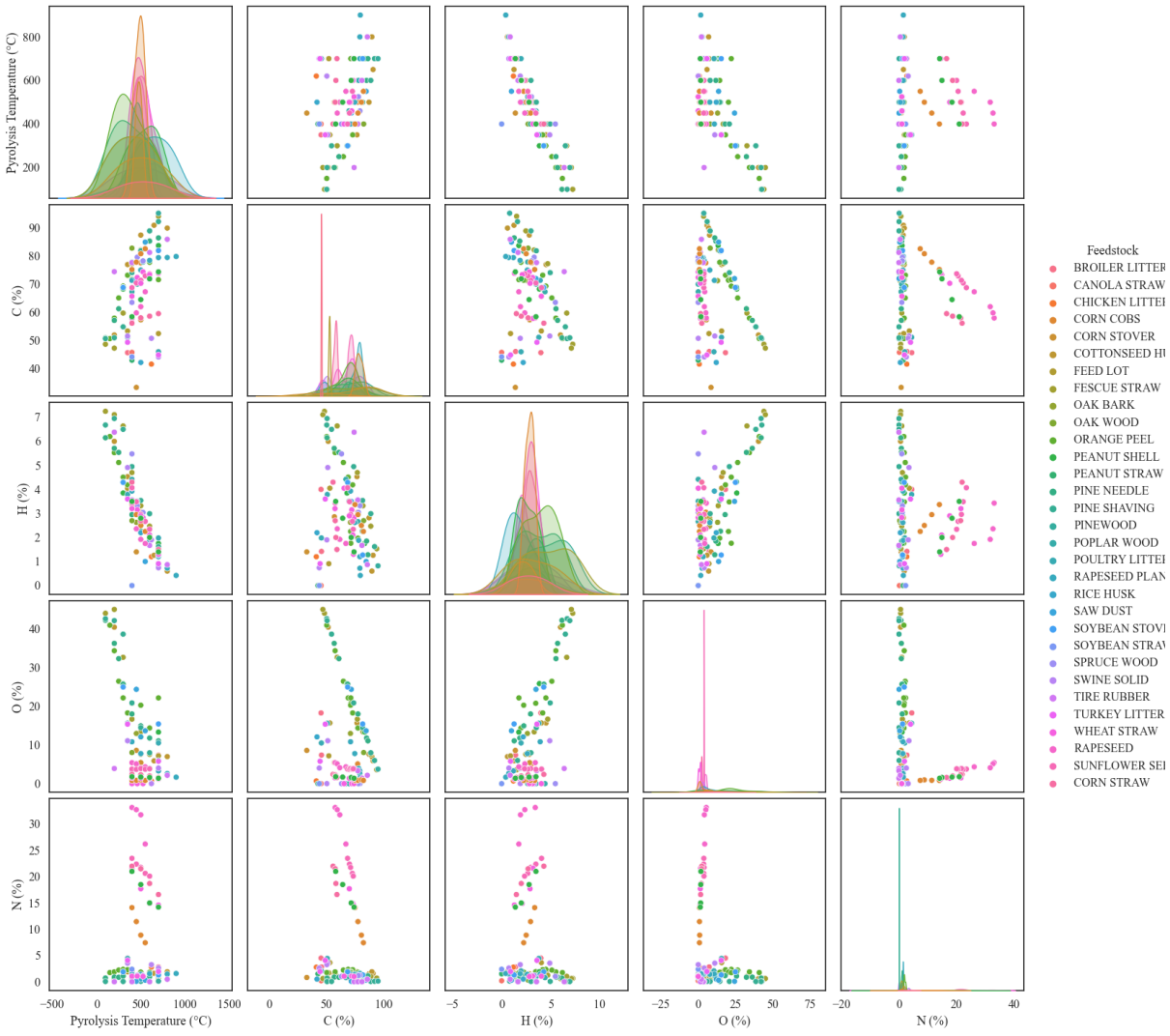

Figure 2.3: Biochar elemental composition based on feedstock at different pyrolysis temperatures (Ahmad *et al*, 2014; Panwar, Pawar & Salvi, 2019; T Xie *et al*, 2015).

2.3.3 Non-condensable gases

The non-condensable gas fraction of the pyrolysis vapours, to be referred to as NCG, is produced as a co-product of each pyrolysis regime. A typical composition of NCG is made up of CO_2, CO, H_2, CH_4 and additional C_2, C_3 and C_4 hydrocarbons (Wright *et al*, 2010). NCG is commonly used to supplement the energy requirements of the endothermic process of pyrolysis. Although NCG can be sold as a product, the wide process conditions result in a wide variety of properties, and thus it would be beneficial to use this as an additional energy source instead of a final co-product (Swart, 2012).

Different chemical structures of the biomass components affect the chemical makeup of gaseous products. The higher carboxyl content of hemicellulose is responsible for a higher CO_2 yield. As a result of the thermal cracking of carboxyl and carbonyl, cellulose exhibits

a higher CO yield. The pyrolysis of lignin releases significantly more H_2 and CH_4 when aromatic rings and functional groups of methoxyl are present. Non-condensable gases can be combusted to provide process heat for large-scale operations or usefully recycled back into the reactor to support fluidisation. Recycling was found to increase liquid yield while simultaneously decreasing biochar yield. According to the 13C NMR analysis, recycling NCG results in an increase in aromatic fractions while a decrease in methoxy, carboxylic, and sugar fractions. The pyrolysis oil's pH and heating value increased as a result of recycling NCG, while viscosity, oxygen content, and density decreased (Mante *et al*, 2012).

2.4 Applications of Biochar

Biochar is the specific focus of this study and therefore further investigation and explanation is supplied on the applications of biochar.

2.4.1 Water Treatment

2.4.1.1 Inorganic Pollutant Removal

Heavy metals pose risks to human health, ecosystems, and food safety due to their toxicity and ability to accumulate. Many studies have assessed the removal of heavy metals from soil/water as well as their conversion into oxidizable and residual fractions to weaken their toxic impact and lower potential health risks.

Listed below are generalizations made about the components that influence the adsorption and immobilization of large metals onto biochar: the substance's properties, environmental temperature, pH benefit, and dosage. Recently this area of study has been minimally investigated and therefore further investigation into the application of biochar in heavy metal remediation is required (Zhang *et al*, 2018; Mohan, Pittman & Steele, 2006; Blanco-Canqui, 2019).

Surface complexation, adsorption, chemical precipitation and electrostatic interaction are the main biochar immobilizing mechanisms for heavy metals. Analysis shows that the phytoavailability and extractable fraction of heavy metals decreases with the application of biochar to the solution (Mohan *et al*, 2006; Enaime *et al*, 2020).

The mechanisms of interaction between the biochar and heavy metals are as follows (Zhang *et al*, 2018),

1. The biochar's surface possesses negative charges, and electrostatic adsorption causes heavy metal ions to be adsorbed.

2. Physical adsorption takes place due to the biochar's unique surface area and pore structure, which are advantageous for the absorption of heavy metals as these properties serve as the sites for this process.

3. Biochar raises the pH of the soil and sewage, thus the precipitation of heavy metal ions with hydroxyl, carbonate, or phosphate radicals is a result.

4. Once the proper range of pH values has been achieved, cation exchange occurs and the heavy metals undergo an exchange interaction on the surface of biochar.

5. Surface complexation occurs between the present heavy metals and the biochar which produces the resulting heavy metal ions and functional groups.

6. Oxygen function groups on the biochar undergo chemical reduction on the biochar. This changes the high valence metal ions in an aqueous solution to low valence ions.

In terms of phosphorus removal, Biochar is promising. When biochar contains a lot of Ferrum (Fe), calcium (Ca), aluminium (Al) and magnesium (Mg), it absorbs phosphorus more effectively. Biochar's phosphorus adsorption capacity is nearly seven times greater than activated carbon (Zhang *et al*, 2018). The phosphorus-impregnated biochar is suitable for improving soil fertility. Applications of biochar make extensive use of resources in addition to resolving the serious issues of water body eutrophication (Mohan *et al*, 2006; Xiang *et al*, 2020).

2.4.1.2 Organic Pollutant Removal

Biochar has demonstrated exceptional adsorption capacity for organic pollutants(such as antibiotics, dyes and herbicides). The results showed that biochar could be used to amend poly-cyclic aromatic hydrocarbon (PAH) contaminated soils in an environmentally friendly and economically beneficial way (Blanco-Canqui, 2019; Enaime *et al*, 2020).

The primary mechanisms of biochar differ somewhat from those used to remove heavy metals when it comes to adsorbing organic contaminants (Zhang *et al*, 2018).

1. Partitioning mechanisms, in which the carbonated organic matter on the biochar's surface adsorbs non-polar organic pollutants.

2. Hydrophobic effects, in which the surface of biochar is contaminated by organic hydrophiles and groups of hydrophytes.

3. Organic contaminants and the functional groups on the biochar surface form hydrogen bonds.

4. Biochar pores' micro-pore filling, which causes organic pollutants to be absorbed and immobilized by swelling after adsorption and preventing desorption.

5. Physical adsorption, in which organic pollutants are absorbed by sites on the biochar's specific surface area and pore structure.

2.4.2 Soil Improvement

The growth of plants and the removal of pollutants are both benefited by the application of biochar to the soil. Although the impact on plant growth and pollution is apparent, it is not significant enough to guarantee the safety of the contaminated land for food production crops because pollution could spread throughout the food chain (Ahmad *et al*, 2014). By enhancing the microbial activity and organic content of the soil, biochar can reduce the bioavailability of heavy metals (Lehmann *et al*, 2011). The type of pyrolysis feedstock, the crop being studied, and specific environmental factors of the location all have an impact on the aforementioned benefits (El-Naggar *et al*, 2019; Beesley *et al*, 2011; Zhou *et al*, 2017; Oram *et al*, 2014; Zhang *et al*, 2018).

Biochar is often infused with fertilizer and therefore as the concentration in the surrounding soil decreases, due to plant consumption, biochar provides slow release and, consequently, lessens the loss of fertilizers (Clough *et al*, 2013). Biochar's extensive pore structure offers beneficial soil microorganisms a favourable habitat, which may further encourage crop growth and boost yields (Zheng, 2010; Yang *et al*, 2019).

Organic carbon, which is abundant in biochar, can increase soil nutrients and increase the amount of organic matter and humus in the soil. Biochar can be used to improve cation exchange capacity and pH value in soil. Due to biochar's well-studied large surface area and pore structure, soil microorganisms have improved habitats owing to its ability to hold more water, ventilate soil, and provide nutrients (Lehmann *et al*, 2011; Jeffery *et al*, 2011; Sohi *et al*, 2010).

As the bulking agent for aerobic composting, biochar has demonstrated significant environmental benefits. This is closely related to biochar's properties, such as its surface functional groups, high porosity, absorption capacity and high cation exchange capacity

(CEC) (Zheng, 2010). Biochar and compost are complementary to one another. One benefit of environmentally friendly biochar is that it improves the physicochemical properties of the compost mixture, reduces greenhouse gas emissions, lowers ammonia emissions and total nitrogen loss, speeds up the growth of beneficial microorganisms, decreases heavy metal bioavailability, adsorbs organic pollutants, and enhances composting quality in the end (Ekebafe, Ekebafe & Ugbesia, 2015). The physicochemical characteristics of biochar, such as the improvement of the CEC, the quantity of surface functional groups, and organic matter, can be altered by the composting process through oxidation and adsorption. It appears promising that dredged sediment can be stabilized, made harmless and used more effectively owing to biochar, an aerobic composting bulking agent. Even though there have been brief studies, applying biochar to the intricate and practical environment restoration is still lacking (Clough *et al*, 2013). It is crucial to concentrate further research on longer experiments in the in-*situ* environment to maximize the potential advantages of biochar. To fully comprehend the underlying application mechanisms of biochar additional research is necessary.

In a triple-win scenario, the addition of the aforementioned composts to agricultural soils may result in higher yields for farmers and compensation for environmental services, reduced eutrophication and less harmful environmental effects from intensive farming practices, and sustainable food production for humanity while also reducing the effects of climate change and the associated risk of reaching climate tipping points (J Singh & C Singh, 2020; Filiberto & Gaunt, 2013; Sánchez-Reinoso, Ávila-Pedraza & Restrepo-Díaz, 2020). By putting an end to the cycles of arable land and human habitation, biochar composts and composites help create a sustainable society for future generations. The method is universal because it is unrestricted by economic, technical, or infrastructure development and can be used anywhere in the world where plants are growing (Ekebafe *et al*, 2015).

2.4.3 Carbon Sequestration

One of the biggest problems we face right now is climate change. Biochar, which is made from carbon crop residues and thereafter returned to the soil, can serve as a sink for atmospheric carbon dioxide (Downie *et al*, 2012).

Carbon sequestration is the process of removing and storing carbon from the carbon cycle, either naturally or through human intervention, to lessen atmospheric greenhouse gas emissions and help combat climate change (Zhang *et al*, 2018; Tan, 2019; Brassard, Godbout, Raghavan, *et al*, 2017).

Carbon can be sequestered in several ways as shown in Figure 2.4. Effective measures must be instituted to increase carbon sequestration and decrease the carbon dioxide concentration in the atmosphere to address the urgent issue of global warming. Due to the stable and concentrated carbon nature of biochar, the conversion of waste biomass into it results in carbon sequestration (J Wang & S Wang, 2019). Following its application to soil, Biochar can not only sequester carbon but also lessen the amount of CO_2, N_2O, and CH_4 that is released, thereby reducing the effect of these greenhouse gasses. Preference for biochar application should be given to neutral and alkaline soils rather than acidic ones to achieve better carbon sequestration since the organic carbon in the soil will degrade more quickly (Jeffery *et al*, 2011).

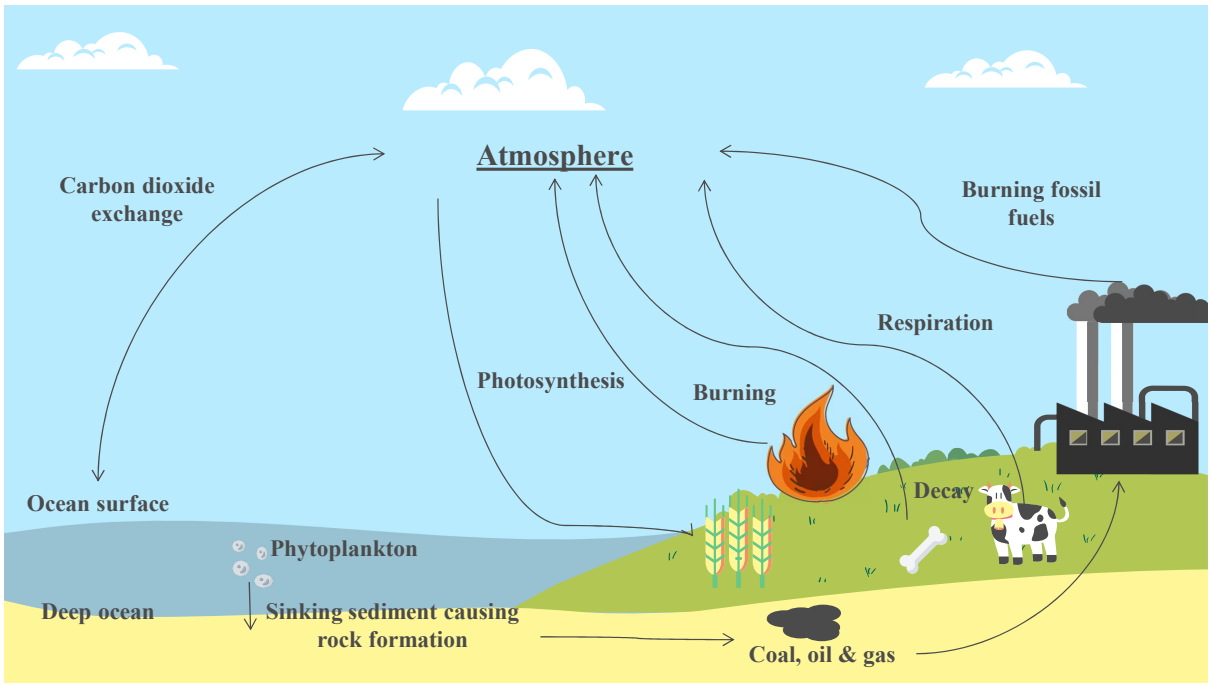

Figure 2.4: Simple representation of the Carbon Cycle (NASA, 2024).

2.5 Pyrolysis types

2.5.1 Slow pyrolysis

Throughout the process of slow pyrolysis, biomass experiences a sequence of intricate physical and chemical reactions. Initially, in the drying phase, biomass is subjected to the removal of heat and moisture, which releases volatile compounds. As the temperature increases, the biomass undergoes pyrolysis, leading to the primary reaction of devolatilisation. This process involves the decomposition of biomass into solid biochar, pyrolysis vapour, and noncondensable gases (Sohi *et al*, 2010; Tomczyk, Sokołowska & Boguta, 2020).

The pyrolysis oil produced from slow pyrolysis is a dark and dense liquid containing a variety of organic compounds like phenolics, acids, and oxygenated hydrocarbons. This pyrolysis oil with a high oxygen content and low heating value can be employed for heating and electricity production or further processed to generate transportation fuels (Cai *et al*, 2017).

On the other hand, the solid biochar produced during slow pyrolysis is a high-carbon solid that possesses a porous structure, enabling it to enhance soil fertility and reduce greenhouse gas emissions. Biochar is also capable of adsorbing contaminants from water and soil, and as a soil amendment, it can enhance soil structure, nutrient retention, and water retention (Panwar *et al*, 2019).

Slow heating rates, low temperatures, and longer residence times (typically several hours) are used to perform slow pyrolysis. Typically, woody biomass will produce 30–35 % biochar, 45–50 % pyrolysis oil, and 20–25 % non-condensable gas when subjected to slow pyrolysis at a temperature range of 300–500 °C. This pyrolysis regime generally results in high-quality biochar and pyrolysis oil due to the extent to which the reactions may reach completion (Al Arni, 2018).

Kiln, retort, and converters are a few slow pyrolysis reactor examples. Retorts and converters are industrial-scale reactors that can recover biochar and a volatile fraction. Rotating kilns, augers, and drums are the three reactors that are most frequently used in slow pyrolysis (Boateng & Barr, 1996). Long-standing and still widely used in developing countries is the use of the kiln. The kilns are simple to build and suitable for heating various biomass types. The kiln reactor's liquid and vapour products are exposed to the soil and atmosphere due to its simplicity which can pollute and emit greenhouse gases.

This technology doesn't need any additional process equipment and is better suited for woody biomass in the form of logs as a feedstock (Dhyani & Bhaskar, 2018).

For biomass pyrolysis, the rotary drum reactor is a very dependable system. It is further divided into two categories: direct heating and indirect heating. The heat needed for the pyrolysis process is produced by the indirect heating process, which involves the combustion of pyrolysis gases and vapours. This kind of reactor can achieve biochar and pyrolysis oil products which exhibit excellent stability (Al Arni, 2018).

The auger reactor is employed to produce biochar continuously. Biomass is typically fed through a hopper in the auger reactor. The biomass is moved by a screw to the heated area of the pyrolysis reactor. To obtain liquid and gas yields, the solid yield is collected from the screw's end, and vapours are taken out of the reactor and transferred to a condenser where the pyrolysis vapour is recovered and the non-condensable gases are allowed to continue through and be collected (Campuzano, Brown & Martínez, 2019; Brassard, Godbout & Raghavan, 2017).

2.5.2 Intermediate pyrolysis

Intermediate pyrolysis occurs between 400-600 °C and can be characterised as having shorter residence time than slow pyrolysis, typically ranging from a few seconds to a few minutes (Dhyani & Bhaskar, 2018; Yang *et al*, 2019; Mohan *et al*, 2006).

Thermal decomposition occurs during intermediate pyrolysis, causing the biomass to break down into simpler molecules and producing a mix of pyrolysis vapours, biochar, and non-condensable gas. The main reactions that happen during intermediate pyrolysis include dehydration, decarboxylation, and depolymerization (Tinwala *et al*, 2015).

The pyrolysis oil created is a dark and thick liquid with a higher heating value than that produced by slow pyrolysis. It has various organic compounds like oxygenated hydrocarbons, phenolics, and acids, and can be used as fuel for heating and electricity, or upgraded to transportation fuels. The liquid byproducts of transitional pyrolysis are less viscous and have a lower tar yield than those produced by fast pyrolysis. The reaction conditions in intermediate pyrolysis provide a wide range of variation for process optimization because more controlled chemical reactions occur(Bieniek, Jerzak & Magdziarz, 2021).

The biochar produced from intermediate pyrolysis is less stable and less porous than slow pyrolysis biochar, with a lower carbon content. Nevertheless, it still has potential applications as a soil amendment, carbon sequestration agent, or precursor for activated carbon production (Tinwala *et al*, 2015).

Overall, intermediate pyrolysis provides faster reaction times than slow pyrolysis and a better-quality pyrolysis oil with a variety of potential uses. While the biochar produced from intermediate pyrolysis has different characteristics from slow pyrolysis biochar, it still has potential applications.

2.5.3 Fast pyrolysis

Fast pyrolysis is a process that involves the breakdown of biomass through a series of chemical reactions, including depolymerization, deoxygenation, and cracking. These reactions break down complex organic molecules in the biomass into simpler molecules, resulting in a liquid pyrolysis oil, a solid biochar, and a non-condensable gas mixture composed primarily of carbon monoxide, carbon dioxide, and methane (A Ahmed *et al*, 2020; Sakhiya *et al*, 2020).

The pyrolysis oil produced during fast pyrolysis is a thick, dark liquid with an energy content similar to conventional fossil fuels. It contains a variety of organic compounds, such as oxygenated hydrocarbons, phenolics, and acids, and can be utilized as a fuel for electricity generation or upgraded to produce transportation fuels (Wright *et al*, 2010).

Fast pyrolysis also produces biochar with high porosity, high surface area, and low carbon content. The biochar can be utilized as a soil amendment, carbon sequestration agent, or precursor for activated carbon production (Joubert *et al*, 2015).

The gas generated during fast pyrolysis contains carbon monoxide, carbon dioxide, and methane and can be used as fuel for heating or upgraded to produce syngas, which can be further processed into transportation fuels (Wright *et al*, 2010; Mohan *et al*, 2006)

Fast pyrolysis is a promising technology for converting biomass into pyrolysis oil, biochar, and non-condensable gas. The process is fast and efficient in producing high-quality pyrolysis oil that can be used as a renewable source of energy or as a precursor for transportation fuels. The biochar and gas produced during fast pyrolysis also have potential applications, making it a desirable option for biomass conversion.

Fast pyrolysis is thought of as a direct thermochemical process that can transform solid biomass into liquid pyrolysis oil with significant potential for energy use. Fast pyrolysis conditions are characterized by the following: biomass particle warming rates ($<$ 100 $^{\circ}$C min^{-1}), coupled with short times of the biomass particles and the gaseous reaction(0.5–2 s) at high and moderate treatment temperatures (450 - 600 °C) (Al Arni, 2018; Oasmaa *et al*, 2010; Heidari *et al*, 2014). The residence time of the fume produced within the hot

zone of the reactor is closely controlled to achieve excellent pyrolysis oil quality. This is a key distinguishing feature of fast pyrolysis. This can be achieved by ensuring that the fumes are quickly quenched in the reactor effluent stream.

2.6 Pyrolysis Reactor Technology

Three types of reactor technology are discussed below. The identified reactors are chosen due to their prevalence in pyrolysis academic research, their ability to achieve all regimes of pyrolysis and that they are continuous process equipment thereby lending themselves to future scalability and use.

2.6.1 Fluidised Bed Reactors (FBR)

The most extensively studied and effective pyrolysis reactors are those of Fluidized Bed Reactors (FBR). FBRs are used for a variety of chemical processes, including pyrolysis and gasification of solid feedstocks like biomass, waste materials, or coal. FBRs work by suspending solid particles in an upward flow of gas, creating a fluidized bed of particles that behaves like a liquid.

The fluidized bed provides excellent mixing and heat transfer between the solid particles and gas, which makes chemical reactions more efficient. Depending on the size and flow rate of the particles, the fluidized bed can be either bubbling or circulating. Bubbling beds have a lower gas velocity and can't carry the solid particles out of the bed while circulating beds have a higher gas velocity that entrains the particles and carries them up into a cyclone separator, which separates the solid particles from the gas stream (Suliman *et al*, 2016).

Compared with other reactor types, FBRs offer several benefits, such as high heat transfer rates, excellent mixing and mass transfer, and good control over the reaction conditions. FBRs have a large surface area, which provides ample contact between the solid particles and gas, resulting in high heat transfer rates. The excellent mixing and mass transfer properties of FBR ensure uniform reaction conditions throughout the bed, making the conversion of feedstock more efficient. FBRs can also operate at low temperatures and pressures, which reduces the cost of materials and energy (Heidari *et al*, 2014). While the FBR features high heat transfer rates and efficiencies, its operation can be troublesome for even consistent feeds. Biomass provides a new challenge in that different feedstocks that produce vastly different product properties could lead to unstable operation of the reactor. Long start-up times should also be considered due to the high mass of the fluidised bed that needs to be brought up to the set process temperature.

FBRs are used in many industries, including energy production, chemical manufacturing, and waste treatment. They are particularly suitable for converting solid feedstocks into valuable products such as synthesis gas, pyrolysis oil, and biochar.

High heat and mass transfer coefficients are produced when sand and biofuel particles are combined, which is ideal for fast pyrolysis. Unfortunately, this inherent high heat and mass transfer lend the reactor to be identified for high-quality pyrolysis oil production. By externally combusting the non-condensable gases/biochar produced, the heat is transferred directly to the bed (adding hot solids) or indirectly (hot gas/steam is passed through bed tubes) (Al-Farraji, Marsh & Steer, 2017).

Additionally, FBR has a more straightforward layout, simple scaling, and effective time management. However, the drawbacks are the large reactor size and the higher operating and construction costs (Swart, 2012).

2.6.2 Auger Reactor (AR)

Auger reactors are a type of reactor used for the thermal treatment of solid materials, such as biomass, waste, or coal. The auger reactor consists of a hollow, rotating screw or auger, which moves the solid material through a heated cylindrical chamber. The auger serves to convey the solid material through the reactor while also providing mixing and heat transfer (Campuzano *et al*, 2019; Funke *et al*, 2018; A Ahmed *et al*, 2020).

The thermal treatment of the solid material occurs as the material moves through the heated chamber, which is typically maintained at temperatures ranging from 400 to 800°C. During this process, the solid material undergoes pyrolysis or gasification, resulting in the production of gas, liquid, and solid products (Sakhiya *et al*, 2020).

Auger reactors offer several advantages over other types of reactors, such as low capital and operating costs, high conversion efficiency, and feedstock flexibility. The low capital and operating costs are due to the simple design of the auger reactor, which consists of a single rotating screw and a heated chamber (Brassard, Godbout & Raghavan, 2017). The high conversion efficiency is achieved due to the excellent mixing and heat transfer provided by the rotating auger, which ensures uniform reaction conditions throughout the solid material. The flexibility in the feedstock is due to the ability of the auger reactor to handle a wide range of solid materials, including biomass, waste, and coal (Funke *et al*, 2018). It should be considered that the Auger reactor requires specifically machined components and due to the additional rotating equipment, it will require maintenance which other reactors may not.

The heat needed for pyrolysis is transferred through the wall of an auger reactor. As a result, the screw serves two functions: first, it mixes the feed; and next, it regulates how long the biomass stays in the reactor. This reactor's configuration has the benefit that it

can be built very small and requires very little in terms of utilities. This makes it possible to construct the reactor as a portable unit and use it where biomass is abundant or on the site of biomass generation. This avoids the expense of transporting the feedstock and therefore lowers the operating costs (Brassard, Godbout, Raghavan, *et al*, 2017; A Ahmed *et al*, 2020).

Auger reactors have found applications in various industries, including waste treatment, energy production, and chemical manufacturing. They are particularly well-suited for the conversion of solid materials such as woody biomass into useful products, such as syngas, pyrolysis oil, and biochar.

2.6.3 Rotary Kiln Reactor (RKR)

A rotary kiln reactor is a type of reactor that is used for a variety of chemical processes, such as pyrolysis, gasification, and calcination. The unique feature of the rotary kiln reactor is that the reactions occur in a rotating cylindrical shell, which is inclined at a slight angle to the horizontal. The cylindrical shell is rotated slowly around its axis, which causes the solid feedstock to move along the length of the kiln due to gravity. The kiln is heated by a burner that is located at one end of the kiln and the feedstock is fed into the other end. As the feedstock moves along the length of the kiln, it is subjected to a range of temperatures and residence times, which promote the desired chemical reactions (Boateng & Barr, 1996; Conto *et al*, 2016; Phounglamcheik *et al*, 2017; Babler *et al*, 2017).

The advantages of rotary kiln reactors include high processing capacity, low capital cost, and excellent heat transfer. The large capacity of the kiln allows for the processing of large quantities of feedstock, making it suitable for commercial-scale applications (Proch, Bauerbach & Grammenoudis, 2021). Additionally, the simple design of the kiln and low capital cost make it an attractive option for small-scale applications. The excellent heat transfer properties of the kiln are due to the large surface area of the cylindrical shell and the use of hot gases to transfer heat to the feedstock (E Hu *et al*, 2022).

Rotary kiln reactors are widely used in the chemical, mineral, and energy industries. They are particularly well-suited for the processing of solid feedstocks, such as ores, coal, and biomass. The rotary kiln reactor is an effective and versatile reactor type that can be used for a range of chemical processes, making it a popular choice for many industries. While it is a popular choice in many industries research could be expanded on the use of rotary kilns for pyrolysis (Pichler *et al*, 2021; Benanti *et al*, 2011).

2.6.4 Technology Comparison

A technology comparison between the fluidised bed reactor (FBR), auger reactor (AR) and rotary kiln reactor(RKR) is demonstrated in Table 2.4. Advancements in technology and ongoing research may influence these comparisons over time. Additionally, specific project requirements and economic considerations should be taken into account when selecting a pyrolysis reactor for a particular application. The chosen reactor design is selected in Section 3.2.1.

Table 2.4: Technology Comparison (Piersa *et al*, 2022; Al-Farraji *et al*, 2017).

Reactor Type	FBR	AR	RKR
Feed Stock Compatibility	Versatile, suitable for a wide range of feedstocks.	Limited to finely chopped or ground feedstocks.	Suitable for various feedstocks, including larger and more heterogeneous materials.
Temperature Range	400-600 °C	400-500 °C	500-800 °C
Pressure Range	Atmospheric to slightly above atmospheric pressure.	Atmospheric pressure.	Atmospheric pressure.
Residence Time	Short residence time (seconds to minutes).	Moderate residence time (minutes to tens of minutes).	Longer residence time (tens of minutes to hours)
Product Yield	Balanced liquid, gas, and char yields.	Moderate liquid, lower gas yield.	High liquid yield, lower gas yield.
Typical Composition	Balanced pyrolysis vapour, biochar, and syngas production.	Emphasis on pyrolysis gas production.	Higher pyrolysis vapour production.
Energy Efficiency	Moderate to high efficiency.	Moderate efficiency.	Moderate efficiency.

Scale / Throughput	Suitable for medium to large-scale operations.	Typically smaller scale.	Can be adapted for various scales, including large-scale operations.
Operation Control and Automation	Good control and automation capabilities.	Moderate control and automation.	Generally good control with potential for automation.
Environmental Impact	Moderate emissions, efficient heat transfer.	Moderate emissions.	Moderate emissions.
Capital Costs	Moderate to high capital cost.	Lower to moderate capital costs.	Moderate to high capital costs.
Operating Costs	Moderate Operating Costs.	Generally lower operating costs.	Moderate to high operating costs.
Technology Maturity and Reliability	Well-established Technology.	Emerging technology.	Established, but continuous improvements are made.
Waste Handling and Residue Management	Efficient char separation, manageable waste.	Moderate waste management.	Efficient char separation, manageable waste.
Regulatory Compliance	Generally compliant with regulations.	Compliance considerations may vary.	Compliance with regulations is achievable.
Case Studies / References	Numerous studies on various feedstocks.	Limited case studies, more research needed.	Various studies on larger-scale applications.

2.7 Influences on pyrolysis products

Due to the nature of this study specific focus is provided to the produced biochar.

2.7.1 Feed stock

Biomass is regarded as a complex solid substance made up of biological, organic, and/or inorganic materials which is typically derived from living organisms or are the result of living organisms such as wastes. Biomass can be divided into two categories: (1) Woody biomass and (2) Non-Wood biomass.

Woody biomass primarily consists of forestry and tree residues. Low dampness, low debris, less voidage, high density, and calorific value are characteristics of wood biomass. Animal waste and industrial and agricultural solid wastes make up non-woody biomass (Suliman *et al*, 2016; Ippolito *et al*, 2020; S Li *et al*, 2019). Non-woody biomass has characteristics like high debris, high dampness, large voidage, low density, and calorific value. Moisture content, among other characteristics of biomass feedstock, has a significant impact on biomass formation. The moisture in biomass can take many different forms, including liquid water, water vapour, and adsorbed within the biomass's pores. Higher biomass moisture content primarily prevents the formation of biochar and increases the amount of energy required to reach the pyrolysis temperature. Due to the significant decrease in heat energy and the shorter amount of time required for the pyrolysis process, low moisture content in the biomass is preferable for biochar formation, making it economically feasible when compared to biomass with high moisture contents (Suliman *et al*, 2016).

Four main elements that make up the bulk of the biomass are lignin, cellulose, hemicellulose and inorganic matter. Depending on the type of biomass, different organic and inorganic compounds have different mass ratios. Similar to this, biomass composition has a significant impact on the production of pyrolysis products. Biochar yield is significantly influenced by the feedstock type and its form, as well as its physical characteristics like surface area, pH, EC, and CEC (Ippolito *et al*, 2020).

Hemicellulose decomposes at temperatures ranging from 200-260 °C, cellulose at 240-350 °C, and lignin between 280-350 °C. More liquid yield (pyrolysis oil) is produced as a result of the pyrolysis of cellulose and hemicellulose, and biochar yield is provided by the lignin (S Li *et al*, 2019). Therefore, biomass with a higher lignin content can be used to make biochar. These components also have an impact on the characteristics and final

product yield of pyrolysis because the mineral matter found in raw biomass catalyzes the process.

2.7.2 Process Temperature

The most well-known and easiest-to-control process parameter for converting biomass to biochar is the temperature at which the conversion occurs otherwise known as the "Process Temperature".

Section 2.2 provides a discussion on the regimes through which biomass can be converted. Pyrolysis regimes can be simplified into three main categories in which process temperature increases: Slow, intermediate, and fast pyrolysis. The physicochemical properties and structure of biochar, such as elemental components, pore structure, surface area, and functional groups, are influenced by the pyrolysis temperature (Tomczyk *et al*, 2020).

When compared to residence time, particle size, and heating rate, the reaction temperature is a crucial factor that determines the biochar yield and properties (Tomczyk *et al*, 2020; S Li *et al*, 2019; Ippolito *et al*, 2020; Ghorbannezhad & Abbasi, 2021).

The bond cessation, which favours the release of a volatile constituent from the biomass, may be exceeded by the energy given to biomass at high temperatures. Limited biochar yield results from the further division of this volatile component into liquid and gas components. Therefore, it follows that biochar production is better suited to low temperatures. The ideal temperature for biochar production is very difficult to report because it depends on biomass type, composition, etc (Ippolito *et al*, 2020; Ghorbannezhad & Abbasi, 2021).

Additionally, it was noted that pH and specific surface area increased at higher temperatures. The ash content is shown to "increase" but this is independent of the pyrolysis temperature in the identified range and rather its presence in the final biochar fraction is better represented since the organic component of the biochar has been reduced thereby implying the ash content has increased (Tomczyk *et al*, 2020).

The biochar produced at lower temperatures, typically between 300-400 °C, has a higher surface area, pore volume, and oxygen content, and is known as "raw biochar". It is highly reactive and more susceptible to chemical and biological degradation. When the temperature of the pyrolysis process is increased between 400-700 °C, the biochar produced is referred to as "activated biochar", with lower surface area, pore volume, and oxygen content, and lower reactivity, resulting in a more stable and resistant product.

At even higher temperatures, usually above 700 °C, the biochar has a graphite-like structure, fewer functional groups, and a highly ordered crystal structure, known as "graphitic biochar", and has high stability and low reactivity (Ippolito *et al*, 2020; Sakhiya *et al*, 2020; S Li *et al*, 2019). The properties of biochar can be tailored to specific applications by controlling the pyrolysis temperature, making it important to have precise temperature control during the process.

2.7.3 Residence Time

Residence time in pyrolysis refers to the amount of time that the biomass spends in the pyrolysis reactor. During this time, the material undergoes a series of complex chemical reactions that result in the production of biochar, pyrolysis oil, and non-condensable gases (Tomczyk *et al*, 2020; Sakhiya *et al*, 2020; Yang *et al*, 2019).

The residence time is an important parameter in the pyrolysis process, as it can have a significant impact on the quality and quantity of the final products.

A longer residence time generally leads to higher yields of biochar and pyrolysis oil, as well as a greater degree of degradation of the biomass. However, a longer residence time also increases the risk of product degradation and the formation of unwanted byproducts. Therefore, it is important to carefully balance the residence time with other process parameters, such as temperature and feedstock composition, to optimize the pyrolysis process and maximize the desired product yields (Tomczyk *et al*, 2020).

Due to the slower rate of organic matter removal, which sets off the secondary reaction, longer vapour residence times typically favour the production of biochar. Low temperatures and extended residence times are ideal for maximizing tar decomposition and coking. To maximize biochar yield through pyrolysis, it is frequently advised that the vapour residence time be between a few minutes and several hours. However, heat transfer and reaction times on particle surfaces increase during high residence times, which improves biochar yield. To achieve high biomass conversion and yield, the vapour residence time must be shorter than the residence time for biomass decomposition. The quality of biochar may be obtained by optimizing residence time while taking into account a variety of factors (Sakhiya *et al*, 2020).

2.7.4 Pretreatment of Biomass

Before pyrolysis, biomass can undergo pretreatment to improve its properties and enhance the efficiency of the pyrolysis process. Pretreatment involves subjecting the biomass to various physical, chemical, or biological processes that alter its structure and composition (Cai *et al*, 2017; Pichler *et al*, 2021).

Physical pretreatment methods include milling or grinding the biomass to reduce its particle size, which increases the surface area available for pyrolysis. Chemical pretreatment methods involve treating the biomass with acids, alkalis, or solvents to remove impurities or modify its chemical composition. Biological pretreatment methods involve using microorganisms to degrade or modify the biomass (Yaashikaa *et al*, 2020).

Pretreatment can improve the yield and quality of the biochar produced from pyrolysis, as well as reduce the energy required for the pyrolysis process. It can also make the biomass more suitable for specific applications, such as biofuel production or soil amendment (Pichler *et al*, 2021).

Biochar characteristics are influenced by treating the biomass before pyrolysis. The most popular pretreatment techniques are submerging the raw materials in solution and reducing biomass particle size. The size reduction of biomass particles produces a high biochar yield. While the baking of biomass can increase the carbon content and reduce the oxygen and moisture content of biochar, pretreatment techniques like nitrogen and metal doping can affect the production and properties of Biochar and elemental composition.

The potential biomass for the production of biochar is used either alone or in combination with other biomass. The practical implementation is frequently constrained by the biomass's moisture or mineral content. For instance, consumption can result from the presence of chlorine and soluble base metals. The characteristics of the produced biochar can vary greatly due to various production technologies and biomass.(Yaashikaa *et al*, 2020)

2.8 Biochar characterisation

Carbon-based biomass feedstock under a wide range of process conditions creates a wide variety of properties. Neat biochar may undergo further upgradation such as through thermochemical activation in the presence of steam, carbon dioxide, oxygen, or any applicable chemical oxidant. Its physical characteristics are dependent on the process conditions used in its synthesis, and include the surface morphology, pH, surface area, and sorption capabilities (Suliman *et al*, 2016).

Biochar is well-known to enhance soil properties by aiding moisture retention, increasing the ratio between macro- and micro-porosity, reducing bulk density, and improving overall soil stability. Its application in agriculture has led to an increase in photosynthesis, stomatal conductance, and leaf relative moisture content (under adequate water availability). Its ability to improve soil fertility, retain soil moisture, and stabilise soil nutrient presence and uptake is extensively substantiated but depends strongly on the method of synthesis and upgradation used (Zheng, 2010).

2.8.1 Elemental Analysis

The elemental analysis of biochar involves the determination of the elemental composition of the material, which includes the amounts of carbon, hydrogen, nitrogen, sulfur, and other elements present in the sample. This analysis provides valuable information about the biochar's potential uses, such as its suitability as a soil amendment or as a precursor for activated carbon production. Elemental analysis is typically performed using techniques such as combustion analysis or elemental analysis with mass spectrometry, which can accurately quantify the amounts of each element present in the sample (Heidari *et al*, 2014; Tinwala *et al*, 2015).

The ratio of different elements in biochar, such as the carbon-to-nitrogen ratio (C/N), is used to evaluate the biochar's stability and its ability to function as a soil amendment. A higher C/N ratio signifies that the biochar is more stable and will gradually release nitrogen, thus providing a consistent nutrient source for plants (Al Arni, 2018).

The hydrogen-to-carbon ratio (H/C) can indicate the biochar's aromaticity or the presence of ring structures. If the H/C ratio is high, it means the biochar is less aromatic and more aliphatic, implying it contains more straight-chain carbon structures (Pimenta *et al*, 1998).

The oxygen-to-carbon ratio (O/C) is another important elemental ratio, which indicates the biochar's energy content and suitability as a feedstock for energy production. If the O/C ratio is higher, it indicates the biochar contains more oxygen and, therefore, has a higher energy content (Suliman *et al*, 2016).

Ultimate and proximate analysis are two types of analytical methods used to determine the composition of biomass or biochar. The ultimate analysis provides information on the percentage of the elemental composition, including carbon, hydrogen, nitrogen, sulfur, and oxygen. The proximate analysis, on the other hand, provides information on the percentage of volatile matter, fixed carbon, and ash content in the biomass or biochar. These analyses are commonly used in the evaluation and characterization of biomass or biochar for various applications.

2.8.2 Thermo-gravimetric analysis

Thermo-gravimetric analysis (TGA) is an analytical method for determining a material's thermal stability and decomposition behaviour. In a controlled setting, it entails gauging how much weight changes from sample to sample over time and temperature changes.

A small portion of the sample is heated continuously in a furnace while being placed in the crucible for the TGA experiment. A balance keeps an ongoing eye on the sample's weight, and the data is collected and analyzed. The TGA measurement can be used to examine the thermal stability of materials in a variety of gas atmospheres, including air, nitrogen, and helium (Felix *et al*, 2022).

Pharmaceuticals, materials science, and polymer science all frequently use TGA. The onset and rate of decomposition, thermal stability, and mass loss that happens during thermal processing are just a few examples of the materials it is used to characterize, as well as to study their thermal behaviour.

TGA can also be used to determine a substance's purity and to control material quality during the manufacturing process. It can offer crucial details for the design and improvement of manufacturing processes and is a potent method for the characterization of the thermal stability and decomposition behaviour of materials (Saldarriaga *et al*, 2015).

TGA is applied for thermal analysis to observe the physical and chemical properties of materials which are measured as a function of a temperature rise. This examination is planned to look at the ignition attributes of biochar and the biomass/ biochar mixes by thermogravimetric examination. Additionally, the normal weighted average of the

individual part was inspected whether synergic activity happened between the segments of the blends. The outcomes may assist with bettering comprehending the procedure and attributes of the examples from a major perspective and for the examination of tests. During this process, the heating of biochar initiates from room temperature and is increased up to 1000 °C (Anca-Couce *et al*, 2020).

2.8.3 Higher Heating Value

The energy content of biochar can be measured using its higher heating value (HHV), which represents the heat that can be generated by burning the material. The HHV of biochar depends on its chemical composition, particularly the amount of carbon, hydrogen, and oxygen it contains, as well as its ash content (Saldarriaga *et al*, 2015). Biochar with a higher carbon content and lower ash content typically has a higher HHV. This parameter is useful in evaluating the potential of biochar as a fuel source for energy production, such as in combustion or gasification processes. It can also be used to estimate the amount of carbon dioxide emissions that would result from burning the biochar (Hosokai *et al*, 2016).

A bomb calorimeter is a device used to measure the heat of combustion of a sample by igniting it in a high-pressure oxygen environment and measuring the resulting temperature change. This allows for the determination of the sample's calorific value, which is a measure of its energy content. The sample is placed in a metal container called a bomb, which is filled with pure oxygen and sealed tightly. The bomb is then placed in a container filled with water and an ignition wire is used to ignite the sample. The resulting heat is absorbed by the water and the temperature change is measured. The heat of combustion can be calculated by dividing the energy released by the mass of the sample (Hosokai *et al*, 2016).

The higher heating value can also be determined via correlations designed to predict these values for organic combustible material. Such a correlation is provided in Equation 2.1 (Merckel, Labuschagne & Heydenrych, 2019).

$$\Delta_c h_{HHV} = -13.87 m_{O_2} \tag{2.1}$$

2.8.4 Functional Groups

A molecule's reactivity, physical characteristics, and interactions with other molecules are all determined by its functional groups. By offering locations for the adsorption or complexation of other molecules, functional groups in biochar are crucial to the substance's ability to absorb.

The feedstock, pyrolysis conditions, and post-treatment of the material all affect the type and quantity of functional groups in biochar. Biochar contains typical functional groups such as quinone, hydroxyl, and carboxyl groups.

Acidic functional groups known as carboxyl groups (-COOH) can join polar and basic molecules to form hydrogen bonds. They are abundant and have a strong affinity for metal ions, which helps biochar absorb heavy metals.

Polar functional groups known as hydroxyl groups (-OH) can interact with water and other polar molecules to form hydrogen bonds. They improve biochar's hydrophilicity and its ability to absorb water-soluble molecules like phenols and dyes. A hydroxyl group is also present in the aromatic functional groups known as phenolic groups ($-C_6H_4OH$). They are in charge of helping biochar absorb organic pollutants like polycyclic aromatic hydrocarbons (PAHs) because they have a strong affinity for metal ions (Tomczyk *et al*, 2020).

The functional groups that contain oxygen and can interact with other molecules to form redox reactions are the quinone groups ($-C_6H_4O_2$). They are crucial for biochar's ability to absorb electron-donating molecules such as polyamines and metal ions (Kazemi Shariat Panahi *et al*, 2020).

Additionally, there is a chance of reduction in biochar functional groups when other properties such as pH, surface area, and porosity are increased. Fourier transform infrared (FTIR) spectroscopy and nuclear magnetic resonance spectroscopy (NMR) are used to characterise surface functional groups (Cai *et al*, 2017).

Biochar is a promising material for environmental remediation, water treatment, and other applications because of the presence and abundance of functional groups that affect its sorption capabilities.

2.8.4.1 Fourier Transform Infrared Spectroscopy

A type of analytical technique called Fourier Transform Infrared Spectroscopy (FTIR) is used to determine a sample's chemical makeup based on how it is absorbed or transmitted. The method determines which atom vibrations in a molecule cause distinctive infrared spectrum absorption peaks.

An infrared beam is passed through a sample in an FTIR spectrometer, and the frequency or wavelength of the light is used to determine the absorption spectrum. The spectrum is then transformed into the frequency-domain signal(the infrared signal broken down by frequency components) using the Fourier Transform, a mathematical technique. The functional groups and chemical bonds found in the sample are then determined by analysing the resulting spectrum (Sohi *et al*, 2010).

To identify organic and inorganic compounds as well as to ascertain the structure and composition of materials, FTIR is a widely used analytical technique in chemistry, biology, and materials science. It is frequently employed in, among other things, the fields of polymer science, pharmaceuticals, forensic science, and environmental science.

A vibrational technique called FTIR spectroscopy is used to examine the functional groups found on the biochar surface. Massive changes in biochar in the concoction and auxiliary arrangements occurred as the temperature rose. A non-damaging FTIR system could observe these progressions in real time. The spectra revealed an ongoing loss of aromatic groups at temperatures between 650 and 800 °C (Tomczyk *et al*, 2020).

2.8.5 Surface Area and Porosity

The total area of the internal and external surfaces of biochar particles is known as the biochar surface area, which plays a crucial role in determining its properties and applications. A larger surface area results in an increased number of sites for chemical reactions and interactions with other substances. It also enhances the adsorption capacity of biochar for nutrients, water, and contaminants, which makes it useful in soil remediation and water treatment.

Biochar porosity refers to the presence of empty spaces or pores within the biochar particles. Porosity is an important factor that influences the properties and applications of biochar. The greater the porosity of biochar, the larger the surface area available for chemical reactions and interactions with other substances. Higher porosity also increases the ability of biochar to absorb and retain nutrients, water, and contaminants, making it

useful for soil remediation and water treatment. When there is an increase in the loss of water during dehydration, the porous surface in biochar is created during the pyrolysis process. The pores found in biochar may be micro, meso, or macro. The pore size of the produced biochar can restrict the ability of the biochar to absorb certain molecules despite favourable polarity and charges (Zheng, 2010).

The surface area and porosity in biochar can be increased by controlling the pyrolysis temperature and duration, as well as by modifying the production process through techniques such as steam activation and acid treatment.

Temperature plays an important role in biochar formation, and the surface area is the key factor in determining the ability of biochar to absorb different compounds. Between treated and untreated raw materials, the surface area may differ. Commercially activated carbon has a larger surface area and naturally, the biochar created without activation has a smaller surface area and is less porous. Therefore, an activation process can be involved in the biochar production process to increase porosity and surface area. The activation process may involve both the physical and chemical processes (Suliman *et al*, 2016).

2.8.5.1 Scanning electron microscopy (SEM)

Scanning electron microscopy (SEM) images of biochars showed that the initial particle surface morphology underwent significant changes as a result of various processes and temperatures. Additionally, the pore characteristics of biochar may significantly improve as a result of the improvement of pores in tests that upgrade with rising temperatures. Additionally, it's possible that as pyrolysis temperature rises, mineral segment crystallinity increases and specially requested sweet-smelling structures form in biochar. SEM images provide a thorough description of the biochar's mesoporous and microporous distributions as well as its pore arrangement. SEM can be used to predict surface morphology before and after adsorption (Suliman *et al*, 2016).

2.8.5.2 Braunauer-Emmett-Teller Analysis (BET)

Braunauer-Emmett-Teller (BET) analysis can be used to determine the biochar surface area. Because the ability of biochar to remove pollutants from soil and aqueous environments is primarily responsible for this property, the study of surface area is crucial. The crude examples show a significant increase in the BET surface zone after pyrolysis in comparison to their biochar counterparts. Most noticeably, while new micropores were produced in the biochar during pyrolysis, the crude feedstocks lacked these material ones.

The porosity results for both feedstock types, including the surface area of the BET and the micropore region, improved as the force level increased from 2100 to 2400 W, which can be inferred from the faster stabilisation discharge rate and the expansion of the micropowder improvement. Biochar with high porosity, a variety of pore structures, and low density is the result of the release of an enormous amount of volatile matter (MB Ahmed *et al*, 2016).

A method for determining a solid material's surface area is BET (Brunauer-Emmett-Teller) analysis. The analysis is based on the idea that by measuring the amount of gas adsorbed at various pressures, it is possible to determine the surface area.

The specific surface area of porous materials such as activated carbon, zeolites, and metal-organic frameworks (MOFs) is typically determined using BET analysis. Due to their porous structure, these materials have a large surface area, which makes them useful for separation, catalysis, and gas storage (H Li *et al*, 2017).

2.8.6 Biochar Stability

Biochar stability is an important factor for its potential use in carbon sequestration. The stability of biochar refers to its ability to resist degradation and decomposition over time. If biochar is not stable, it can potentially release carbon back into the atmosphere, which would undermine its usefulness as a tool for carbon sequestration. Stable biochar has a high resistance to decomposition, which means that it can store carbon in the soil for longer periods. Factors that influence biochar stability include feedstock type, pyrolysis temperature, and post-processing treatments. Optimising these factors may allow the production of biochar with enhanced stability for use in carbon sequestration (Tan, 2019).

The ability of biochar to sequester carbon has been measured by its stability or resistance to degradation via biotic and abiotic mechanisms in the soil. The stability of biochars has been the subject of numerous studies (Yaashikaa *et al*, 2020; Tan, 2019; Brassard, Godbout, Raghavan, *et al*, 2017). Biochar stability is regarded as being determined by the temperature used during the pyrolysis process. This prediction is straightforward and inaccurate. The nature of biochar; moisture, volatile matter, ash, and fixed carbon has long been studied using proximate examination. For an extended period, the approximate examination requires high temperatures (900 °C for the assurance of volatile matter and 750 °C for the determination of ash). This has drawbacks and can lead to an exaggerated estimate of carbon by underestimating the amount of ashes present (Yaashikaa *et al*, 2020).

Direct or indirect qualification or quantification of biochar carbon structures, such as aromaticity, and thermal, chemical, or thermochemical methods like chemical oxidation, thermal degradation, etc., can be used to categorize the methods for determining stable carbon. The modelling of carbon mineralization and incubating biochar in soil requires further investigation (Brassard, Godbout, Raghavan, *et al*, 2017; Ekebafe *et al*, 2015).

Determining the longevity of the biochar practically is impossible because it takes hundreds of years for biochar to completely degrade (Roberts *et al*, 2017). However, the incubation and modelling procedures are pricey and time-consuming but they can provide some clarity on the expected performance and stability of the sequestered carbon. Biotic and abiotic degradation are made possible by the evaluation of thermochemical oxidation stability. However, the current methods for determining biochar stability do not yield precise results and can be used as a tool for many different applications. Biochar will therefore be used more effectively to mitigate climate change if new techniques for assessing biochar stability are developed (Yaashikaa *et al*, 2020).

2.9 Modification techniques

The process of modifying biochar involves altering its surface properties to enhance its performance in various applications. This is usually done by treating the biochar with certain chemicals or by physical methods such as grinding or crushing (Y Xie *et al*, 2022).

Chemical modification can be achieved by treating the biochar with various compounds such as acids, bases, or oxidizing agents. This can improve the biochar's sorption capacity, stability, and reactivity (H Li *et al*, 2017).

Physical modification, on the other hand, can alter the biochar's particle size, shape, and surface area, which can affect its performance in different applications.

Biological modification methods involve treating biochar with microorganisms, such as bacteria or fungi, to improve its nutrient content or to enhance its ability to support plant growth. Microbial treatment can also alter the surface chemistry of biochar and enhance its adsorption capacity for nutrients (Yang *et al*, 2019).

The modified biochar can be used in a variety of applications, such as water treatment, soil remediation, and energy storage. The specific modification method used will depend on the desired properties of the biochar for the intended application (Zhang *et al*, 2018).

2.9.1 Chemical Modifications

2.9.1.1 Acid Modification

The process of acid modification involves the treatment of biochar with various acids, such as hydrochloric acid or sulfuric acid, to alter its surface chemistry and improve its functionality. Acid modification can increase the biochar's surface area and porosity, as well as introduce functional groups such as carboxylic and phenolic groups onto the surface. These functional groups can enhance the biochar's ability to adsorb and remove contaminants from water or soil, making it a useful material for environmental remediation applications. Additionally, acid-modified biochar has shown promise as a potential catalyst for various chemical reactions due to its unique surface chemistry (Blanco-Canqui, 2019).

Eliminating impurities and increasing the presence of oxygen-containing functional groups like -OH and -COOH are the main goals of acid modification. Biochar is frequently activated using oxidants like HCl, HNO_3, H_2O_2, and H_3PO_4 (Y Xie *et al*, 2022).

The type and concentration of the acid will affect the microstructure and specific surface area of biochar, as well as the pore size and structure. The source material and the preparation conditions have a significant impact on the characteristics of acid-modified biochar. Acid modification can also affect the biochar's ability to absorb substances and how well it performs in a variety of applications (Mohan *et al*, 2006).

2.9.1.2 Alkaline Treatment

Alkaline treatments are a type of biochar modification that involves the use of alkaline substances such as sodium hydroxide or potassium hydroxide to alter the properties of biochar. This process can increase the biochar's pH, surface area, and nutrient availability, making it more effective as a soil amendment. Alkaline treatments can also remove contaminants such as heavy metals from biochar, making it useful for environmental remediation. The effectiveness of alkaline treatments depends on factors such as the type and concentration of the alkaline substance used, the duration and temperature of the treatment, and the properties of the original biochar (J Wang & S Wang, 2019).

Increased biochar's specific surface area and the quantity of oxygen-containing functional groups present on its surface are the main goals of an alkaline treatment. For this purpose, alkaline substances like potassium, ammonium, and sodium hydroxide are frequently used (Y Xie *et al*, 2022).

The type of feedstock and the production environment have an impact on the alkaline treatment's specific surface area of the biochar. For instance, calcination and potassium hydroxide treatment can significantly increase the surface area of sewage sludge and rice straw biochar. The specific surface area of bamboo-derived biochar, in contrast, was unaffected by sodium hydroxide treatment. Additionally, sodium hydroxide treatment can boost biochar's ability to exchange ions and the quantity of oxygen-containing functional groups (Ahmad *et al*, 2014).

2.9.1.3 Metal salts/oxides

Metal salt and metal oxide modification are two methods used to enhance the properties of biochar. In the metal salt method, a solution containing a metal salt is added to the biochar, followed by drying and heating to convert the metal salt to the corresponding metal oxide. The metal oxide is then bound to the biochar surface, providing functional groups that can enhance its properties for various applications.

In the metal oxide method, metal oxide particles are directly mixed with biochar during its production. The metal oxide particles can act as a template for the formation of biochar, resulting in biochar with enhanced properties. These modifications can improve the biochar's ability to adsorb and retain nutrients, contaminants, and other substances, making it useful for applications such as soil remediation, water treatment, and energy production (Y Xie *et al*, 2022).

In recent years, there has been an increasing interest in using metal salts or metal oxides to modify the properties of biochar. This method allows for the alteration of key biochar properties, leading to improvements in characteristics such as adsorption capacity, catalysis strength, and magnetism. For example, zinc chloride has been utilized to enhance the porosity, specific surface area, and adsorption capacity of biochar. The use of different metal salts and oxides (MgO, $ZnCl_2$, and K_2SO_4) on biochar produced the highest increase in phosphorus adsorption with zinc chloride at an impregnation ratio of 1:1 and an activation temperature of 600 °C (J Wang & S Wang, 2019). Interestingly, a higher impregnation ratio of 1:3 did not lead to an increase in specific surface area or pore volume.

2.9.2 Physical Modifications

Physical modification of biochar involves altering its physical properties, such as its surface area, pore structure, and particle size, without changing its chemical composition. This can be done using techniques like grinding, milling, sieving, and pelletizing. Modifying the physical characteristics of biochar can enhance its storage, handling, and application. For instance, reducing the particle size can increase the surface area, leading to better adsorption of pollutants in soil and water. Pelletizing biochar can increase its density, making it more convenient for transportation and application. Furthermore, physical modification can affect the biochar's capacity to hold nutrients and water, as well as its stability in soil (Ahmad *et al*, 2014).

Biochar can undergo physical activation by being exposed to a variety of reductive agents at various temperatures, including steam, CO_2, air, and ammonia. There are two ways that this gas purging technique can alter the characteristics of biochar. Biochar first reacts with reductive agents and consumes carbon, then releases and loses volatiles and condensates. Physical activation causes more pores to form, increasing the porosity, specific surface area, and micro-porous structure of biochar. Temperature, the mass ratio of biochar to activation agents, and activation time are just a few factors that affect the efficiency and process of activating biochar (Y Xie *et al*, 2022; H Li *et al*, 2017).

Chapter 3

Experimental

3.1 Introduction

Throughout the exploration of this research topic the design, construction, commissioning and operation of a biochar-focused reactor was a major objective. This objective was much more difficult to achieve due to the complexities of the processing material and the products produced. Therefore this trial and error method required four different methods of production to be investigated resulting in three prototype versions which were constructed and commissioned. The first rendition was prototype 1 where areas of improvement were identified and the the lessons learnt from the execution of the first prototype were implemented on the second prototype (prototype 2). Thereafter, the second prototype was analysed and further modifications were made to improve the operation and quality of the products produced which produced prototype 2.1.

3.2 Design

3.2.1 Process Design Considerations

Biochar is our primary focus for this reactor and therefore the operating conditions of the proposed reactor should be closer to the identified parameters for slow and intermediate pyrolysis as outlined in Section 2.2. Additionally, it has been identified that this process would provide the research group with an ample supply of pyrolysis products to perform independent research.

Previously the production of biochar for research purposes is produced using a batch method that provides high-quality biochar at the cost of time and yield. Thereafter the biochar is upgraded via another batch process that introduces super-heated steam into the neat biochar converting it to activated biochar, unfortunately, more biochar is lost to this process due to the formation of hydrogen and carbon monoxide. This process takes multiple days to complete a ridiculously small batch of activated biochar and the process yields are far from optimal.

It is proposed that the future pyrolysis reactor provides the outcomes of both batch processes in one conversion step thereby activating the biochar as it is being created *in-situ*. This could be achieved easily in a batch process but due to the high demands for pyrolysis products, the future system needs to be continuous or at the very least semi-batch. The combined activation and biochar production reduces the production time greatly at the potential reduction of the biochar quality but this would need to be investigated.

Feed stock variability was of interest, as we could pretreat biomass samples (such as loading biomass with fertiliser agents), which may alter the ease of charging the pretreated biomass into the reactor. The temperature range of a rotary kiln is in the optimum range for experimentation planned in future, particularly the in situ activation of biochar using steam. Residence time is much longer for rotary kilns and can be easily adjusted compared to the FBR and Auger reactor types. While the fluidised bed reactors tend to be more energy efficient, the energy optimisation of the rotary kiln reactor can be improvised in the future by recycling/returning the pyrolytic fluids to the reactor to promote auto-thermal pyrolysis. The rotary kiln is also a mature and well-understood technology, and was considered to be a better option for establishing a pyrolysis rig that could be used in future studies for exploring modifications to the pyrolysis process.

Due to our specific goals, requirements, information provided in Section 2.6.4 and the existence of an operational FBR on campus, it was decided that the rotary kiln type design was chosen as it supplies the platform to develop a continuous biochar process. The chosen type of reactor can be used to achieve the process conditions required for the identified pyrolysis of biomass into its pyrolysis products.

The bench scale in-situ activation rotary kiln pyrolyser (ISA - RKP) is proposed for this purpose. The ISA-RKP should allow the integration of a heat exchanger and electrostatic precipitator to ensure a proper mass balance may be completed for the system as shown in Equation 3.1. NGC would be determined by mass difference.

$$\text{Biomass} = \text{Biochar} + \text{PyroVapour} + \text{NGC} \tag{3.1}$$

The rotary kiln design can be separated into 3 broad categories; biochar synthesis system, measurement and data storage system and finally the in-situ activation system. A full process flow diagram of the proposed process is given as Figure 3.1

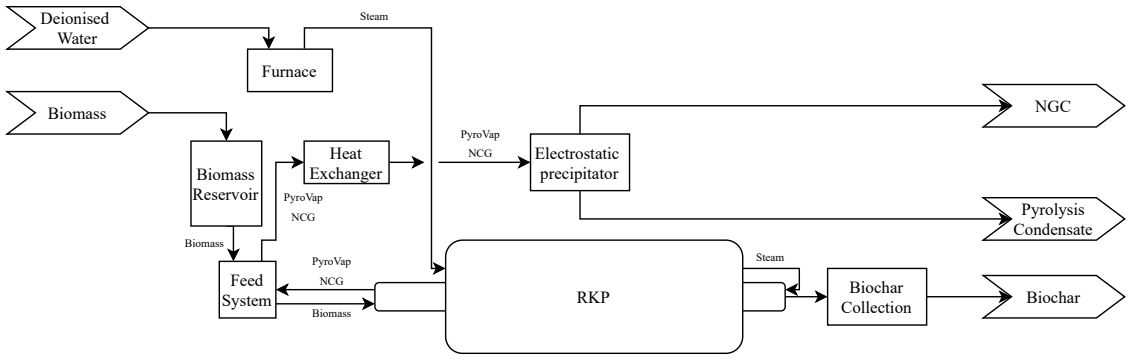

Figure 3.1: Process Sketch of *In-Situ* Activation - Rotary Kiln Pyrolyser process.

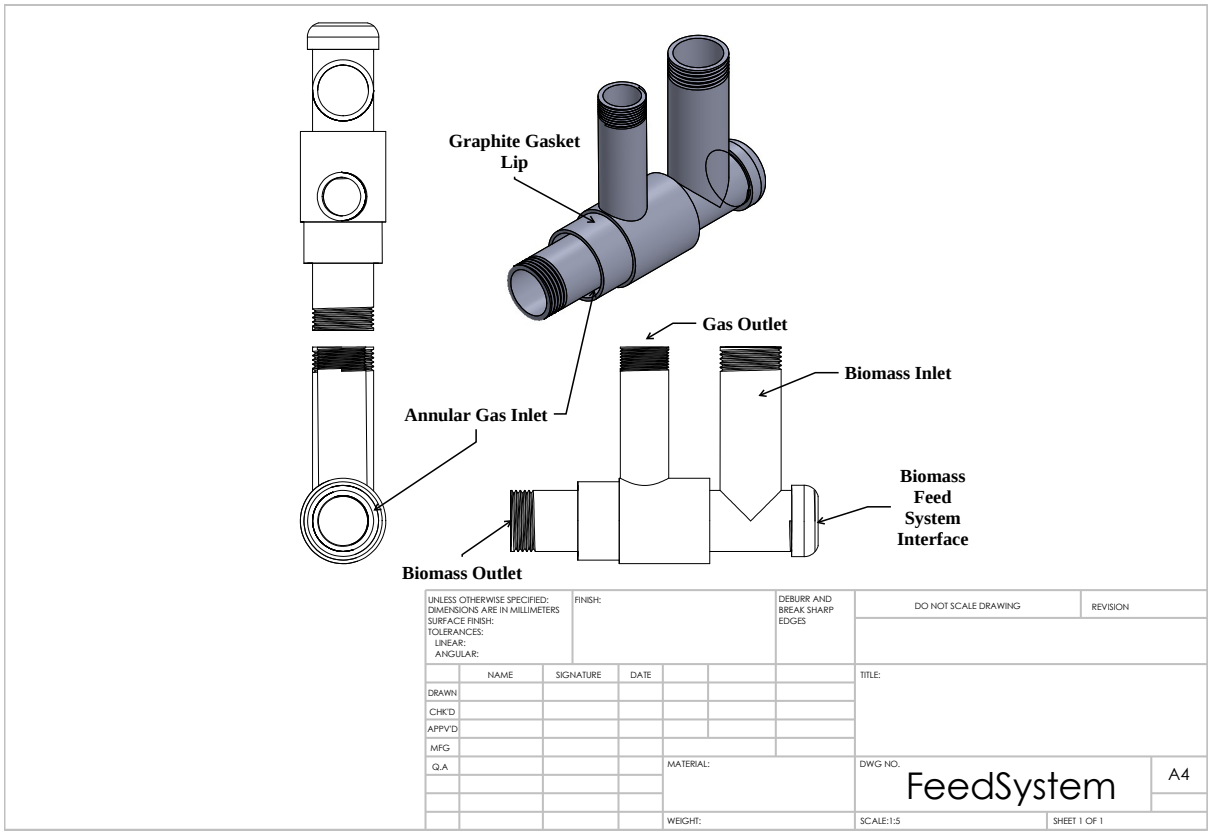

Figure 3.2: Preliminary feed system design.

Preliminary design drawings completed on Solidworks are given as Figures 3.3 and 3.2. The preliminary feed system design given as Figure 3.2 shows the gas outlet and biomass inlet. The annular space indicated shows where the gas flows into the gas outlet and thus around the biomass outlet. The biomass outlet is extended to ensure the biomass is unable to block up the gas outlet when it is introduced to the rotary kiln. It is intended for this system to remain stationary while the kiln tube rotates therefore the indicated lip is designed for graphite gaskets to be mounted thus providing a gas seal which has the ability to spin due to its low friction coefficient. The graphite gasket also acts as a sacrificial component which is easily replaced and relatively low cost. The system should be designed to allow for ease of disassembly to service and troubleshoot. This design is utilised on both prototypes of the reactor system with a few minor modifications.

Figure 3.3 shows the preliminary reactor body design. The Kiln tube, insulating material and the annular space for the heating element are indicated in this drawing. The kiln tube is not fixed to the insulating material and must have the freedom to rotate thus accomplishing the requirements for a rotary kiln. The system should be designed to allow for ease of disassembly to service and troubleshoot. This design is utilised on both prototypes of the reactor systems with a few minor modifications.

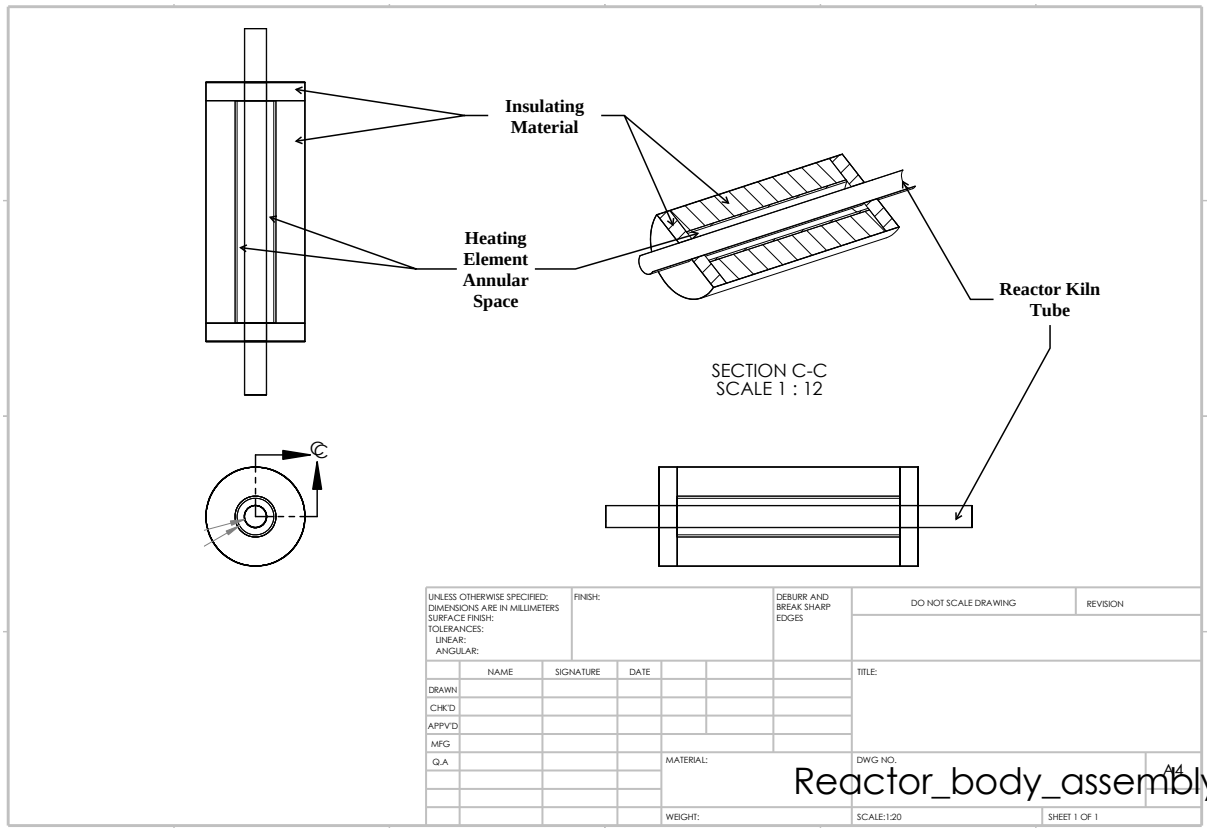

Figure 3.3: Preliminary reactor body design.

3.2.2 Operating Conditions and Products

Based on the principles outlined in Section 2.2 the following temperatures for pyrolysis are from 300 to 550 °C. This is well within the limit of the heating element as well as being firmly in each of the different pyrolysis regimes.

The following experimental plan is suggested to characterise the biomass and the resulting pyrolysis products. The number of experiments is subject to change but the process variables and their possible range are given in Table 3.1

Table 3.1: Process Operating Conditions.

Particle Size (mm)	Temperature (°C)	Rotation speed (rpm)	Kiln Angle (°)
varies	300-550	30-60	5

The conditions outline would be repeated for multiple different biomass sources starting with just three; Eucalyptus wood chips (*Eucalyptus Grandis*), Peanut shells (*Arachis Hypogaea*) and Macadamia shells (*Macadamia Integrifolia*). These sources would need to be fully characterised. Thereafter the biomass can be modified before pyrolysis and the above process variables would be repeated. The proximate analysis and the higher heating values are given in Table 3.2.

Table 3.2: Key feedstock typical characteristics (Heidari *et al*, 2014; Fan *et al*, 2018; Wu *et al*, 2019)

Property	*Eucalyptus Grandis*	*Macadamia Integrifolia*	*Arachis Hypogaea*
Common name	Eucalyptus Wood	Macadamia Nut Shell	Peanut Shell
Moisture (%)	7.9	10.1	5.8
Ash (%)	0.5	2.3	4.3
Volatile Matter (%)	78.2	69.8	76.6
Fixed Carbon (%)	13.4	17.8	13.4
HHV ($MJ\,kg^{-1}$)	19.42	18.78	18.55

Once the ISA is implemented and constructed the same process variables can be manipulated and tested but with the added variable of steam feed rate. These tests would operate at a minimum steam inlet temperature of 850 °C.

3.2.3 Heat Flow and Distribution Investigation

3.2.3.1 Heat Loss to Environment

The pyrolysis tube, at 500 °C, is surrounded by the heating element which is maintained at a temperature of approximately 500 °C. The outer vessel wall surrounding the heating element chamber is of the greatest importance as it must prevent excessive heat loss from the system. The basic wall design is provided in Figure 3.4. In the prototype 1 design the insulation zone consists of a mixture of 10 % concrete and 90 % perlite. In the prototype 2 reactor the insulation zone consists of glass wool. The two materials are compared by determining the heat lost to the environment.

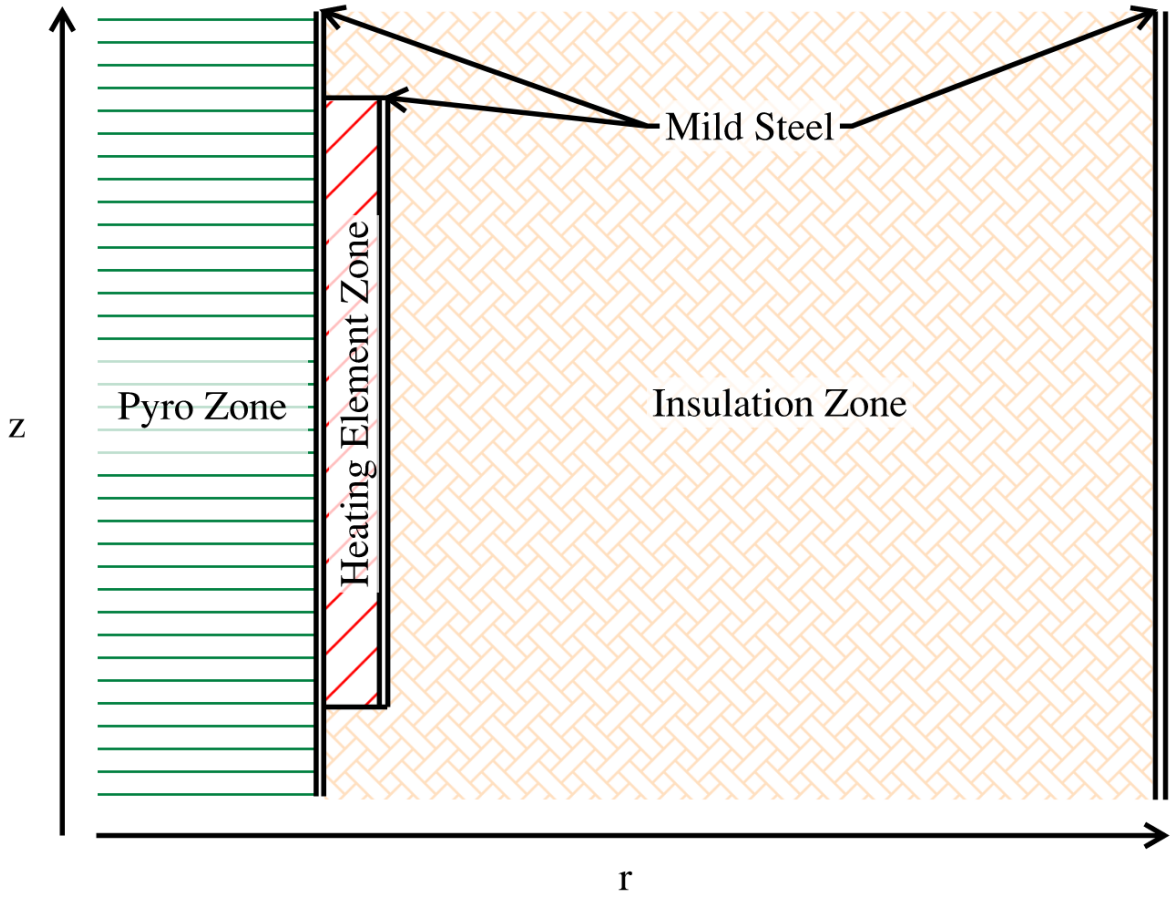

Figure 3.4: Reactor internal wall design.

The resistance coefficient method was used to determine the surface temperatures of the outer wall in order to determine the amount of insulation required to obtain the minimum heat losses (Cengel & Ghajar, 2015).

Equation 3.2 and Equation 3.3 were used to determine radial heat transfer through the outer shell through convection and conduction respectively. The surface area for heat

transfer was calculated according to Equation 3.4.

$$Q_{conv} = hA(T_p - T_w) \tag{3.2}$$

$$Q_{cond} = \frac{kA}{\ln(r_2/r_1)}(T_p - T_w) \tag{3.3}$$

$$A = 2\pi r_1 L \tag{3.4}$$

With the resistance through the material determined according to Equation 3.5.

$$R_i = \frac{ln(\frac{r_{i+1}}{r_i})}{k_i A} \tag{3.5}$$

An acceptable outer wall temperature for the fluidised bed was estimated to be approximately 60 °C for both safety and acceptable heat losses. Thus the material was chosen to match the temperature profile across the wall.

Material	Conductivity ($kJ.kg^{-1}.K^{-1}$)	Thickness (mm)	Heat Loss (W)
Concrete/Perlite Mix	0.17	75	176
Glass Wool	0.0385	75	59

Table 3.3: Material Properties

Using the specified materials and thicknesses the energy loss through the reactor wall is found to be 176 W for the prototype 1 insulation and 59 W for the prototype 2 insulation. Therefore the change in insulating material decreased the energy loss to the environment by 2.98 times. The heat loss from the prototype 2 system approximately 1.07 % of the heating element rated power of 5.5 kW and therefore this insulating material is deemed sufficient.

3.2.3.2 Transient Heat Distribution Model

As part of the development of the reactor an indicative transient heat flux model has been developed. The intention of the model is to inform further improvements, intelligent design decisions and the heat losses of the system to the environment. A heat transfer

model that approximates the behavior of the new experimental rig is of great value as it allows for greater understanding of the system and provides estimates that quantify the impact of changes to the system in the form of multi-dimensional heat transfer. As this system relies almost completely on conduction as the mode of heat transfer, the general heat conduction equation may be modified and implemented to assess the raised concerns.

The general heat conduction equation in cylindrical coordinates (Cengel & Ghajar, 2015).

$$\frac{1}{r}\frac{\partial}{\partial r}\left(r\frac{\partial T}{\partial r}\right)+\frac{1}{r^2}\frac{\partial}{\partial \phi}\left(\frac{\partial T}{\partial \phi}\right)+\frac{\partial}{\partial z}\left(\frac{\partial T}{\partial z}\right)+\frac{e_{gen}}{k}=\frac{1}{\alpha}\frac{\partial T}{\partial t} \tag{3.6}$$

Where ρ and C_p is the density and thermal conductivity of the material through which the heat is transferred (Cengel & Ghajar, 2015).

α is known as the thermal diffusivity of the material through which heat is being transferred can be calculated by Equation 3.7. This allows for easier manipulation of the general heat conduction equations and provides a comparison between the heat that is conducted and heat that is stored in the system.

$$\alpha=\frac{k}{\rho C_p} \tag{3.7}$$

The temperature variation inside the solid annular space along the ϕ-axis is minimal and therefore the conduction term associated with this axis is removed. The experimental analysis is completed on a steady state basis but, to improve the heat transfer model's ability to converge the theoretical model will be transient with a constant heat flux at the inner boundary of the annular space and therefore will only make an appearance at that specific boundary and not within the internal conduction equations. With these assumptions Equation 3.6 the general heat conduction equation for the internal nodes of the cylinder is demonstrated is Equation 3.8 (Lestrange, 2019).

$$\frac{1}{r}\frac{\partial}{\partial r}\left(r\frac{\partial T}{\partial r}\right)+\frac{1}{r^2}\frac{\partial}{\partial \phi}\left(\frac{\partial T}{\partial \phi}\right)+\frac{\partial}{\partial z}\left(\frac{\partial T}{\partial z}\right)=\frac{1}{\alpha}\frac{\partial T}{\partial t} \tag{3.8}$$

The method of finite differences will be used analyse and create the transient heat transfer model. This method approximates the changes of a function over finite steps, thereby approximating the derivative of the function over a specified range. As the size of the step over which the system is approximated becomes smaller, the accuracy of the approximation increases but a relationship exists between the size of the step and computation

time. If a minuscule step is used the computation time will be increased and therefore a compromise has to be struck between the accuracy of the model and the computation time required.

The finite difference method approximations can be calculated using, the backwards difference, central difference and forward difference methods. The three approximations are indicated below respectively for the radial direction of cylindrical coordinates (Welty *et al*, 2008).

$$\frac{\partial T_r}{\partial r} = \frac{T_r - T_{r-1}}{\Delta r} \tag{3.9}$$

$$\frac{\partial T_r}{\partial r} = \frac{T_{r+1} - T_{r-1}}{2\Delta r} \tag{3.10}$$

$$\frac{\partial T_r}{\partial r} = \frac{T_{r+1} - T_r}{\Delta r} \tag{3.11}$$

These approximations can also be extended to higher order partial differential equations as seen in Equation 3.12 for the backwards difference method.

$$\frac{\partial^2 T_r}{\partial r^2} = \frac{T_r - 2T_{r-1} + T_{r-2}}{\Delta r^2} \tag{3.12}$$

This can be expanded for the central and forward difference methods as demonstrated in Equations 3.13 and 3.14.

$$\frac{\partial^2 T_r}{\partial r^2} = \frac{T_{r+1} - 2T_r + T_{r-1}}{\Delta r^2} \tag{3.13}$$

$$\frac{\partial^2 T_r}{\partial r^2} = \frac{T_{r+2} - 2T_{r+1} + T_r}{\Delta r^2} \tag{3.14}$$

3.2.3.2.1 Two-dimensional Model Development

The radial and vertical dimension will be considered for the two-dimensional model. Therefore the general heat conduction equation for the internal nodes shown in Equation 3.8 is reduced Equation 3.15 below.

$$\frac{1}{r}\frac{\partial}{\partial r}\left(r\frac{\partial T}{\partial r}\right) + \frac{\partial}{\partial z}\left(\frac{\partial T}{\partial z}\right) = \frac{1}{\alpha}\frac{\partial T}{\partial t} \tag{3.15}$$

The finite difference method form is found by approximating the partial derivatives using the central difference method for space and backwards difference method for time which are Equations 3.10 and 3.9 respectively. The final finite difference general heat conduction equation is demonstrated in Equation 3.16 below.

$$T_{r,z}^{j} = T_{r,z}^{j-1} + \alpha\Delta t \left(R\,\frac{T_{r+1,z}^{j-1} - T_{r-1,z}^{j-1}}{2\Delta r} + \frac{T_{r+1,z}^{j-1} - 2T_{r,z}^{j-1} + T_{r-1,z}^{j-1}}{2\Delta r^2} \right) + \alpha\Delta t \left(\frac{T_{r,z+1}^{j-1} - 2T_{r,z}^{j-1} + T_{r,z-1}^{j-1}}{2\Delta z^2} \right) \tag{3.16}$$

A two-dimensional model requires four boundary conditions therefore the conditions are as follows. The initial boundary condition occurs along the center of the system next to the cartridge heater which applies a constant heat flux. Therefore a constant heat flux boundary condition is required. Two initial boundary conditions are shown in Equation 3.17 which shows the requirements for the two conditions. Fortunately this apparatus experiences two axes of symmetry in both dimensions and thus the model can be simplified.

$$\begin{aligned} T_0^j &= T_0^{j-1} + \alpha\Delta t \left(\frac{\dot{Q}}{k} + \frac{T_{r,z+1}^{j-1} - 2T_{r,z}^{j-1} + T_{r,z-1}^{j-1}}{2\Delta z^2} \right) \text{ when } r = 0 \text{ and } 0 \leq z \leq L \\ T_0^j &= T_0^{j-1} + \alpha\Delta t \left(\frac{T_{r,z+1}^{j-1} - 2T_{r,z}^{j-1} + T_{r,z-1}^{j-1}}{2\Delta z^2} \right) \text{ when } r = 0 \text{ and } L < z < Lt \end{aligned} \tag{3.17}$$

where L is half of the length of the heating element inside the experimental unit and L_t is the total length of the unit including the material used to insulate the system from the sides.

The convection boundary condition is taken at the external nodes of the apparatus as indicated by Equation 3.18.

$$\begin{aligned} T_{r,z} &= \frac{\frac{\Delta rh}{k}\,T_\infty + T_{r-1,z}}{1 + \frac{\Delta rh}{k}} \text{ when } r = R \text{ and } z = z \\ T_{r,z} &= \frac{\frac{\Delta rh}{k}\,T_\infty + T_{r,z-1}}{1 + \frac{\Delta rh}{k}} \text{ when } r = r \text{ and } z = Lt \end{aligned} \tag{3.18}$$

Equations 3.16, 3.17 and 3.18 may be used to model the behavior of our system.

3.2.3.2.2 Transient Model Results and Discussion

The transient models are used to approximate the systems to an array of operating times of 1 s, 15 minutes, 30 minutes, 45 minutes, 1 hour, 2 hours 45 minutes and the final time of 13 hours 53 minutes. Python was used to create the analysis but as discussed a compromise between model accuracy and computation time has to be made. Table 3.4 indicates the chosen finite steps for the transient models. A simple temperature controller is built into the model, ensuring the element's internal temperature is maintained at the required 500 °C (at point $z = 0$) by terminating the heat generation of the heating element when its temperature exceeds the defined temperature.

Table 3.4: Transient model simulation details.

# Dimensions	Final Time (s)	Δt (s)	Δr (m)	Δz (m)	Figure Number
2-D	1	1	0.006	0.035	1
2-D	900	1	0.006	0.035	1
2-D	1 800	1	0.006	0.035	1
2-D	2 700	1	0.006	0.035	1
2-D	3 600	1	0.006	0.035	1
2-D	10 000	1	0.006	0.035	1
2-D	50 000	1	0.006	0.035	1

Figure 3.5 features the temperature profile in the middle of the reactor when $z = 0$ at the defined time points given in Table 3.4 for the Prototype 1 and Prototype 2 reactors. As one can determine when comparing the identified figures, the Prototype 2 reactor reaches a heating element temperature of 500 °C much faster than that of the Prototype 1 reactor. This is due to the informed decision to reduce the thermal mass of the reactor units which in turn reduces the startup and heating time of the reactor unit. The added benefit of reducing the thermal mass but selecting a Glass Wool as the material of insulation results in the reduction of the conductive heat transfer but an increase in convective heat loss to the environment as the system reaches the steady state surface temperature sooner. This trade-off is beneficial as the purpose of the reactor unit is to complete fast turnaround experiments continuously and not to operate commercially where energy efficiency is paramount for the profitability of the process.

Figure 3.6 features a two-dimensional temperature distribution for the experimental apparatus. The central core seen in Figure 3.6 that does not feature a calculated temperature is the edge of the heating elements and the reactor tube. This model assumes a heating element has a consistent heating profile but this is not always the case as parabolic heating elements are typical for heating elements (de Beer, 2018).

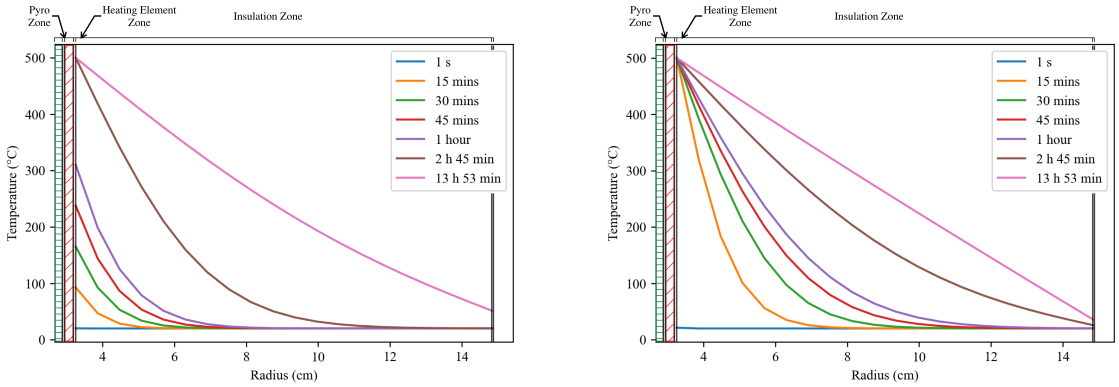

(a) Prototype 1 Perlite/Concrete insulation.

(b) Prototype 2 Glass Wool insulation.

Figure 3.5: Summarised transient heat flux profile development of Prototype 1 (a) and Prototype 2 (b).

The reactor unit is drawn over the figures to show the material which is used to insulate the top and bottom of the apparatus. What we can conclude from Figure 3.6 that as the heat distributes over time the center of the reactor maintains the required reaction temperature for pyrolysis which could indicate that the residence time of the reactor is shorter than expected. Further steps can be taken to ensure the required residence time is achieved for the type of pyrolysis such as baffles or adjusting the kiln tube angle. Figure 3.17 shows the manipulation of the kiln angle as a solution to influencing the residence time of the material within the reactor. This is deemed a more elegant solution when compared to baffles since the internal baffles have the ability to develop blockages in the main reactor tube.

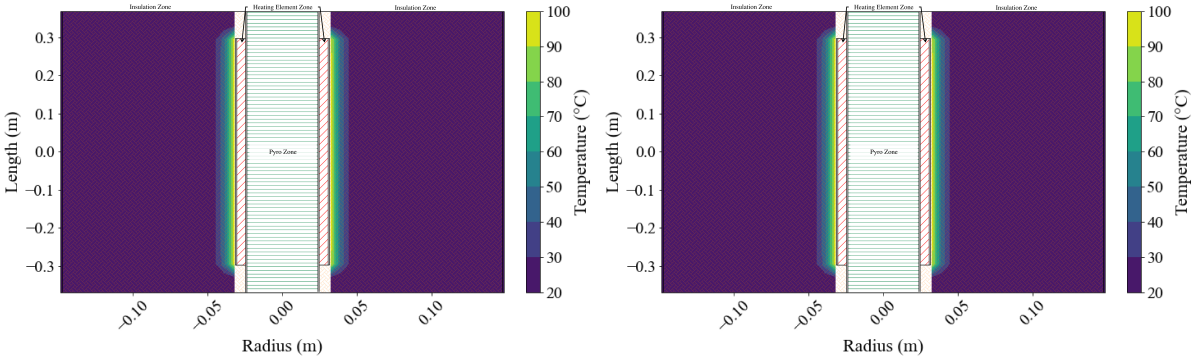

(a) Prototype 1 - 15 minutes.

(b) Prototype 2 - 15 minutes.

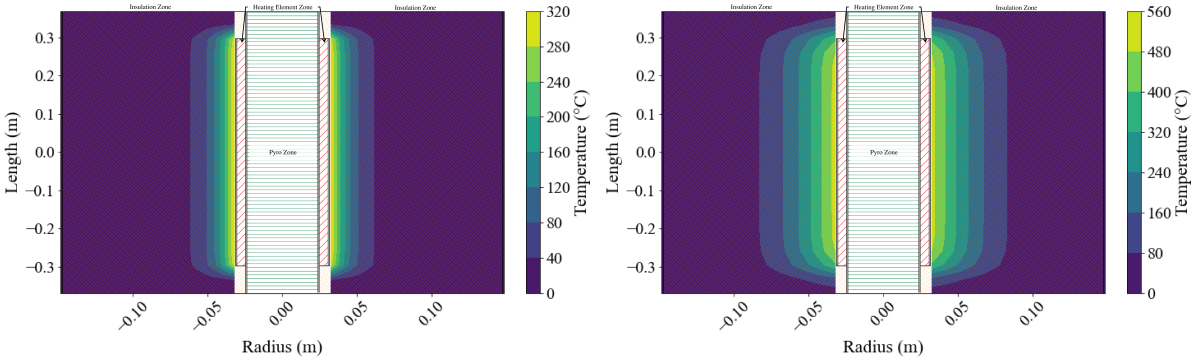

(c) Prototype 1 - 1 hour.

(d) Prototype 2 - 1 hour.

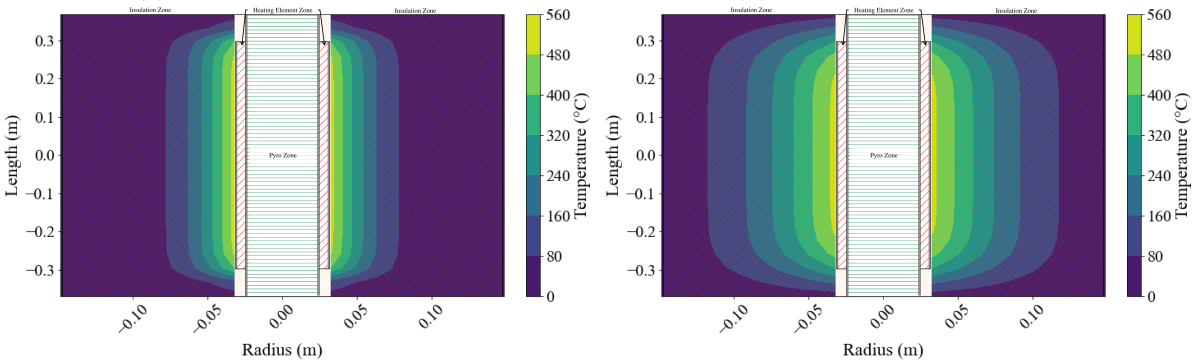

(e) Prototype 1 - 2 hours 45 minutes.

(f) Prototype 2 - 2 hours 45 minutes.

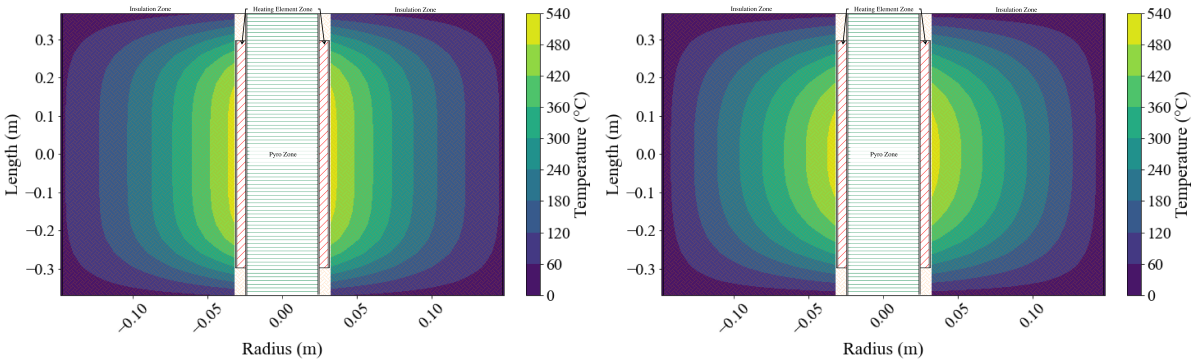

(g) Prototype 1 - 13 hours 53 minutes.

(h) Prototype 2 - 13 hours 53 minutes.

Figure 3.6: Transient Heat Flux map development of Prototype 1 (a) and Prototype 2 (b) at differing points.

3.2.4 Process Design Mass and Energy Balance

Figure 3.7 show the pyrolysis reactor inputs (Energy from the Heating Element, biomass feed stock) and outputs (Non-condensable gases, pyrolysis Vapour, biochar and heat loss to the environment). The biomass is transformed into assumed mass fractions of non-condensable gas, pyrolysis and char as a consequence of the pyrolysis at the set reaction temperature of 500 °C.

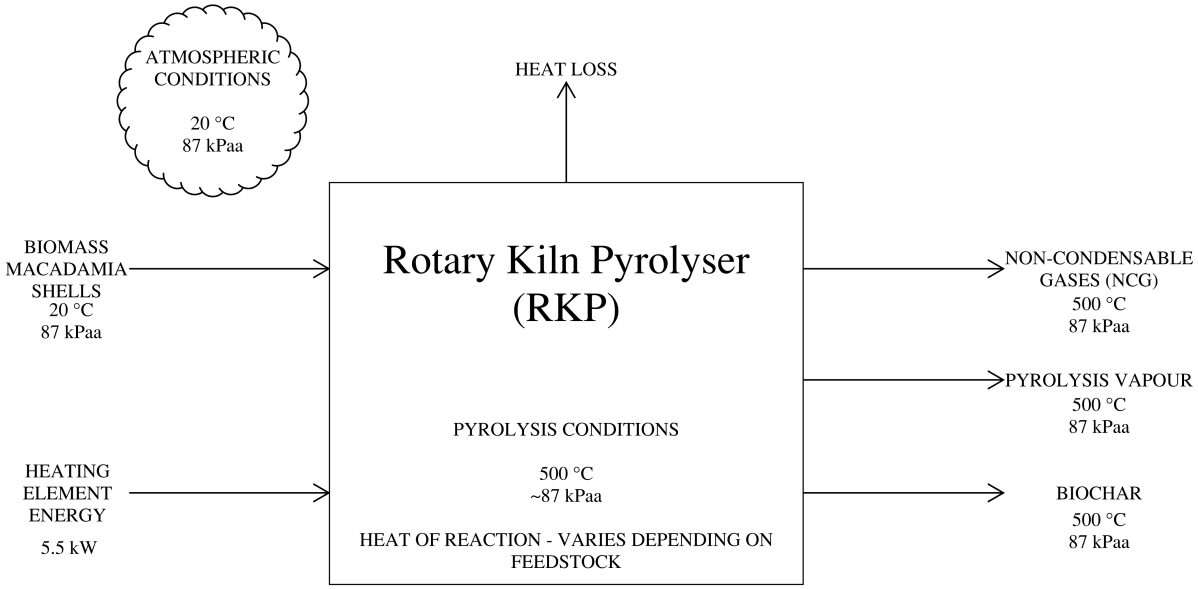

Figure 3.7: Mass and Energy Balance sketch demonstrating inputs and outputs of the Rotary Kiln Pyrolyser (RKP).

The following assumptions are made to assist in the execution of the design Mass and Energy balance for the pyrolysis reactor (Y Wang *et al*, 2018):

1. Dry Macadamia shells are the chosen biomass for this mass and energy balance with a heat of reaction for pyrolysis of $-0.73\,\mathrm{MJ\,kg^{-1}}$.
2. The reactor is at steady state.
3. At Steady state the reactor is evacuated from residual oxygen. Therefore no combustion occurs in the reactor unit.
4. The heating element has a functional power supply of 5.5 kW but it is connected to a temperature controller which maintains its operating temperature to 500 °C and thus only the energy required by the reaction is delivered to the unit and not the full 5.5 kW.
5. The Rotary Kiln Pyrolyser (RKP) Mass and Energy Balance is completed. Further planned expansions are excluded from this analysis.

6. Effect of internal convection on heat transfer through the wall of the reactor is not negligible.

Figure 3.8 shows the culmination of the system Mass and Energy Balance. The Product recovery refers to the NCG and Pyrolysis vapours in the system as per the assumptions. This indicates that biochar is produced and not consumed as per this studies requirements.

Two Cases have been considered in the Mass and Energy Balance. The first case is the maximum theoretical case without combustion where the heating element is utilised 100 % is shown in black dots and produces the limit at which the reactor can operate. The maximum case sized on the max heating input of the heating element (100 % utilisation, plotted in red) results in 6.38 $\mathrm{kg\,h^{-1}}$ of biomass processing which in turn produces approximately 2.02 $\mathrm{kg\,h^{-1}}$. The second case is the experimental case where the biomass flow rate is known is shown on Figure 3.8 as the green square. The flow rate is determined, as per the experiments completed in Section 4, as 1.71 $\mathrm{kg\,h^{-1}}$ which results in a produced biochar flow rate of 0.54 $\mathrm{kg\,h^{-1}}$ at a heating element utilisation of 29 %plotted in blue. The demonstration of the two identified cases on Figure 3.8 shows that the experiments completed operate within the maximum theoretical operation without combustion and follow the initial maximum design case.

While the maximum design case has in turn set the maximum biomass inlet flow to the system it does not consider the physical restrictions and limitations which exists for the system. Therefore it remains a theoretical maximum but it is not an operational maximum which is expected to be much lower flow rates.

A further sensitivity for the auto-thermal operation of the reactor can be completed with the following assumptions (Shoaib *et al*, 2018):

1. For the purposes of completing a sensitivity the higher heating values of NCG is approximately 62.4 $\mathrm{MJ\,kg^{-1}}$.
2. For the purposes of completing a sensitivity the higher heating values of Biochar is approximately 31.3 $\mathrm{MJ\,kg^{-1}}$.
3. For the purposes of completing a sensitivity the higher heating values of Pyrolysis Vapour is approximately 21.0 $\mathrm{MJ\,kg^{-1}}$.
4. For the purposes of completing a sensitivity the gases will combust preferentially to that of biochar due to improved mixing with oxygen.

The auto-thermal energy surplus point via combustion is determined by the sensitivity completed and is also demonstrated on Figure 3.8 as a vertical orange line. This line is approximately 86 % thus indicating the reactor will be self sufficient of its energy requirements if approximately 14 % of the gaseous pyrolysis products (NCG, pyrolysis vapour) are combusted. If one were to include the biochar in the combusted products less "product" would be required to meet the energy surplus point.

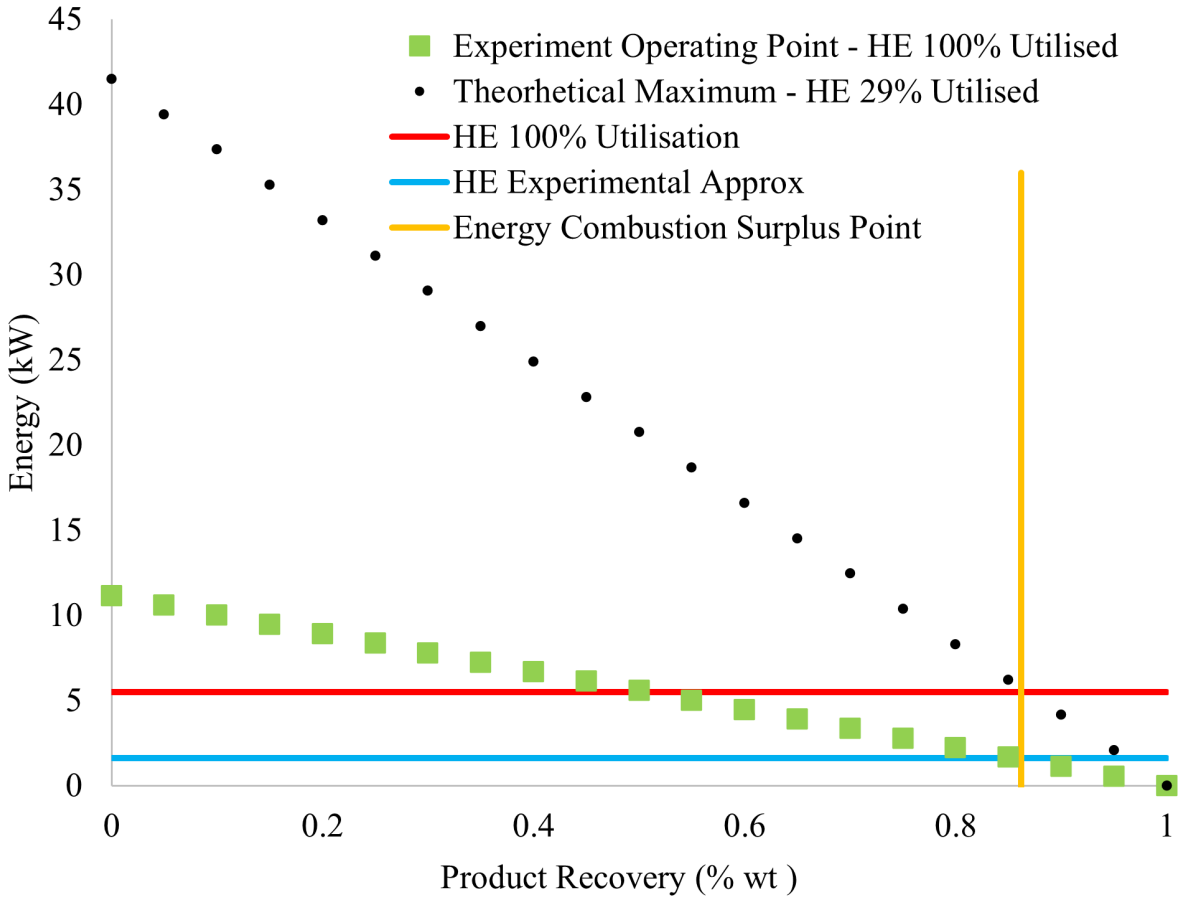

Figure 3.8: Mass and Energy Balance representation.

3.2.5 Design of Experiments (DoE)

3.2.5.1 Key Independent Process Variables

The development and design of the ISA-RKP allow the operator to manipulate a variety of process variables which may impact the final characteristics and yields of the pyrolysis products. The impact of common process parameters has been briefly discussed in Section 2.7 based on published experimental work. The performance and optimisations which the

ISA-RKP introduces are required to be quantified which can be achieved by investigating the impact of the key process parameters.

There exist a multitude of different process parameters which can be investigated but the effect of the following key process parameters are chosen to be determined first due to their already identified impact on the characteristics of the pyrolysis products. The feedstock, process temperature and a reactor-specific optimisation in the form of in *situ*-activation are chosen as the key factors which should be considered which impact the final properties of the produced biochar. The residence time within the reactor shall be kept constant by ensuring the angle and the rotation of the reactor tube is held constant throughout the experiments. The pretreatment of biomass will not be controlled and therefore a "neat" biomass shall be introduced.

The chosen independent variables are expected to impact the properties of the final biochar product which are discussed in depth in Section 2.8.

Three biomass feed-stocks are chosen due to their availability and prevalence as common waste materials; *Eucalyptus Grandis* wood chips (paper industry waste) - EG, *Macadamia Integrifolia* shells (agricultural waste) - MS, and *Arachis Hypogaea* shells (agricultural waste) - PS.

The internal temperature within the ISA-RKP at the initial steady state before the feed is set to vary between a minimum value of 300 °C to a maximum value of 500 °C. The lower limit is chosen due to it being the beginning of pyrolysis regimes. The upper limit is chosen due to the design temperature limit of 600 °C of the coiled heating element.

High temperature (850 °C) steam can be introduced into the pyrolysis zone of the ISA-RKP which can provide further reduction and therefore activation of the produced pyrolysis products. The steam flow rate is to be maintained at a set value and for simplification it will be compared with no in-*situ* activation and traditional batch steam activation. The summary of the key process variables to be considered is provided in Table 3.5.

Table 3.5: Key Independent process parameters to be investigated.

		Factor Level		
Factors	Unit of Measure	1	2	3
Feed-stock	-	EG	MS	PS
Temperature	°C	300	400	500
Activation Method	-	In-*situ*	Neat	Batch

3.2.5.2 Factorial design

Full factorial design is utilised when the effect of the identified independent variables should be fully quantified from not knowing the impact of the variables at all.

Factorial experimental design is an effective and efficient method which can be utilised to quantify the impact of multiple variables using fewer isolated experiments. This method can only be utilised if there exist at least two independent parameters. The following advantages of factorial experiments are provided below.

- Factorial designs are more efficient than one-factor-at-a-time experiments.
- Factorial design allows for additional factors to be examined at no additional cost.
- Factorial designs allow the effects of a factor to be estimated at several levels of the other factors, yielding conclusions that are valid over a range of experimental conditions.

Factorial experiments work on two important considerations. The number of variables and how many different options those variables can utilize. As we can see from Table 3.5 above there exist three *factors* which need to be quantified. For each *factor* there exist three discrete *levels*. Therefore to investigate the impact of these simple variables the number of experiments required for a full factorial design is 3^3 which results in the 27 experiments provided in Table 3.6.

3.2.5.3 Box-Behnken Experimental Design

Box-Behnken design is a response surface design technique that is frequently used in the Design of Experiments (DOE) to create models that show the connection between a response variable and predictor variables. This design incorporates three different levels of the predictor variables, which are often set to -1, 0, and +1. By evenly distributing these variables within the range of (-1, +1), and adding a center point at level 0, the design estimates the error variance and verifies the model fit.

This design is a variation of central composite design (CCD), as it allows for the estimation of second-order models with three factors, and requires fewer runs than a CCD. The Box-Behnken design can estimate the main effects and two-factor interactions of the predictor variables and typically requires fewer runs than a full factorial design.

Table 3.6: Full factorial experimental design.

Experiment Count	Temperature (°C)	Feed-stock	Activation Method
1	300	EG	N
2	400	EG	N
3	500	EG	N
4	300	MS	Y
5	400	MS	Y
6	500	MS	Y
7	300	PS	SA
8	400	PS	SA
9	500	PS	SA
10	300	EG	N
11	400	EG	N
12	500	EG	N
13	300	MS	Y
14	400	MS	Y
15	500	MS	Y
16	300	PS	SA
17	400	PS	SA
18	500	PS	SA
19	300	EG	N
20	400	EG	N
21	500	EG	N
22	300	MS	Y
23	400	MS	Y
24	500	MS	Y
25	300	PS	SA
26	400	PS	SA
27	500	PS	SA

The Box-Behnken design comprises of a set of experimental conditions, each involving predictor variables at different levels, grouped into "blocks." The response variable is measured for each block, and the resulting data is used to estimate the coefficients of a second-order polynomial equation to model the connection between the response variable and the predictor variables.

This design is most appropriate when the connection between the response variable and predictor variables is expected to be smooth and without sharp curves or discontinuities. It is commonly used in chemical and process engineering, but it can be utilized in any field where DOE is used to optimize a process or system.

Table 3.7: Box-Benhken experimental design.

Experiment Count	Temperature (°C)	Feed-stock	Activation Method
1	300	EG	Y
2	500	EG	Y
3	300	PS	Y
4	500	PS	Y
5	300	MS	N
6	500	MS	N
7	300	MS	SA
8	500	MS	SA
9	400	EG	N
10	400	PS	N
11	400	EG	SA
12	400	PS	SA
13	400	MS	Y
14	400	MS	Y

3.3 Construction

3.3.1 Rotary kiln pyrolyser construction (RKP)

The synthesis of biochar is relatively simple as discussed, but the wide range of process conditions that result in effective but broad final product properties can be considered a design problem.

Biomass is known to have different properties that affect the final characteristics of the biochar produced. Biomass as a feedstock material imposes multiple problems due to its inherent properties. The solids handling of biomass is extremely important when considering the design of a biochar-producing system. Bridging biomass is a common problem that can lead to a plant shutdown due to the clogging of a process line. The biomass particles compress and form an amalgamation of lignocellulosic feed material that has to be removed. This can not only cause unexpected downtime but also damage process equipment. Bridging is a function of particle size, feed rate as well as pipeline inner diameter. The smaller the biomass feed particles the greater the chance of bridging. This problem must be considered when designing and testing the bench scale pyrolyser.

The internal diameter of the RKP is chosen to be large enough to ensure bridging will not be a problem for nominal feed rates but small enough to ensure that mixing within the tube and heat transfer are effective. The larger internal diameter also allows for a wide range in the particle size of biomass fed to the system.

A 5.5 kW custom-made heating element surrounds the kiln tube in the RKP. The heating element provides the energy required to heat the system to the required temperatures, but it has a limit of 600 °C. If an operation higher than this is achieved, there is the risk of irreparable damage being done to the heating element. The heating element is shown in Figure 3.9.

Figure 3.9: 5.5 kW Heating element, inside the insulation (top left), external to the reactor (top right) and curled around the kiln tube (bottom).

Figure 3.10 shows a compilation of the construction of RKP insulation. The order of materials from outer to inner are as follows; paint can, perlite/concrete mix, outer steel pipe. The inner tube through which the biomass is converted to its pyrolysis products and the completed insulation. The outer shell is painted with matt chalk paint to ensure the infrared temperature sensor can accurately read the wall temperature of the vessel at any point. This can be seen in the final presentation of the design of the prototype.

The first prototype had numerous issues relating to reliable operation which are listed below:

- The support structure of the reactor system required further reinforcement which would add weight to an already extremely heavy reactor due to the chosen insulation

Figure 3.10: RKP Construction 1.

material.

- The rotation system was unreliable in terms of power delivery through the chain system and the power availability. This can have negative effects on the repro-

ducibility of experiments completed on the system. Flexing of the reactor frame and rotation motor mount is common during operation. The system was susceptible to the thermal expansion of the components which made operation at reaction temperature difficult.

- Feed system design is prone to bridging which is difficult to correct due to the complexity of the system. The feed system does not allow for the introduction of differing biomass particle sizes and only is applicable for fine particle sizes.
- The product system design added unnecessary complexity to the system and did not add value.
- The kiln length of the system between the feed system and the pyrolysis zone was too short. This leads to pyrolysis occurring in the feed system which further disrupts and introduces operational challenges.
- The kiln tube diameter was not nominal material and therefore gaskets are required to be specifically manufactured for this system.

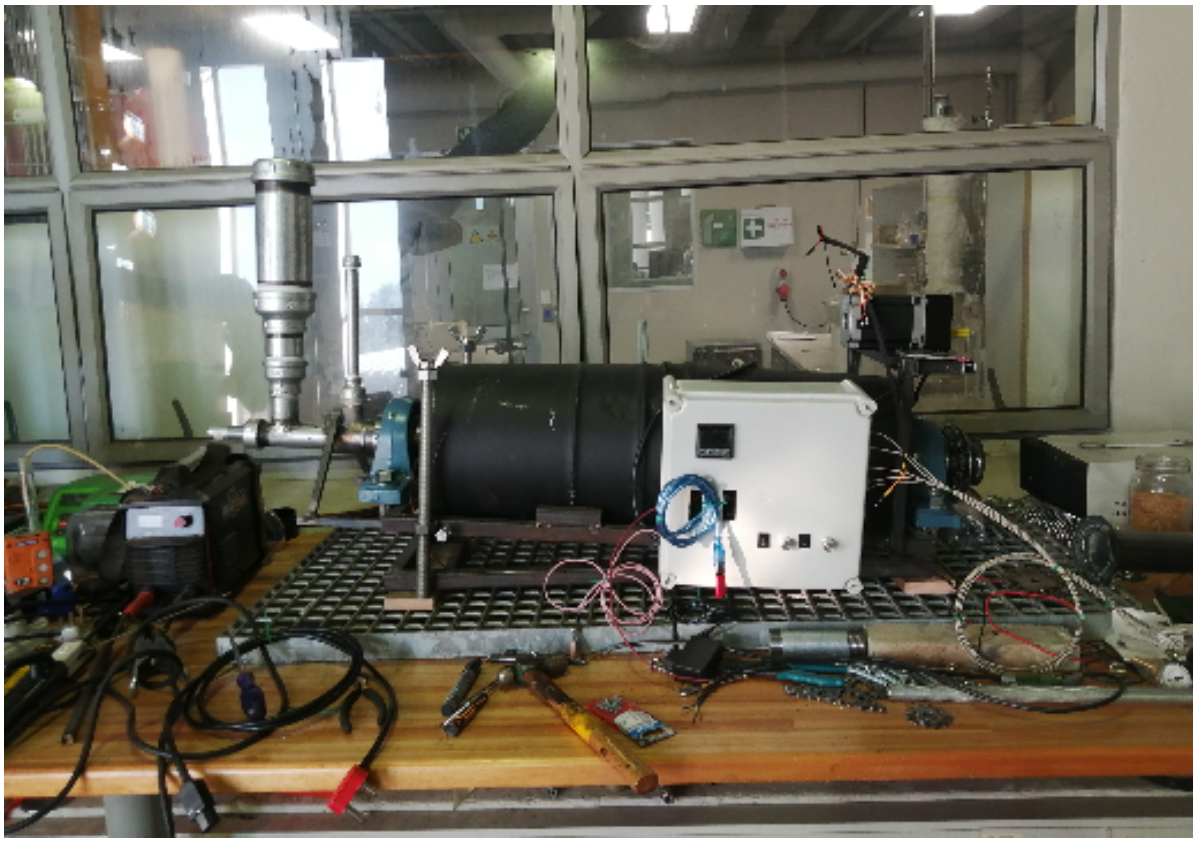

Figure 3.11: Prototype 1 system.

Following the trial and error method of development, the second prototype of the rotary kiln pyrolyser maintains the successful design considerations and removes the items which added complexity but did not add value or improve the reactor operation. The following areas were identified to have lessons learnt and the outcomes of these lessons are implemented in the new design.

The largest lesson learnt in the design and construction of the first prototype is that simplicity is best and complexity can be added to a system after its basic function has been achieved. With this in mind, the new design of the rotary kiln pyrolyser is more focused on achieving reliable operation of its components to produce biochar. The following items were reconsidered and designed according to their purpose. The items identified can be further noted in Figure 3.12. The feed system was simplified to a simple push system which was resealed after feed of the biomass was complete. Included 2 x thermocouple insertion points to read the temperature in the Pyrolysis zone. The product system was simplified to be open to the atmosphere relying on the reactor over pressure created by the pyrolysis vapours. The open end allows the measurement of the pyrolysis zone exit. The rotation system was simplified and reinforced which negated the effects of thermal expansion of the reactor components thereby allowing ease of operation at reaction temperature. The reactor frame and mounting were Reinforced and extended for a longer kiln tube length. The reactor insulation was simplified to glass wool insulation which allows access to the heating element tube as it is removable and light. The kiln tube length and diameter were made longer to increase the distance between the pyrolysis zone and the feed and outlets.

During the commissioning of the second prototype reactor, some areas of concern were identified which are discussed in Section 3.4.2. Analysis of the products was completed and it was determined that the reactor was not performing as expected and the conversion of the biomass to the required quality was not being achieved. Thus the requirement for further modification of the reactor was required. The following modifications were made to the second prototype. The section of the kiln tube from the pyrolysis zone to the gas outlet was insulated to reduce condensation as shown in Figure 3.13a. The length of the outlet kiln tube was greatly reduced and thus the product system at the reactor outlet required modification. The length of the kiln tube removed is shown in Figure 3.13b.The steam injection line which forms part of the ISA was insulated to ensure the steam does not lose too much heat as shown in Figure 3.13b. The operating temperature of the preheating furnace for this stream was further increased to 120°C.

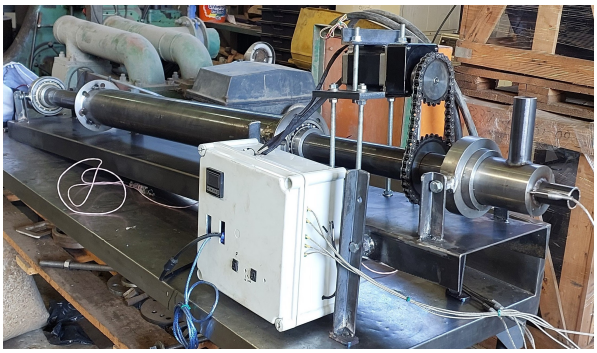

(a) Without insulation.

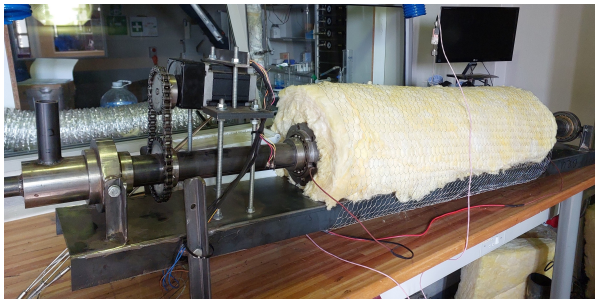

(b) With insulation.

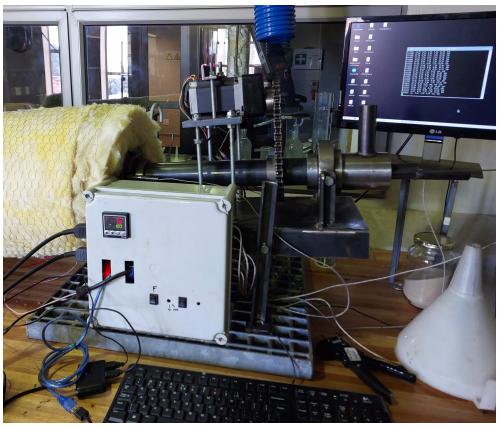

(c) Feed side.

(d) Product side.

Figure 3.12: Reactor Prototype 2.

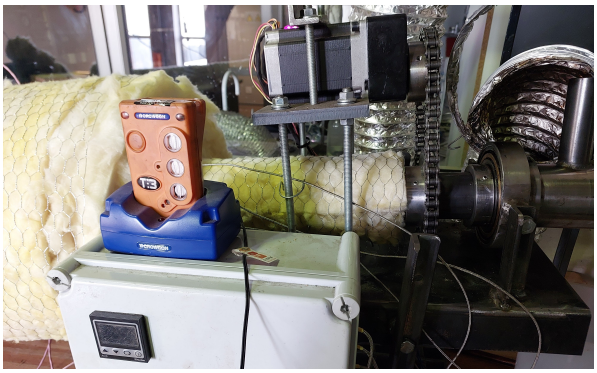

(a) Feed side.

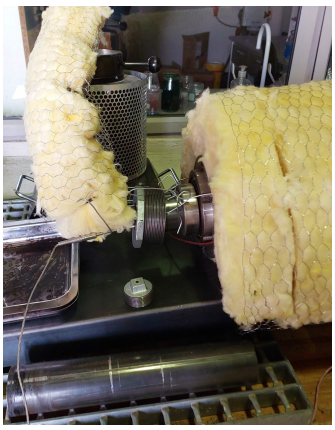

(b) Product side.

Figure 3.13: Prototype 2 feed side and product side modifications.

3.3.2 Electronic control boxes

Waterproof housing that features the heating element temperature control system and two DC variable switches that can reverse the rotation and control the speed of the feed motors. Two override switches were considered, but the incorrect type of switch was purchased and therefore would not be able to supply the required amperage without failure. The override switches are to be included in future improvements as they would greatly assist with the unit's controllability. There were old versions of the electronic control box and the rotation mechanisms, but over time they have been replaced with better options.

The Raspberry Pi provides the human-machine interface and can either have traditional input and output peripherals or can be accessed via a shared wireless network. The Raspberry Pi receives a stream of serial data from the Arduino Leonardo which it parses, displays, and then stores onto the 64 GB Sandisk removable storage device. The Raspberry Pi allows the process operator to start and stop the process and monitor the results live while the process is operating. The current measurement is run through a Python script in the Raspberry Pi kernel and can be stored on the 64 GB SanDisk removable storage disk to be analysed at a later time.

The Arduino is the sensor interface that supplies and collects the data required to run the various pieces of equipment. 5 x K-type thermocouples that are converted from an analogue signal to a digital signal by MAX31855 chips. The MAX31855 is a thermocouple-to-digital converter (TDC) and supplies the information through the serial data interface (SPI) method. The temperature measurement and compounding are completed by the Arduino Leonardo, and the information is supplied to the Raspberry Pi in the form of serial data where it is stored. The data can be downloaded from the Raspberry Pi without the removal of the memory stick via file transfer protocols but the process operator has the freedom to access the data by removing the memory stick if they so wish to complete the analysis.

The rotation speed of the rotary kiln can be set and controlled via an A419 stepper motor driver and a Nema-34 stepper motor with a 3:1 gearbox which is supplied by a 12v 5A DC power supply. This combination provides the required torque at low revolutions per minute to allow adequate residence time of biomass feedstock within the rotary kiln. The adjustable angle combined with the plasticity of this system allows the process operator to investigate the influence of these process parameters on the overall process.

The heating element temperature control system is comprised of three main components. A type N thermocouple in physical contact with the heating element provides the tem-

perature of the heating element to the temperature controller (ACS Shinho) which then provides 12VDC voltage to the steady state relay. The steady-state relay closes the internal switch utilizing the electromagnet and this allows 240VAC to flow to the heating element thus heating the system. This system has large areas for improvement, the biggest concern is that of one thermocouple measuring the temperature of a specific point on the heating element and this introduces the problem of unknown hot spots.

The electronics and the heating element each feature an independent power supply and therefore if one system encounters a fatal flaw the other systems can be shut down safely. This also ensures that the power requirement of each system is separated so that the plug does not pull an extremely high current. The chosen kettle plugs feature space for a fuse which may be beneficial to ensure an automatic shutdown of the system if a failure occurs. Currently, this is not implemented.

The variety and scope of the process variables that are available for the process operator to control using the designed and constructed control system ensures that the system can be used to complete a multitude of studies and the impact of individual process variables can be identified and characterised. If the connection between a desired product property can be quantified the process can be optimised for the creation of the property which would be extremely powerful for further research in bioprocessing.

Figure 3.14 is annotated and features all of the information given in the description above.

The electronic control box is maintained between the prototypes and therefore no further discussion is required for Prototype 2.

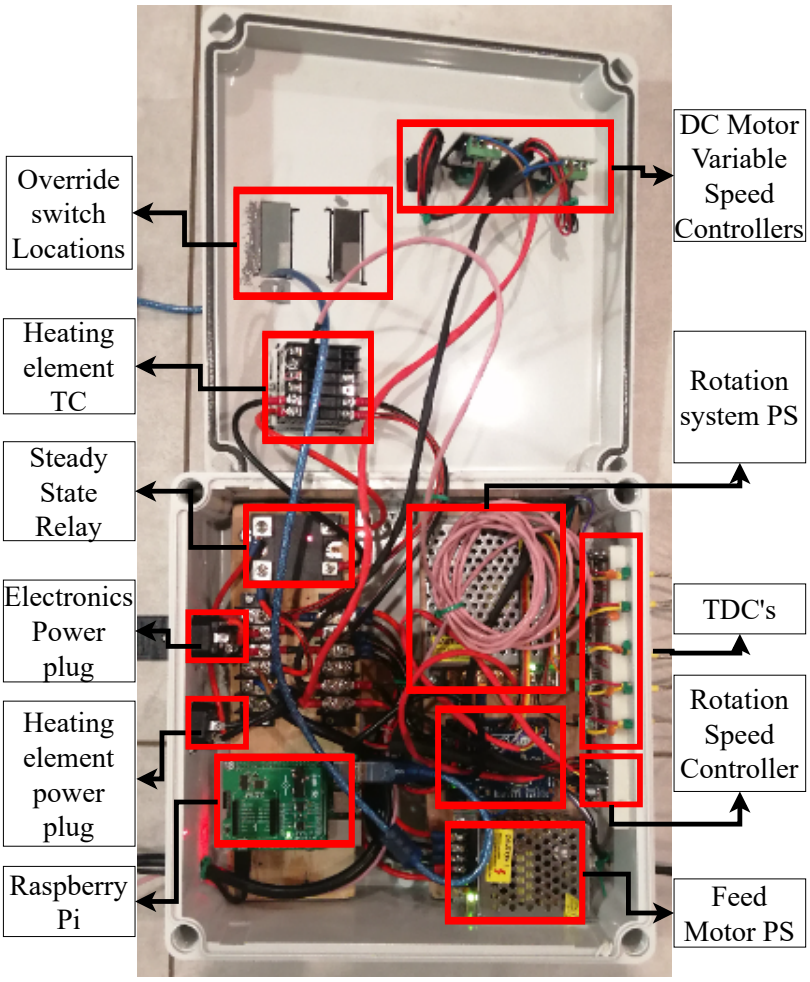

Figure 3.14: Electronic box annotated internals.

3.3.3 *In-situ* activation (ISA)

The *in-situ* activation (ISA) system is comprised of a peristaltic pump, a preheating furnace, and a 2.5 mm stainless steel coil that resides in the same zone as the heating element and feeds counter current into the RKP system, thus feeding the reducing agent into the pyrolysis zone and thereby activating the pyrolysis products as they are being produced.

This system has the potential to not only reduce the processing time but also improve the final quality of the produced biochar. The higher temperature introduced by the steam and the creation of a reducing environment indicates that the biomass feedstock could be further converted. A great concern is that of the increased velocity of the gasses within the rotary kiln and whether this would create entrainment of solid particles. The reducing agent is chosen to be distilled water for its availability, purity and safety when

compared to other common reducing agents. One should note that in using water as the reducing fluid will produce syngas as a resultant and therefore the flammability of the effluent stream should be monitored.

This system was not implemented in Prototype Reactor 1 but it was included in Prototype 2 as shown in Figure 3.12d. The furnace was initially set to 850 °C as that was the desired target steam temperature with a liquid flow rate of 0.121 mL min^{-1} which results in a steam flow rate of approximately 121 mL min^{-1} (volume change of approximately x1000). The operating temperature was chosen due to it being in the correct range for the activation of biochar via reduction and the flow rate was selected as it provided suitable sweep gas velocities and did not introduce the entrainment of solid particles.

Post the commissioning of prototype 2 the following issues were identified. This temperature setting of the furnace did not account for the heat losses the system experienced and therefore there would be condensation which would create condensate slugs and introduce momentum issues to the system in combination with the peristaltic pump's natural pulsation. The condensate introduction to the pyrolysis zone would reduce the temperature of the rotary kiln thereby negatively impacting the conversion of biomass to biochar. To resolve these problems, the steam outlet line was insulated with glass wool, as shown in Figure 3.13b, and the temperature setting of the Furnace was set to 1200 °C which enabled the measured discharge steam temperature of approximately 850 °C.

3.4 Commissioning

3.4.1 Inert commissioning

The commissioning of the first prototype system was completed using inert feed material to begin to understand the energy inefficiencies of the system and the potential operating conditions for effective and safe operation. Figure 3.15 shows the internal temperatures measured by the system over time accompanied by the heating element temperature. The measurement was taken from the very beginning of the system startup to quantify the expected start-up for future runs.

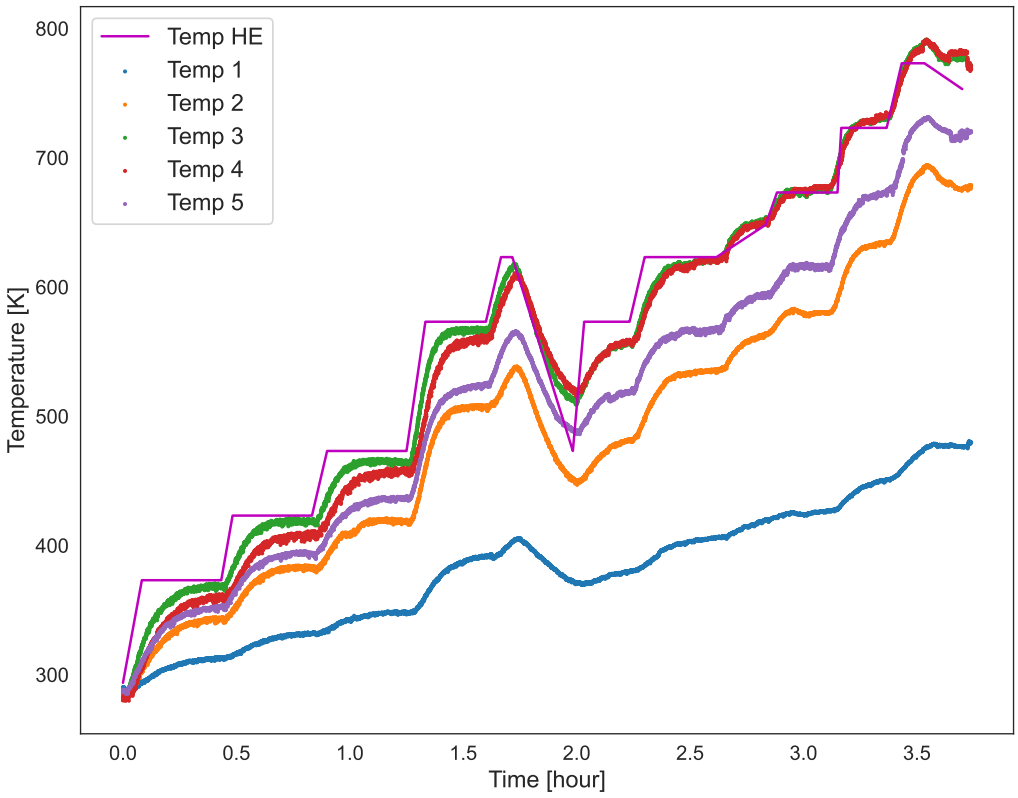

Figure 3.15: Internal kiln temperature vs time.

The thermal images provided in Figure 3.16 highlighted the heat loss areas on multiple parts of the prototype 1 reactor. Water was present in the insulation and steam began to exit the RKP from the show hot spots when $T_{element} = 300$ °C. This prompted the sudden decrease in heating element temperature given in Figure 3.15 at 1.5 hours into the inert commissioning. The thermal images are of the feed system (left-hand side), the

centre of the reactor where the two halves connect, and the biochar collection (right-hand side), respectively. The final two images in Figure 3.15 are of the entire reactor from afar; take note that the electronic box blocks part of the reactor.

High-temperature inert commissioning was not completed on the second prototype due to a mature understanding of the operation and challenges of the system. Furthermore, the materials of construction of the second prototype do not introduce complexities of trapped water and therefore the danger introduced by the release of entrapped steam is greatly reduced. Due to this, the commissioning of the system was completed by proceeding with the experimental pyrolysis runs as discussed in Section 3.2.5.

Post the modifications to the prototype 2 reactor low temperature inert commissioning was completed by feeding Macadamia shells to the reactor. The rotation speed on the kiln tube was kept constant at 10 RPM (120 steps per second). The kiln angle, first product out and last product out were all measured to determine the relationship between the kiln angle and reactor residence time was completed to ensure proper mass transfer is achieved through the reactor tube. Figure 3.17 shows the ability to increase or decrease the residence time within the reactor by influencing the angle of the kiln tube. As the kiln angle is reduced the longer the residence time of the material is. The kiln angle of 5.2° was utilised for these analyses due to the mounding of feed material at the entrance of the pyrolysis zone. The mounding has the potential to block the gas discharge from the pyrolysis zone and a steeper kiln angle reduces this effect. At higher kiln angles the mound of feed material has the potential to push towards the inlet of the system thereby interfering with the graphite gasket and thus making the rotation of the system difficult. The risk of this occurring can be further reduced by increasing the length of the feed tube and introducing a mesh in the gas space of the feed system to stop biomass from entering the area.

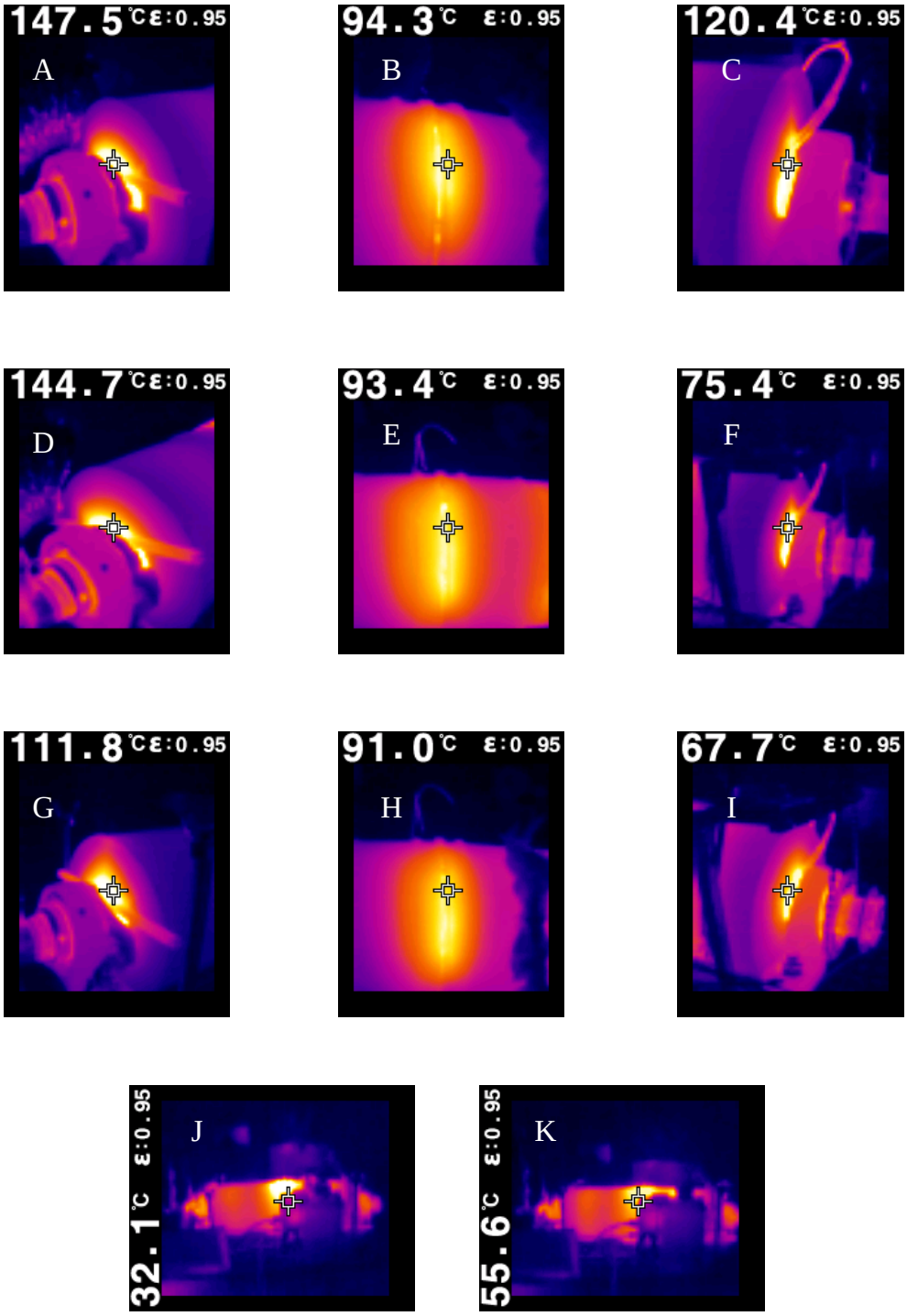

Figure 3.16: Thermal images of inert commissioning at multiple heat loss locations on Prototype 1 reactor. The temperatures on the inlet- (A, D and G) and outlet-sides (C, F, and I) of the rotary kiln inner shell at its interface with the insulation material were monitored and were indicative of insufficient insulation showing temperatures of 147.5°C (A), 120.4°C (C), 144.7°C (D), 75.4°C (F), 111.8°C (G) and 67.7°C (I).

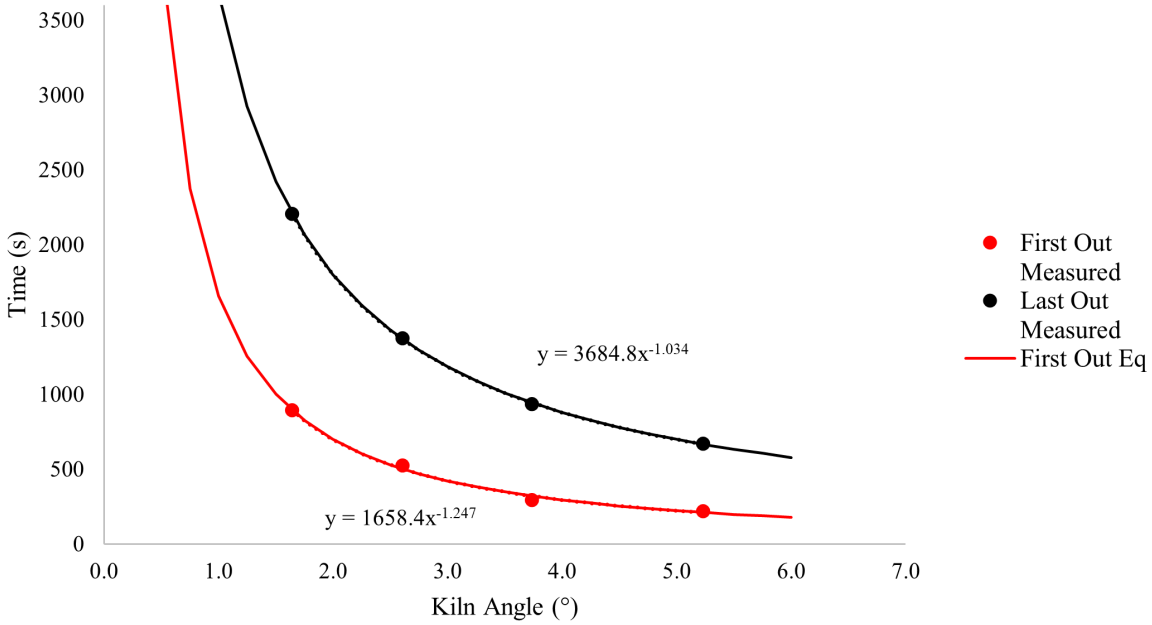

Figure 3.17: Prototype 2.1 Kiln angle vs residence time.

3.4.2 Pyrolysis commissioning

Once the initial inert commissioning was completed, the first prototype reactor remained at the final operating conditions of $T_{element}$ = 500 °C. Woody biomass in the form of *Eucalyptus Grandis* was charged into the biomass reservoir. The rotation stepper motor was set to 100 steps per second which translates to 30 rpm of the kiln tube. The woody biomass was fed to the reactor and pyrolysis began. Figure 3.18 shows the pyrolysis commissioning of the prototype 1 system at steady-state. The product side of the reactor (Figure 3.18.A) is shown next to the feed side of the reactor (Figure 3.18.B). We can also note the colour of the produced vapour in Figure 3.18.B is yellow and not grey/white. This indicates the pyrolysis vapour being entrained in the gas stream which further supports that pyrolysis was achieved during commissioning.

Four concerns were raised by the pyrolysis commissioning; The feed reservoir can be clogged easily so a much larger particle size is suggested. Uniform biomass chips greater than 2 mm to a maximum of 5 mm would flow best. The pyrolysis vapour and NGC should include as little resistance to flow as possible. As shown in Figure 3.18 the restriction had to be removed to ensure that the system did not leak pyrolysis vapour from the various gaskets. Fume extraction methods should be improved. The fourth and arguably the largest concern was the reliability of the reactor. During the pyrolysis commissioning of the reactor, there are constant breakdowns of the rotation system which is crucial for the operation of the system. Multiple modifications and attempts were made to improve the

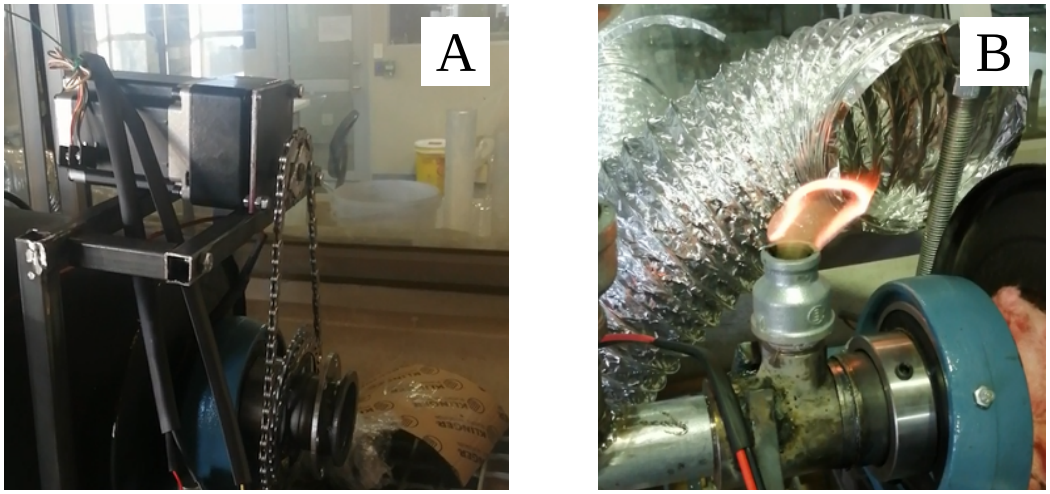

Figure 3.18: Pyrolysis commissioning of product side (A) and feed side (B) of the prototype 1 reactor. The flame and vapour demonstrated in Figure B show we are generating a combustible gas from the pyrolysis unit and sustaining a flame thus indicating continuous conversion. There is no flame within the reaction tube and thus we are achieving an anoxic atmosphere.

rotation system but ultimately the requirement for a next prototype became clear where the rotation system could be redesigned and made reliable.

Fortunately, all of the concerns are addressed in the second prototype of the reactor. The first concern is solved in Prototype 2 by increasing the size of the feed tube and returning to a simplistic push rod manual loading system. The reduced complexity ensures feeding problems can be quickly resolved by the operator. The second issue is solved in Prototype 2 by featuring an increased gas exit line size and insulation up to the feed system which reduces heat loss and therefore condensation in the gas portion of the system. The last concern is solved by improvement to the lab conditions where an extraction hood extension to the gas exit allows for proper fume extraction. The final concern is perhaps the greatest achievement of the second prototype reactor. The rotation system is reliable due to its complete redesign and reinforcement.

Prototype 2 pyrolysis commissioning was approached by performing the experimental runs as originally identified in Section 3.2.5. The runs completed are given in Table 3.8

The pyrolysis commissioning of the system was completed by proceeding with the experimental runs featured in Figure 3.19 and Table 3.8. The pyrolysis commissioning of Prototype 2 covers a large portion of the potential operating conditions of the system as demonstrated in Figure 3.20. Figure 3.20 is divided into three different regions; the Heating Element Temperature readings, the Pyrolysis zone temperature readings and the miscellaneous temperature probe readings used to check key points on the apparatus and

Table 3.8: Prototype 2 pyrolysis commissioning runs.

Experiment Count	Temperature (°C)	Feed-stock	Activation Method
1	400	MS	Y
2	400	EG	N
3	300	MS	Y
4	300	MS	Y
5	300	EG	Y
6	300	MS	N

the ambient conditions. In the execution of the pyrolysis commissioning of Prototype 2, it was noted that the internal pyrolysis feed inlet temperature was lower than expected. Thus the focus shifted from completing the experimental work identified in Section 3.2.5 and rather to identifying the operating capabilities of the reactor. To do this the reactor is required to be operated at its maximum process conditions which can therefore inform on the potential of the reactor. From this information, further suggestions and improvements can be made to the system.

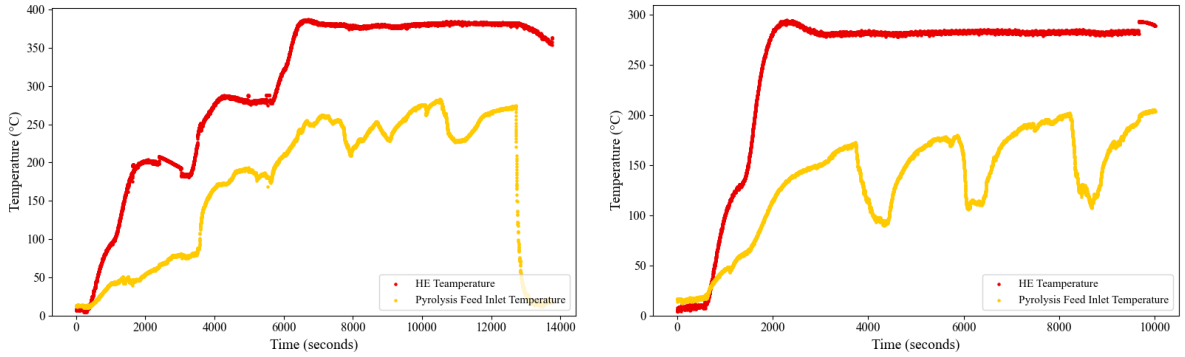

(a) Experimental Runs 1-3 for prototype 2 reactor.

(b) Experimental Runs 4-6 for prototype 2 reactor.

Figure 3.19: Operational data from Experimental runs 1-6 as noted in Table 3.8 for prototype 2 reactor commissioning. The heating element temperature (red) achieves and maintains the required conditions for the reactor commissioning but the pyrolysis zone inlet temperature (yellow) experiences a discrepancy resulting in lower temperatures. As the measured temperature is at the pyrolysis zone inlet it can be assumed that it is the lowest temperature in the pyrolysis zone.

Figure 3.19 shows the experimental commissioning runs of the prototype 2 system. It is hypothesised that the increase of steel in the system leads to increased heat loss in the longitudinal direction which results in the discrepancy in the measured temperatures. It should be noted that the temperature measured within the kiln tube exists at the inlet to the pyrolysis zone and therefore it is likely that the temperature in the centre of the pyrolysis zone is much higher.

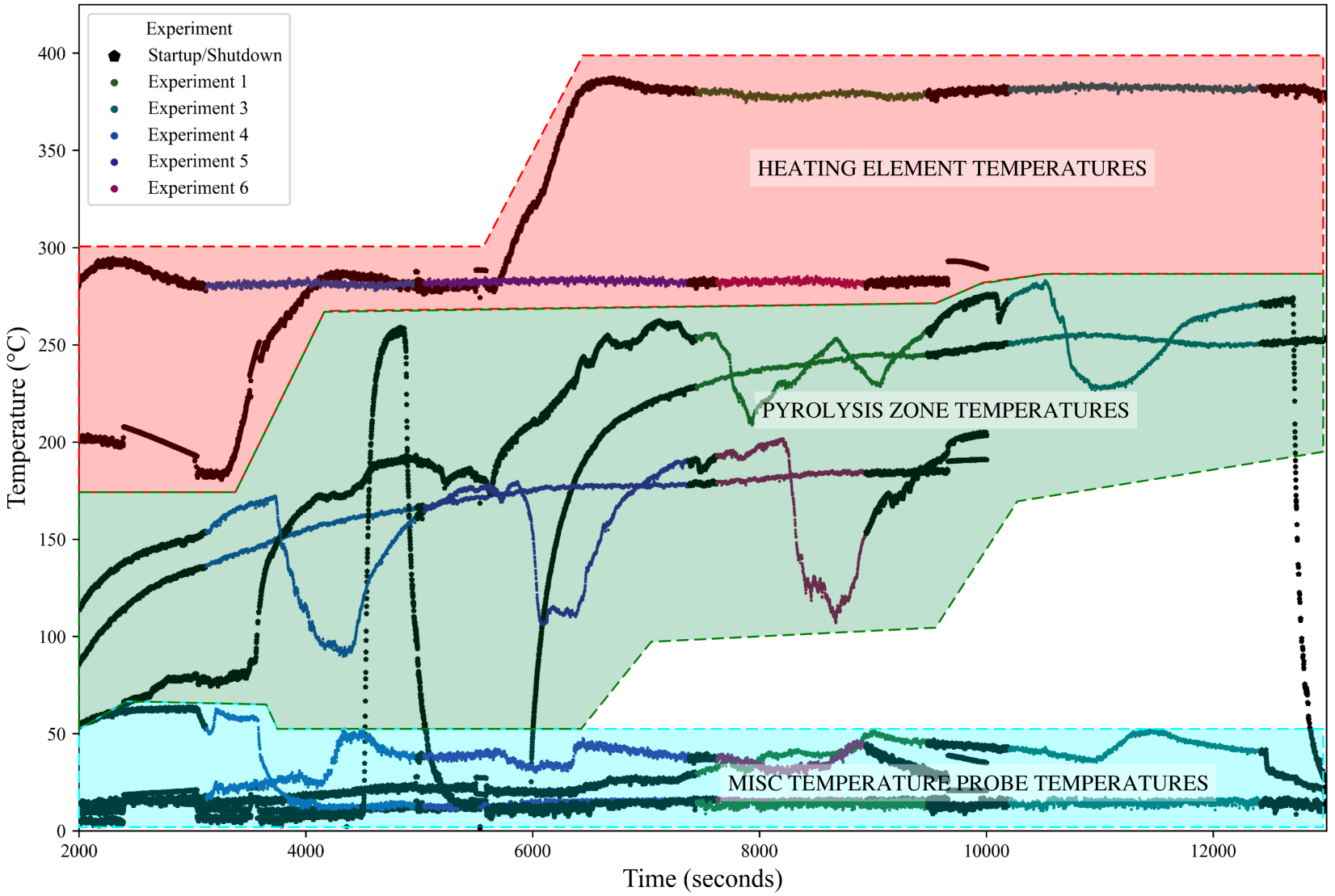

Figure 3.20: Pyrolysis commissioning operating region prototype 2 reactor. Three key zones are demonstrated in the figure. The Pyrolysis zone temperature is of importance showing the drops in temperature as the feed material is introduced. These temperature drops were not identified for the previous version of the reactor.

3.4.2.1 Suggested improvements

The following items are areas of the experimental apparatus that should be improved to ensure consistent and safe operation. The identified areas and items for improvement are derived from the discussions completed in the section above. The improvements are divided into relevant groups.

Unit process additions provide the ability to complete rigorous mass and energy balances. The improvements suggested here would purely assist with the overall analysis and characterisation of the process and the pyrolysis products.

- Low-pressure drop heat exchanger and electrostatic precipitator for pyrolysis vapour collection.
- Current measurement of the 5.5 kW heating element.
- Staged introduction of feed biomass which can reduce the severity of the identified temperature drops.

Improvements that will improve controllability and safety of operation. These items should be addressed first, as they will prove the operator's flexibility and safety while operating the unit.

- Rotation system Override switch.
- Insulation improvement.

Process expansion that could result in improved product properties and allow optimised operation.

- Heating element controller interface with data logger system.

3.5 Operation

3.5.1 Operating Procedures

The operation of the ISA-RKP should be completed using the set of operating procedures described below. Due to the electronic control box being maintained from the first prototype to the second these operating procedures are relevant to both systems. Figure 3.21 shows the order and general process to startup and shutdown the reactor systems. The detailed procedures of the start-up and shutdown of the system are given in Sections 3.5.1.1 and 3.5.1.2.

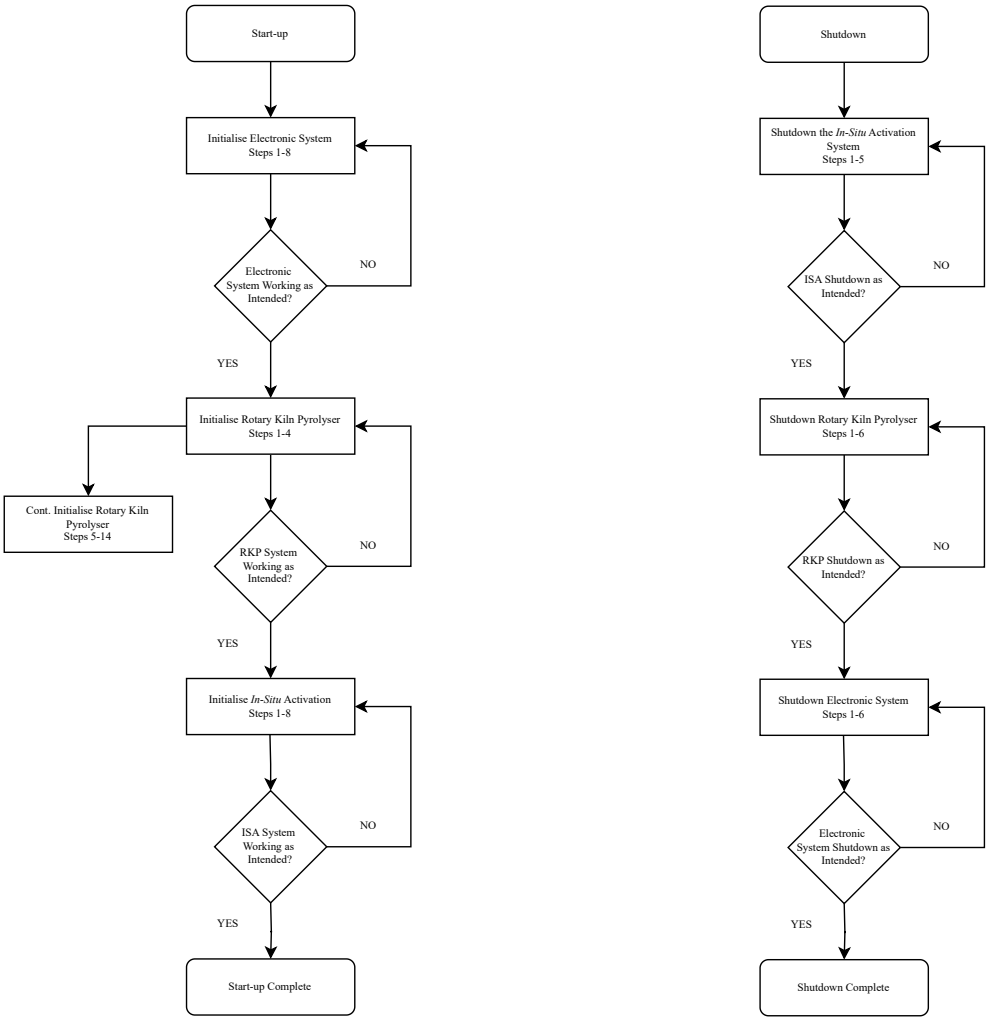

(a) Start-up order for reactor systems. (b) Shutdown order for reactor systems.

Figure 3.21: Order of procedure for Start-up and Shutdown.

3.5.1.1 Start-up

The following process start-up steps apply to either prototype and must be followed to ensure proper and safe operation. The start-up process is split up into three systems; Electronic initialisation, RKP initialisation, and finally ISA initialisation. System start-up is at a maximum of an hour and thirty minutes (1h30min).

The electronic system must be initialised by the following steps:

1. The Raspberry Pi must be plugged in.
2. Login to the Raspberry Pi and launch the Arduino program and the Putty program.
3. Ensure that Raspberry Pi locates the Arduino Leonardo and the 64 GB Sandisk Memory stick.
4. Compile and upload the Arduino program.
5. Prepare the Putty program to complete the data recording of the output serial data. Load the preset configuration called "PyrolysisDataLogger". Rename the data file to be written to.
6. Insert a kettle plug into the TOP socket. The 2 power supplies, the steady state relay and the Heating element Temperature controller will turn on.
7. The Arduino Leonardo waits for a serial connection to begin therefore once the Putty program is initiated, the process will begin.
8. After a preliminary check, the rotary kiln tube will begin to spin and the thermocouples will begin to measure the temperature.

If the power for the electronics is not connected to the top socket, the system will still be able to measure temperature using the thermocouples but none of the other systems will work.

The RKP must be initialised, only after the electronic system, by the following steps:

1. The heating element temperature set value must be chosen to be 100 °C.
2. Check that all other systems are operating as expected.
3. Insert a kettle plug (that is on its wall plug) into the BOTTOM socket to begin heating the system.

4. Watch the system heat up. Once the heating element reaches the set value take note of the time and set a timer for 15 minutes.
5. Select the next set point 100 °C and repeat step 4.
6. Repeat steps 4-5 until the required set-point for operation is reached.
7. At the required set point, initiate the feed motor and begin charging biomass into the kiln tube.
8. Monitor the fumes created by the pyrolysis of the biomass as well as the condition of the feed motor. The fumes should be caramel in colour and be able to produce a flame when ignited.
9. Alter the feed motor speed to ensure that the system converts the biomass to the required pyrolysis products.
10. Monitor the biomass reservoir. If it becomes low, charge more into the reservoir as long as the tube is not empty. This ensures no oxygen enters the system.
11. Repeat steps 8-10 until the required amount of pyrolysis products is produced or until the biochar reservoir is filled.
12. Stop the biomass feed motors and allow the kiln to rotate with continuous heating until the fumes are white/clear.
13. Stop the kiln rotation by switch and connect the system to the fume extraction.
14. Remove the biochar collection unit and collect the sample. Reconnect the collection unit and begin at Step 7 for the next batch.

The ISA can be initialised during Step 4 of the RKP initialisation system. This should only be completed if the intention is to perform in-*situ* activation experiments. These experiments should be prioritised first due to the complexity the ISA introduces to the operation of the system.

1. Collect distilled water in a 250 ml beaker and insert the peristaltic suction line secured as deriving suction from the bottom of the beaker well below the liquid level.
2. Turn on the peristaltic pump and set the flow rate to $0.121\,\mathrm{mm\,min^{-1}}$.
3. Test the flow of distilled water by pumping a small amount into a clean beaker. Once confirmed the system is working this water can be discarded.

4. Turn on the preheating furnace and set the temperature to 150 °C. This furnace heats up very quickly.
5. Watch the system while it heats up.
6. Increase the furnace set temperature by 200 °C once it has reached steady state. Repeat this until you reach a set temperature of approximately 850 °C.
7. Begin to flow steam through the system and increase the temperature to 1200 °C.
8. Once the temperature of the furnace has stabilised at 1200 °C biomass can be fed to the system for an in-*situ* activation experiment.

The benefit of the rotary kiln system is that the high-temperature set point can be maintained while the biochar sample is being collected. This reduces the downtime between a batch system as well as allows for further technological improvement in the future.

3.5.1.2 Shutdown

The following process shutdown steps must be followed to ensure a proper and safe end of operation. The shutdown process is split up into three systems; ISA deactivation, RKP deactivation, and finally Electronic deactivation and data acquisition. The shutdown of the system can be anywhere between an hour thirty minutes (1h30 min) and three hours (3h00 min) due to varying environmental and process conditions.

The ISA must be shut down by the following steps:

1. Change the temperature set point of the preheating furnace to 150 °C.
2. Ensure the flow of distilled water continues.
3. When the furnace reads at maximum 800 °C the water flow through the system can be stopped.
4. Turn off the furnace and open the lid.
5. Turn off the peristaltic pump.

The RKP must be shut down by the following steps once Step 2 of the ISA shutdown procedure is complete:

1. Stop the biomass feed motors and allow the kiln to rotate with continuous heating until the fumes are white/clear.
2. Stop the kiln rotation.
3. Remove the biochar collection unit and collect the sample.
4. Connect the product system to the fume extraction.
5. Remove the heating element kettle plug from the electronic box, which begins the cooling of the system.
6. Monitor the fume output and continue to allow the system to cool down until the temperature of the heating element drops below 100 °C.

The electronic system must be shut down by the following steps:

1. Once the system is cooling down from the target pyrolysis temperature. Stop serial data collection from Arduino.
2. Transfer the resulting data file or remove the 64 GB memory stick by ejecting it first.
3. Remove the electronic kettle plug from the electronics box. This deactivates the temperature control system, so do this only once the temperature of the heating element is below 150 °C.
4. Ensure the system is shut down with a final check.
5. Shutdown the Raspberry Pi.
6. Unplug the Raspberry Pi.

Thereafter the operator can leave the process rig with the resulting Data.

3.6 Experimental Analysis

3.6.1 Sample Preparation

The sample is collected from the reactor unit and the excess quench water is removed from the stainless steel tray. The tray with the sample is then loaded into the large furnace where the samples are dried at 105 °C for 24 hours as shown in Figure 3.22. The samples are then transferred to air-tight glass jars where they can be stored long-term.

Figure 3.22: Produced biochar samples drying in kiln at 105 °C.

The starting biomass and resulting biochar are shown in Figure 3.23. The majority of analysis requires a small amount of homogeneous sample which is difficult to achieve with the resulting biochar shown in Figure 3.23b therefore the biochar must be further processed to provide the identified requirements.

The biochar is ground into a fine powder as shown in Figure 3.24. The resulting powder is suitable for the required analysis and therefore once labelled this is the final form of the biochar.

(a) Macadamia shell biomass.

(b) Macadamia shell biochar.

Figure 3.23: Macadamia shell biomass vs biochar.

(a) Biochar before sample preparation.

(b) Biochar post sample preparation.

Figure 3.24: Biochar Sample preparation.

3.6.2 Analytical Methods and Apparatus

The thermogravimetric analysis was completed using a TA Instruments Discovery TGA 5500. Two types of runs will be completed; The first type will use nitrogen as the inlet gas thereby producing a pyrolysis run, and the second type will use pure oxygen as the

inlet gas thereby producing an oxidation run.

The elemental analysis was completed using an Elementar Unicube Organic Elemental Analyser.

The surface area and porosity analyses were completed using a Micromeritics TriStar II 3020 Version 3.02. The samples will most likely begin to degrade at different temperatures. Biomass will begin to degrade post 110 °C whereas biochar will begin to degrade around 180 °C. The samples should be degassed as follows:

- Biochar - Approximately 150 °C for 2 hours under vacuum.
- Biomass - Approximately 105 °C for 2 hours under vacuum.

The duration for degassing is given as a minimum time and could, in reality, be much longer due to the condition of the sample.

Chapter 4

Results and Discussion

The following experiments were completed to characterise the performance of the prototype 2 reactor and to determine the resulting product quality. The first three experimental runs were completed and analysed. The results from the analysis informed modifications which were made to the reactor. The last three experimental runs are the experimental runs completed after the modifications. These were also analysed and the following results and discussion discuss both sets of data to not only compare the modifications but also to determine the quality of the resulting biochar.

- MS500N 1 - Macadamia shell, 500 °C, Reactor outlet open to atmosphere, Prototype 2 Reactor pre-modifications.
- MS500X 1 - Macadamia shell, 500 °C, Reactor outlet closed to atmosphere, Prototype 2 Reactor pre-modifications.
- MS500Y 1 - Macadamia shell, 500 °C, Reactor outlet steam injection, Prototype 2 Reactor pre-modifications.
- MS500N 2 - Macadamia shell, 500 °C, Reactor outlet open to atmosphere, Prototype 2 Reactor post-modifications.
- MS500X 2 - Macadamia shell, 500 °C, Reactor outlet closed to atmosphere, Prototype 2 Reactor post-modifications.
- MS500Y 2 - Macadamia shell, 500 °C, Reactor outlet steam injection, Prototype 2 Reactor post-modifications.

A summary of the experimental runs detailed above is shown in Figure 4.1. The odd ordering and overall complex plot of the experimental runs can be explained by the fact

that the experiments were done individually and/or sequentially. The figure features only 5 of the 6 experimental runs. This is due to a power cut which caused a minor interruption in the measurement of the final part MS500N 2 experimental run and thus the MS500Y 2 experimental data was lost. While the measurement system was interrupted and required a restart the rest of the systems were able to recover quickly and therefore there is little impact on the final biochar product.

Figure 4.2 features each of the experimental sessions. One can discern the operational procedure discussed in Section 3.5 is followed by the easily identifiable temperature steps. The heating element temperature, Kiln tube skin temperature and Pyrolysis feed inlet temperature are shown in each figure where applicable.

As biomass is fed to the reactor the easiest signifier to identify is that of the sudden temperature decrease experienced by the Pyrolysis feed inlet temperature in Figure 4.2 (yellow dot). This is due to the comparatively cold biomass making contact with the temperature probe at the beginning of the pyrolysis zone. This temperature reaches a minimum value and then quickly rises back once the biochar has passed. At the end of a run when less biomass is present in the pyrolysis area and the conversion to biochar through pyrolysis is reduced the reaction favours combustion instead of pyrolysis which explains the sudden temperature increase.

A less recognisable but still important drop is also mirrored in the Kiln tube skin temperature (orange dot). Figures 4.2c and 4.2d feature the additional temperature measurement of the Pyrolysis product outlet temperature shown in (brown dot) which was only meaningful post the modifications to the unit. Overall one can see the experiments only proceed once the temperature of the kiln tube has reached steady state.

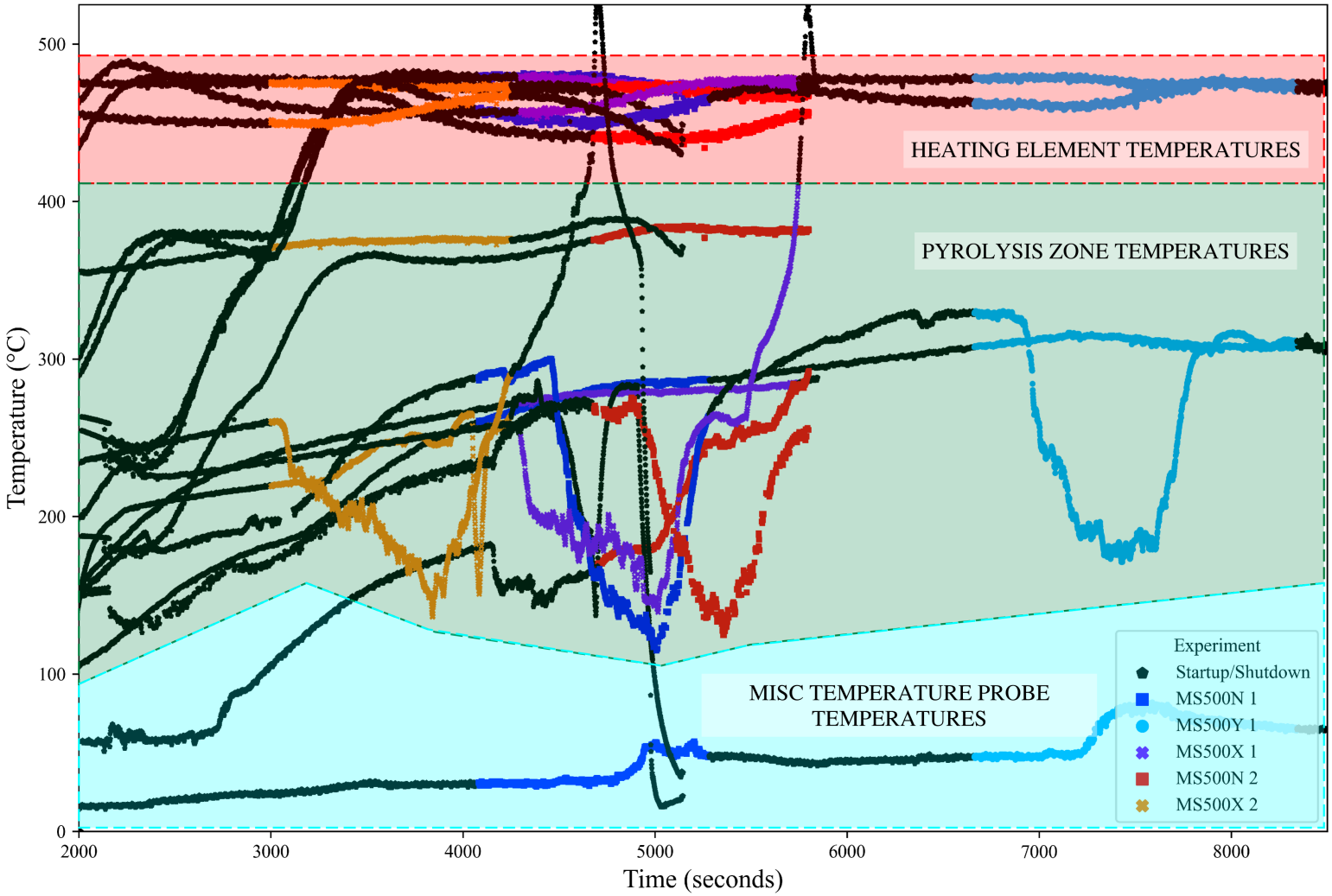

Figure 4.1: Reactor characterisation experimental runs to determine performance/product quality.

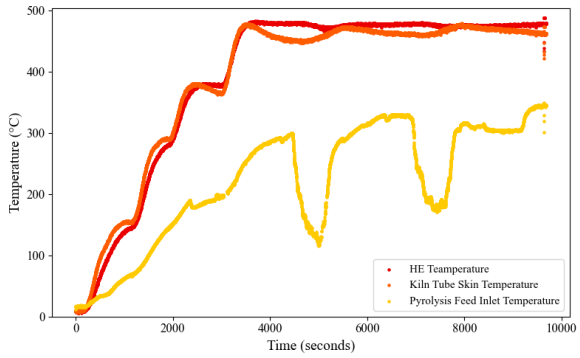

(a) Experiments MS500N 1 and MS500Y 1.

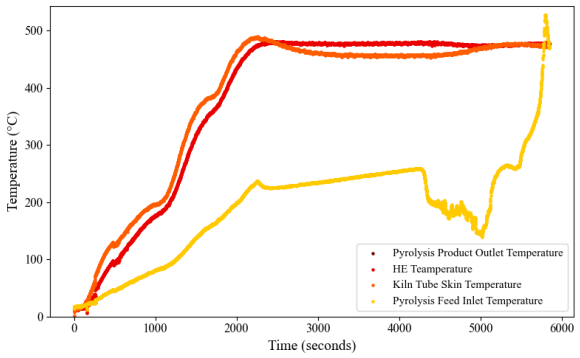

(b) Experiments MS500X 1.

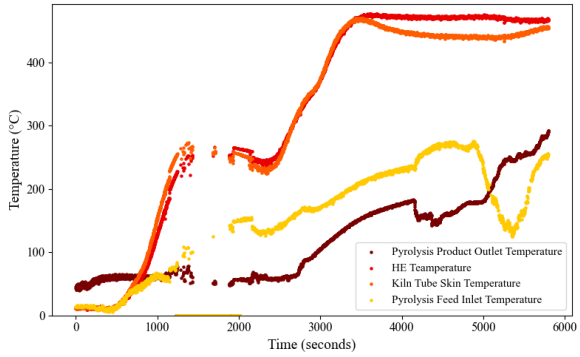

(c) Experiments MS500N 2.

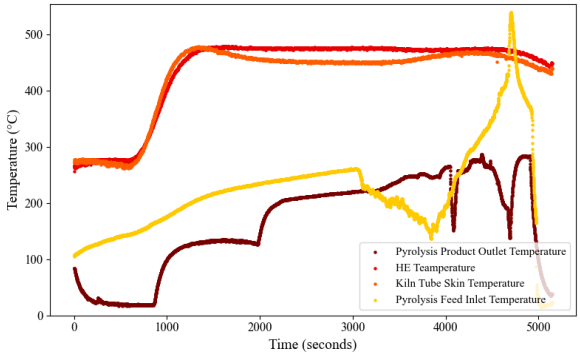

(d) Experiments MS500X 2.

Figure 4.2: Experimental runs completed as required to characterise reactor performance/product quality.

Figures 4.3 illustrate the temperature measurements of each experiment compared with each other over the same time range. The first graph demonstrates the variation in the heating element temperature and its resistance to the energy requirement of the pyrolysis reaction. The heating element temperature is set to 500 °C for this set of experiments and any variation in these values is due to the influences of the process and its requirements. The second illustration shows the kiln tube skin temperature which varies at first negatively and then increases. The temperature of the heating element does not increase in the same way it decreases, this indicates that there is energy being introduced to the system. The third graphic is given as the pyrolysis feed inlet temperature which indicates the above-mentioned signifier of the large temperature drop. This drop quickly recovers in the second half of the experimental run and on occasion overshoots the expected temperature indicating a release of energy. The fourth graph shows the pyrolysis product outlet temperature where a steady and consistent increase in temperature can be noted.

All of these graphs indicate that in the last part of the experimental runs the combustion reaction becomes prevalent which converts the overall energy requirement of the process from being endothermic to exothermic. This is connected to the biomass load of the kiln

tube. If the biomass load of the kiln tube is kept high the prevalent reaction is endothermic and therefore pyrolysis occurs consistently. This can be caused by but is not limited to two things occurring at high biomass load; the conversion through pyrolysis produced off gases in the form of pyrolysis vapours and NCG which will create an overpressure and thus reduce the incursion of oxygen, and secondly the high solids loading reduces the vapour space and high surface area quickly consumes any existing oxygen to kick start the pyrolysis reaction via an exothermic energy injection.

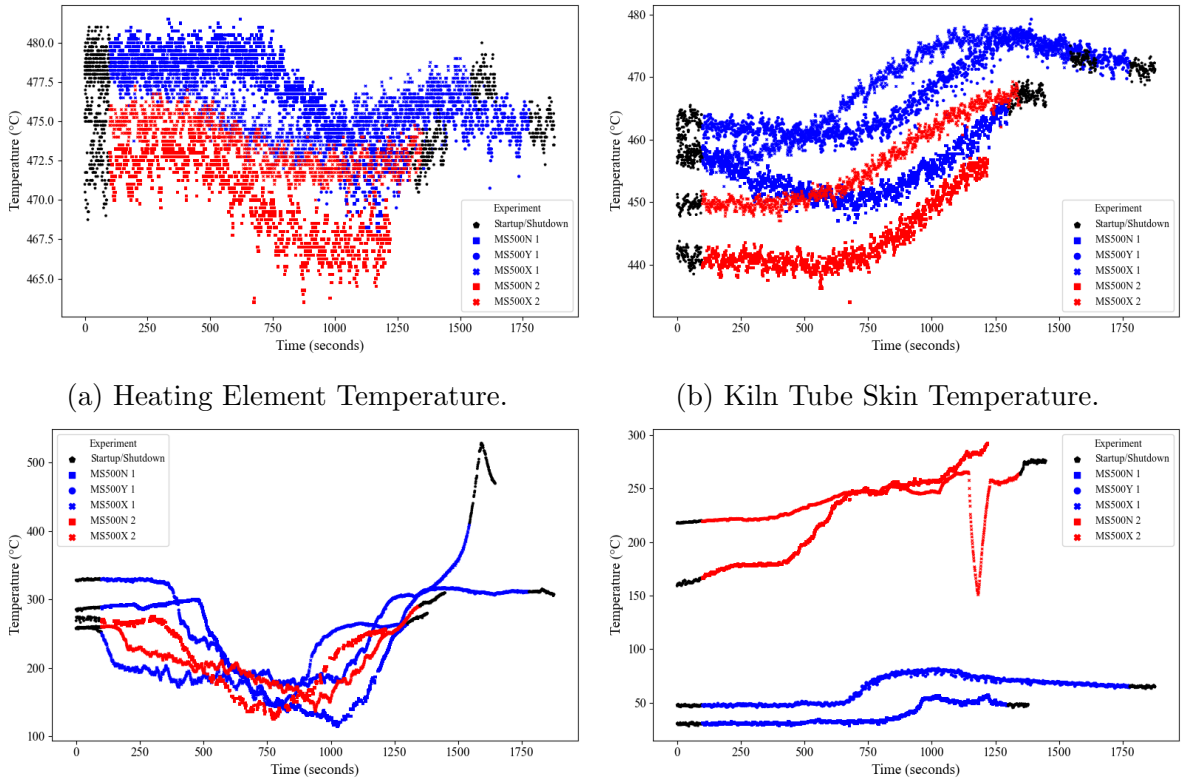

(a) Heating Element Temperature.

(b) Kiln Tube Skin Temperature.

(c) Pyrolysis Feed Inlet Temperature.

(d) Pyrolysis Product Outlet Temperature.

Figure 4.3: Key process parameters during experiments.

The mass yields of the completed experiments are given in Figure 4.4. The behaviour of the results among the three different experimental conditions (MS500N, MS500Y, MS500X) is maintained through set 1 and set 2 with the in-*situ* activation (MS500Y) featuring the highest conversion of biomass to biochar and therefore the highest loss of mass of the experiments. This result is in line with what is expected as the additional activation of the biochar product would induce a mass loss via the reduction of the biochar surface. This logic follows as the least reductive experiment MS500X (closed outlet) has the highest solid yield. Overall the second set of experiments performed after the modifications to the reactor feature lower biochar yield and therefore indicate further conversion of biomass to its pyrolysis products. The second set also features a higher gap between the MS500N/MS500X experimental runs and the MS500Y experimental run which could indicate the effectiveness of the in-*situ* reducing steam.

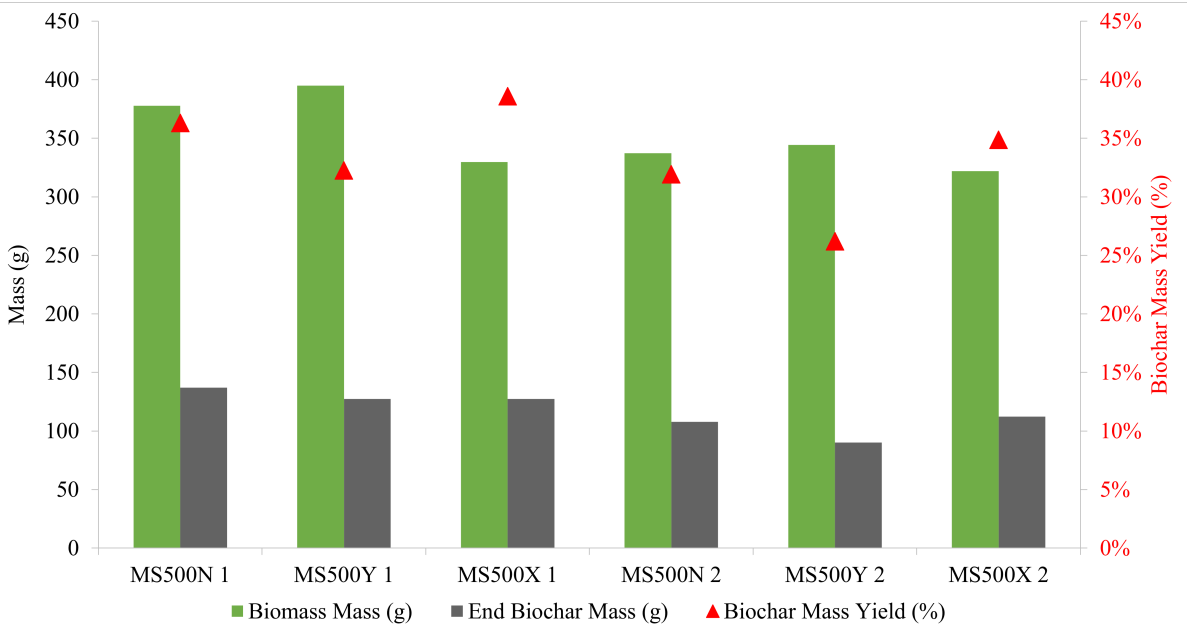

Figure 4.4: Mass yields of experimental runs.

The thermogravimetric analyses of the neat Macadamia Shells shown in Figure 4.5 form a basis for the analysis of the produced biochar. The two figures presented are that of the oxidation and pyrolysis decompositions of the Macadamia shells. The steepness of the mass percent line combined with the height of the derivative weight peak indicates the relative reaction rate of the decomposition occurs.

Figure 4.5a can be deconvolved into four basic components; moisture removal occurs as the first peak, hemicellulose decomposition is the largest peak, cellulose decomposition is the second largest peak and finally lignin decomposition which occurs over the same range as both hemicellulose and cellulose. The resulting figure indicates that the largest reaction rate in the oxidation of the Macadamia shells is that of hemicellulose followed by cellulose. Thus from the oxidation of neat macadamia shells, we can derive the moisture content, ash content and therefore the bounds to which the decomposition of biomass must be kept. Figure 4.5b change in shape can be explained by a preferential decomposition of the hemicellulose and the cellulose. The resulting figure indicates that the largest reaction rate in the pyrolysis of the Macadamia shells is that of cellulose followed by hemicellulose with the decomposition of lignin being considerably reduced. Thus from the pyrolysis of the biomass, we can determine the moisture content, fixed carbon and therefore the bounds to which the pyrolysis of biomass must be kept. The values for the identified information from the oxidation and pyrolysis TGAs are given in Table 4.1.

The oxidation and pyrolysis analyses shown in Figure 4.6 were completed for the biochar produced from the first set of experiments completed on the Prototype 2 reactor. Figures 4.6a, 4.6c and 4.6e show oxidation profiles reminiscent to that of the MS Neat oxidation

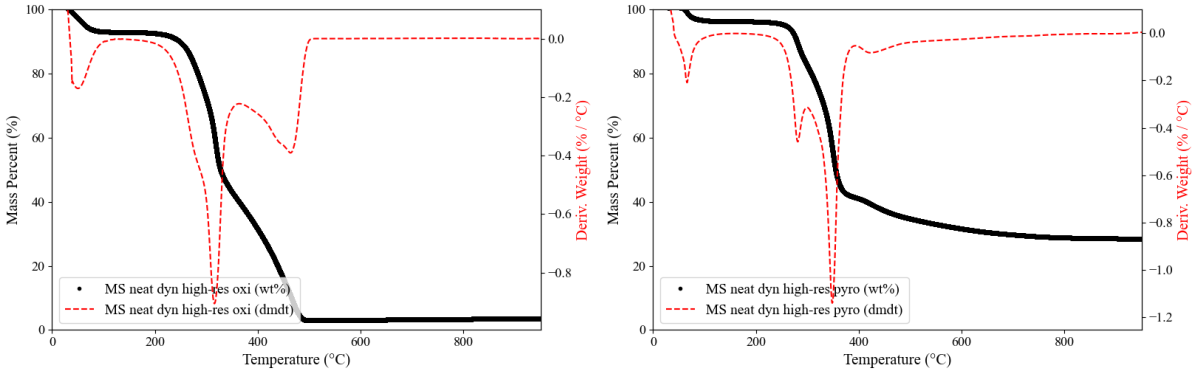

(a) MS Neat Oxidation.

(b) MS Neat Pyrolysis.

Figure 4.5: Thermogravimetric analyses for Neat Macadamia shells.

with the shift in the highest decomposition rate to that of cellulose when compared to the oxidation analysis in Figure 4.5a. Figures 4.6d and 4.6f show the pyrolysis profiles of the produced biochar samples. The resulting profiles vary greatly from the profile given in Figure 4.5b with the greatest change being the final mass percent at the end of the analysis which is shown to be on average much higher than that of the originating biomass. This indicates that the experimental runs completed for set 1 did result in the production of a somewhat stable biochar but the stability of the final product leaves something to be desired. These results informed the decision to make further modifications to the reactor unit. The overall intent was to decrease the efflux of energy from the system by removing unnecessary cooling points. The modifications are discussed at length in Section 3.1.

Figure 4.6b is not included in the above-mentioned discussion due to an unidentified inert which has seemed to interfere with both the oxidation and pyrolysis of the analysis. The measured inert of MS500N 1 is found to be double the average inert measured throughout these analyses. When the pyrolysis profile of this sample is completed the resulting final mass percent remains is much lower than expected. Considering that all other analyses do not have similar issues this could indicate that this sample is contaminated.

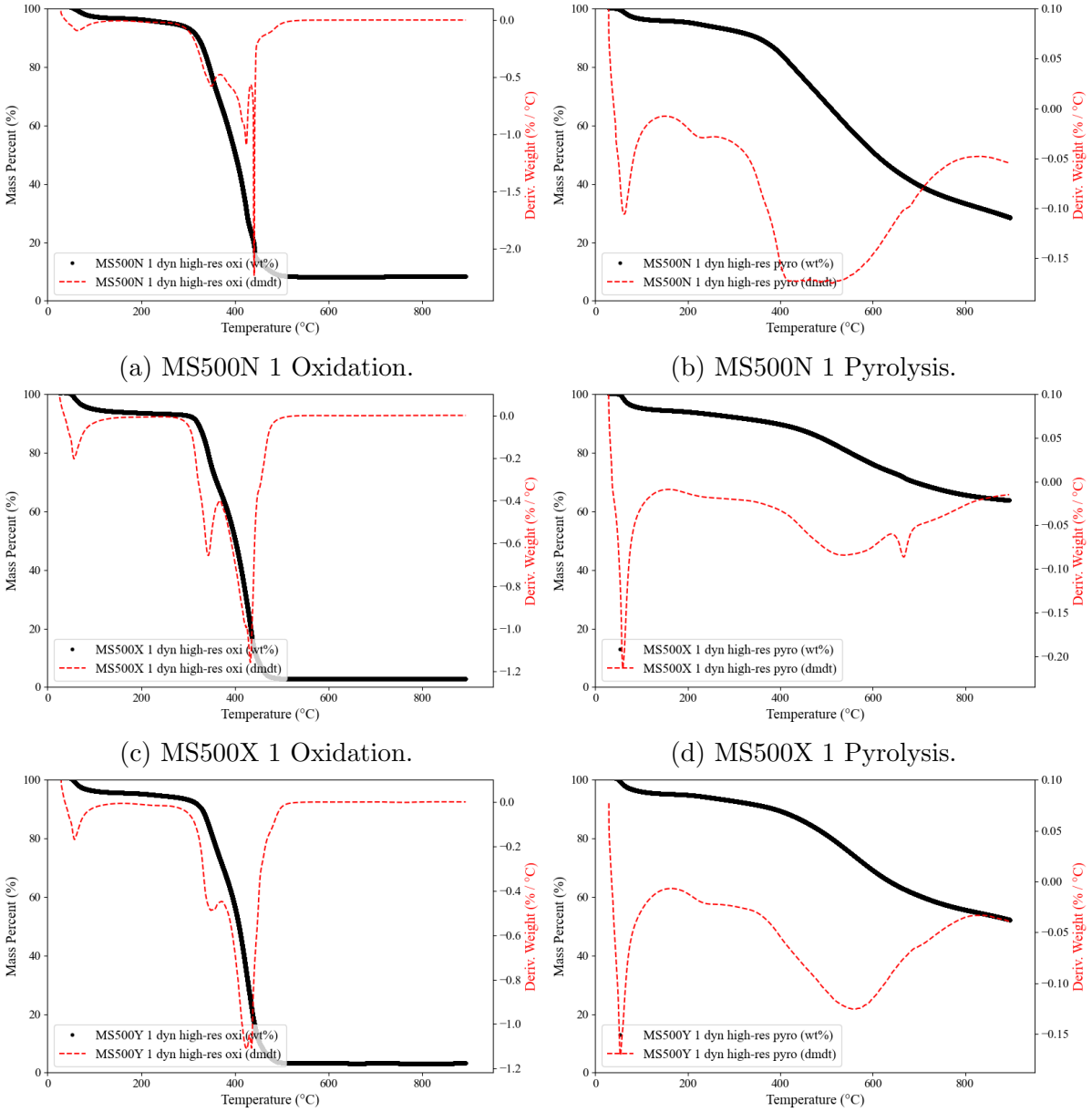

(a) MS500N 1 Oxidation.

(b) MS500N 1 Pyrolysis.

(c) MS500X 1 Oxidation.

(d) MS500X 1 Pyrolysis.

(e) MS500Y 1 Oxidation.

(f) MS500Y 1 Pyrolysis.

Figure 4.6: Thermogravimetric analyses for experimental set 1.

The oxidation and pyrolysis analyses shown in Figure 4.7 were completed for the biochar produced from the second set of experiments completed on the Prototype 2 reactor after the required modifications were completed. Figures 4.7a, 4.7c and 4.7e show oxidation profiles reminiscent to that of the set 1 oxidation profiles demonstrating the same shift in the highest decomposition rate to that of cellulose when compared to the oxidation analysis in Figure 4.5a. When we juxtapose Figures 4.7b, 4.7d and 4.7f to the set 1 pyrolysis figures it is clear that higher biochar stability has been achieved. The resulting profiles vary even further from the profile given in Figure 4.5b with the greatest change being the final mass percent at the end of the analysis which is shown to be on average much higher than that of the originating biomass. This indicates that the experimental

runs completed for set 2 did result in the production of a more stable biochar when compared to the biochar produced in set 1. While this is an improvement to the final product there is still room for further development.

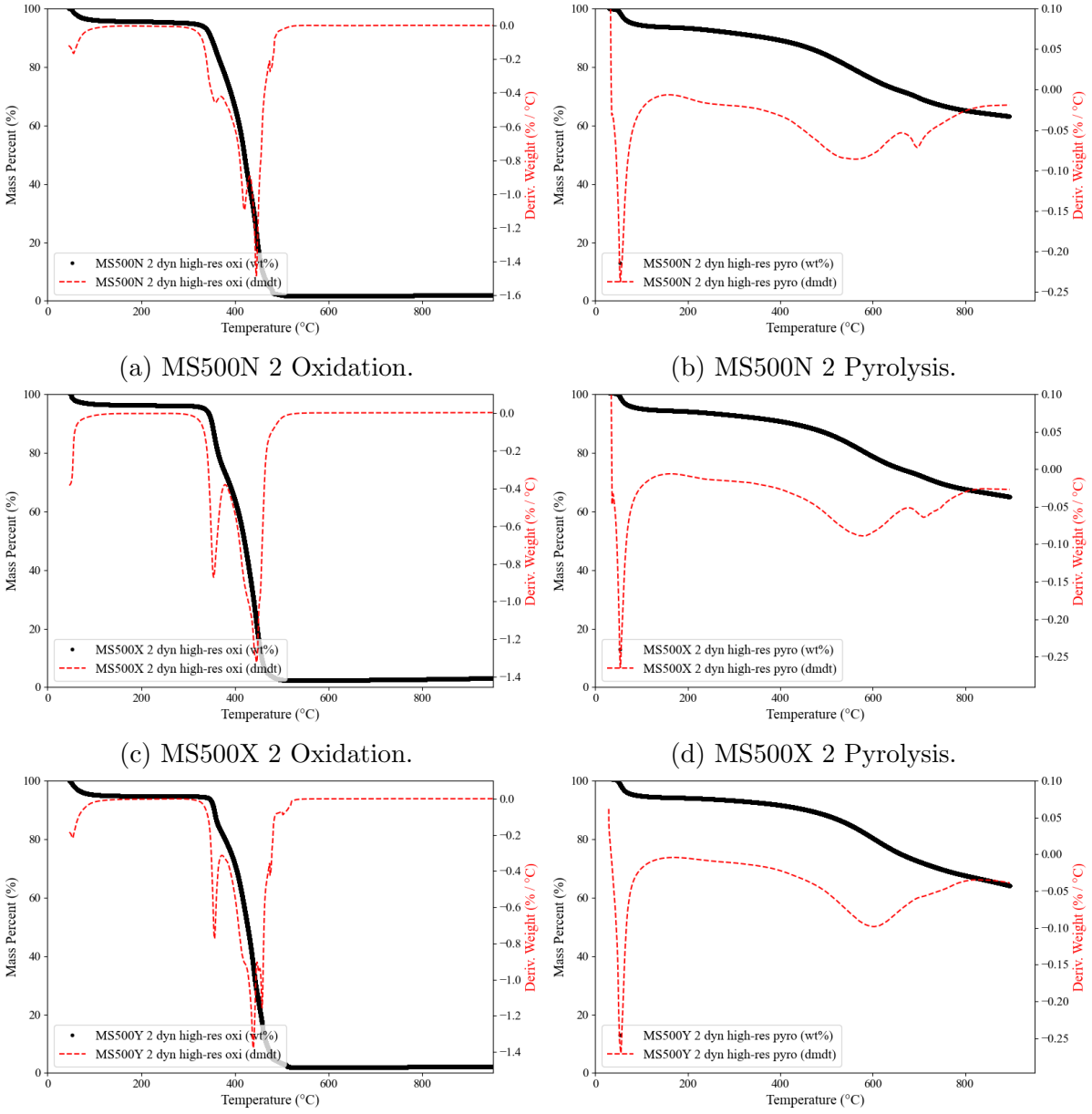

(a) MS500N 2 Oxidation.

(b) MS500N 2 Pyrolysis.

(c) MS500X 2 Oxidation.

(d) MS500X 2 Pyrolysis.

(e) MS500Y 2 Oxidation.

(f) MS500Y 2 Pyrolysis.

Figure 4.7: Thermogravimetric analyses for experimental set 2.

A summary of the proximate analysis of biomass and biochar samples is given in Table 4.1. Figure 4.8 illustrates the pair plot representation of the correlations between the variables of the proximate analyses. We can note that the MS500N 1 does not follow the expected behaviour and often is completely different from all of the other biochar samples. The key variables to be cognoscente of are that of moisture, ash content and fixed carbon where the MS500N 1 sample is shown to be out of the expected range for all. One can also note that the proximate analysis measurements for the second set of

experiments shown in red are grouped in the expected ranges.

Table 4.1: Proximate analyses of neat biomass and produced biochar.

Experimental Code	Moisture (wt.%)	Volatile Matter (wt.%)	Fixed Carbon (wt.%)	Ash Content (wt.%)
MS Neat	5.7	65.4	25.5	3.5
MS500X 1	5.3	30.9	61.0	2.8
MS500N 1	3.5	68.0	20.1	8.4
MS500Y 1	4.7	43.1	49.0	3.2
MS500X 2	4.7	30.3	62.2	2.8
MS500N 2	4.9	31.9	61.3	1.9
MS500Y 2	5.3	30.6	62.0	2.1

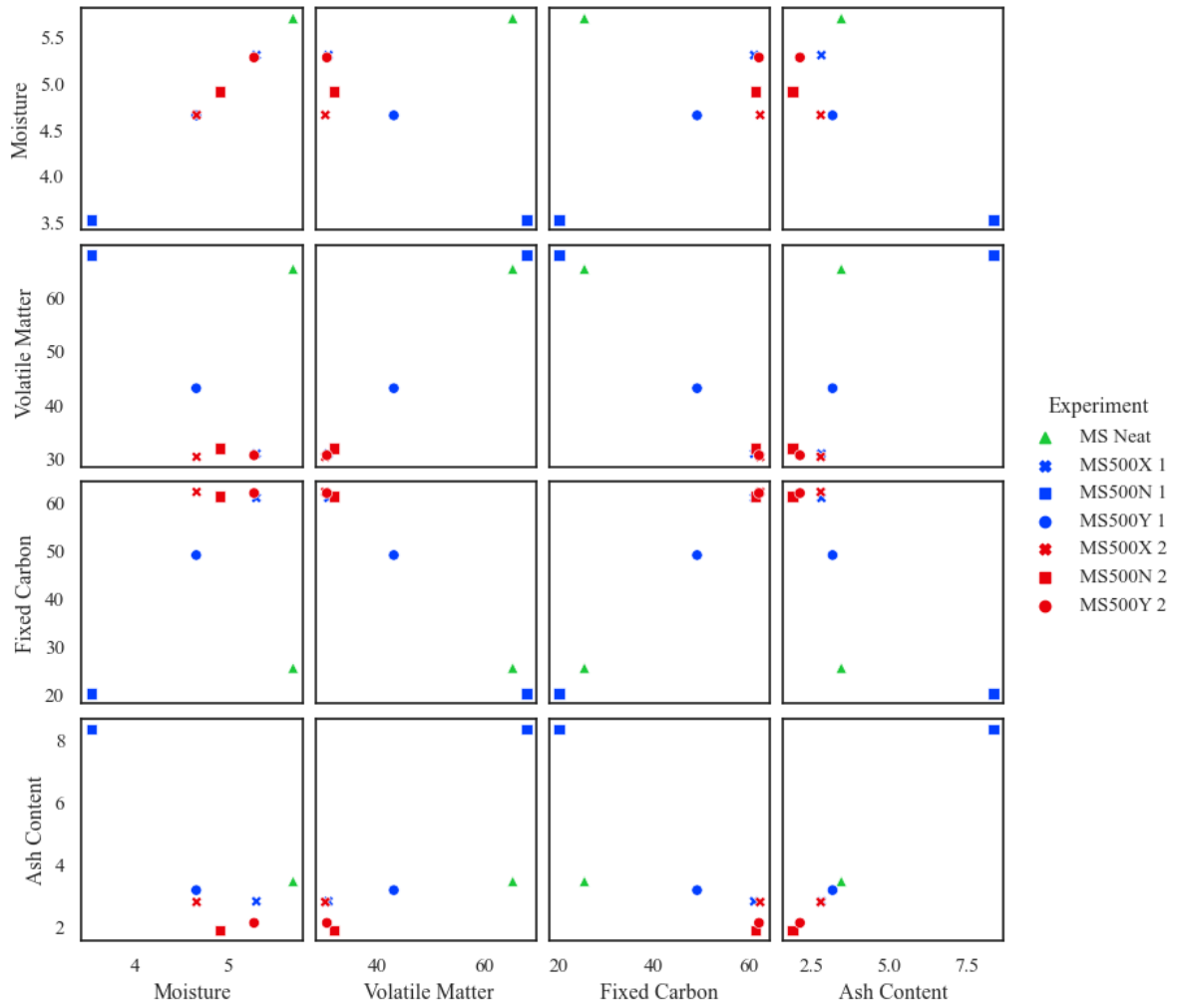

Figure 4.8: Pair plot of Proximate Analysis.

The surface area and porosity of the samples were analysed and the results are summarised in Table 4.2. These analyses were completed in duplicate to confirm the results that were being generated. The biomass and biochar samples were degassed at 105 °C and 150 °C for 17.5 hours respectively. This exceeds the predetermined minimum degas time of 2 hours by a wide margin and therefore due to the length of the degas time this indicates that there is an inhibiting factor. The results in Table 4.2, which show mostly impossible measurements, indicate that the samples and thus the pores of the samples are impregnated with pyrolysis oils. This leads to the conclusion that in the process of the biomass being converted to biochar via pyrolysis the pyrolysis vapours condensed. This should be avoided as to achieve a high-quality final biochar product the sample will be required to undergo more processing to remove the condensed pyrolysis vapours from the solid.

Table 4.2: BET surface area and porosity analyses.

Experiment	BET Surface Area ($m^2\,g^{-1}$)	Pore Volume ($cm^2\,g^{-1}$)	Pore Size (Å)
MS Neat	0.3297	0.000133	143.192
MS500Y 1	-0.0496	0.001091	N/A
MS500X 1	-0.0835	0.000531	N/A
MS500N 1	-0.1283	0.000737	N/A
MS500Y 2	7.1717	0.004782	587.061
MS500X 2	0.0778	0.000921	N/A
MS500N 2	N/A	N/A	N/A

The MS Neat surface area measurement is surprising due to how low the value is. This value could be due to the nature of the starting biomass when compared to that of typical woody biomass is much denser and features much higher yield stresses thereby naturally reducing the available surface of the biomass. The only positive reading shown in Table 4.2 is that of MS500Y 2 which features a measured BET surface area of $7.17\,m^2\,g^{-1}$ which is an improvement of 21.75 times that of the biomass surface area. The existence of a measurement for this mode of operation could be due to the introduced steam performing two functions; firstly acting as a sweeping gas which removes the surrounding pyrolysis vapours from the produced biochars and secondly as a reducing agent thereby increasing the surface area of the biochar. This cannot be substantiated without further investigation but it is an encouraging result for the case of in-*situ* biochar activation.

The elemental analysis of the samples was completed and the colour map representation of the correlation between the resulting variables is given as Figure 4.9. From the given figure we can determine that strong positive correlations exist between Hydrogen percentage and Oxygen percentage. A strong negative correlation is illustrated between Carbon and oxygen percentages. The highlighted correlations are the origin of the weaker correlations also identified in Figure 4.9. These correlations indicate that when the sample is pyrolysed the oxygen mass percentage of the solid biochar product decreases and the carbon percentage increases while the hydrogen percentage decreases. This is expected as the volatile matter in the biomass is decomposed and removed during the process as pyrolysis vapour and non-condensable gases. This is further supported by the proximate analysis summary in Table 4.1 which indicates lower volatile matter mass percentages on biochar samples.

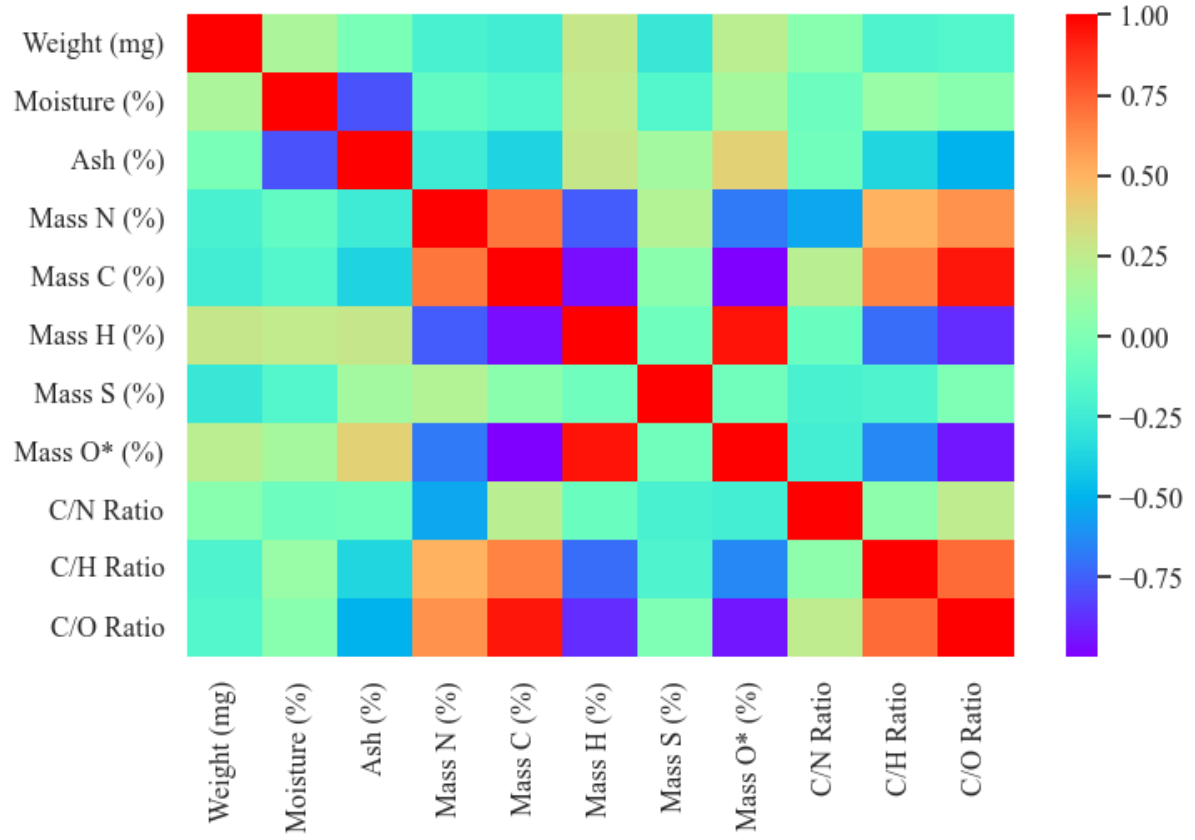

Figure 4.9: Elemental analysis correlation.

These correlations are individually given as Figure 4.10a and 4.10b. The strong negative correlation between oxygen and carbon is demonstrated in the first figure with a weaker negative correlation between hydrogen and carbon being shown in the second figure. There exist a clear separation of the points into three regions and there is very little spread by the measured points into the adjacent regions. The first region given by the green points is for neat biomass, followed by blue for set 1 and finally red for set 2. Set

1 shows the most stable biochar product being that produced by MS500X followed by MS500Y with MS500N producing the least stable product. This outcome informed the degree to which modifications to the prototype 2 reactor were required as the expected outcome would be that MS500Y would produce the most stable biochar. Postmodification as discussed in Section 3.1 the experimental results indicate that MS500Y produces the most stable biochar followed by MS500X with MS500N producing the least stable biochar. Therefore figure 4.10 demonstrates the progression of the product stability as from set 1 to set 2 there is a marked decrease in both oxygen and hydrogen mass percentages. This is a clear indicator that the improvements made to the prototype 2 reactor resulted in an overall improvement in the biochar quality.

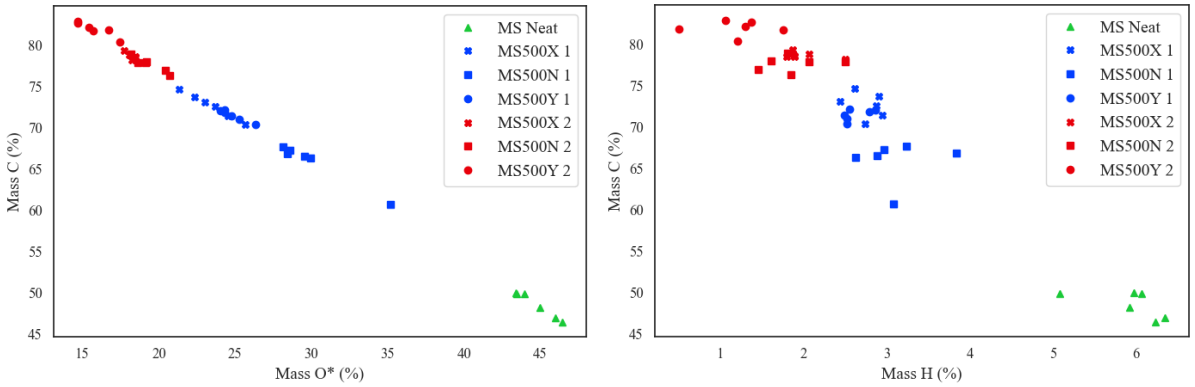

(a) Oxygen vs Carbon.

(b) Hydrogen vs Carbon.

Figure 4.10: Elemental component comparison.

A Van Krevelen plot which features the atomic ratios of the analysed samples is given as Figure 4.11. The Van Krevelen diagram provides a platform to assess the origin and conversion maturity of solid fuels. This plot is accompanied by Table 4.3 which features the calculated higher heating values of the samples. These sets of information are presented together to assist in the discussion of the resulting biochar stability and the degree of conversion achieved by the different experimental sets.

Table 4.3: Higher heating value of experimental samples as per 2.1.

Sample name	Higher Heating Value ($MJ\,kg^{-1}$)
MS Neat	-18.30
MS500X 1	-26.65
MS500N 1	-23.64
MS500Y 1	-25.88
MS500X 2	-28.78
MS500N 2	-28.11
MS500Y 2	-29.44

Once again the improvement of the produced biochar stability is clearly illustrated by

displayed in Figure 4.11 with set 2 showing the highest stability followed by set 1 as compared with the originating biomass. This trend is also demonstrated in the higher heating values presented in Table 4.3 with the highest heating value indicated as MS500Y 2. From the complete discussion above it is clear that the produced biochar stability has been improved by the introduction of in-*situ* activation. While the stability of the product has been improved there still exists areas of development and post-treatment of biochar samples has the potential to produce an improved final product.

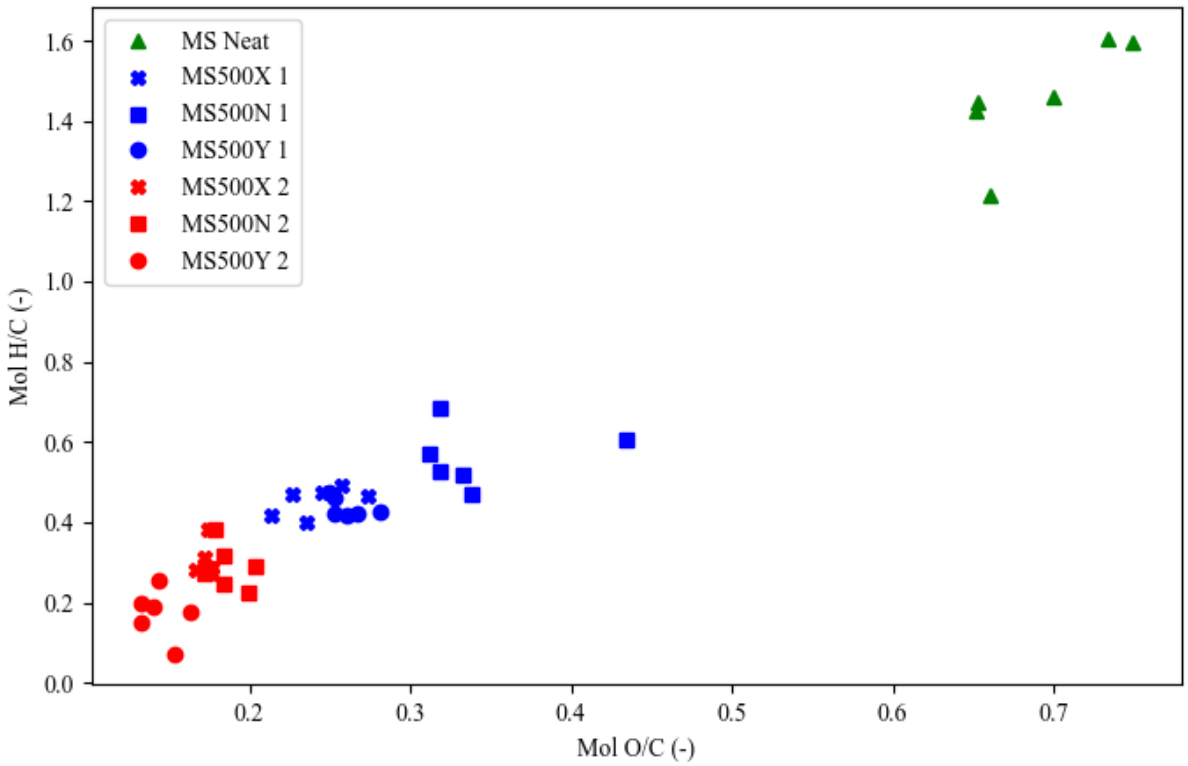

Figure 4.11: Van Krevelen diagram of samples.

Chapter 5

Conclusions and recommendations

In the investigation of biochar as a value-adding product, a biochar-focused pyrolysis reactor was identified, designed, constructed, commissioned and operated. This objective was much more difficult to achieve due to the complexities of the processing material and the products produced. Therefore three versions of the prototype were constructed after the research. The first rendition was prototype 1 where areas of improvement were identified and the lessons learnt from the execution of the first prototype were implemented on the second prototype. Thereafter the second prototype was analysed and further modifications were made to improve the operation and quality of the products produced.

Recommendations for future experiments are to complete additional sample post-processing to remove the impregnated pyrolysis oils in the solid biochar product. The following items are areas of the experimental apparatus that should be improved to ensure consistent and safe operation. The identified areas and items for improvement are derived from the discussions completed in the section above. The improvements are divided into relevant groups.

Unit process additions provide the ability to complete rigorous mass and energy balances. The improvements suggested here would purely assist with the overall analysis and characterisation of the process and the pyrolysis products. Low-pressure drop heat exchanger and electrostatic precipitator for pyrolysis vapour collection. Current measurement of the 5 kW heating element.

Improvements that will improve controllability and safety of operation. These items should be addressed first, as they will prove the operator's flexibility and safety while operating the unit. Rotation system Override switch. System insulation improvement.

Process expansion that could result in improved product properties and allow optimised operation. Heating element controller interface with data logger system.

A final suggestion would be to utilise the produced biochar for some of the discussed applications to test its effectiveness. This type of investigation would allow for the tailoring of the biochar's final characteristic for the defined use case.

The completed modifications have improved the overall biochar stability and degree of conversion. The introduction of in-*situ* activation shows a marked improvement in biochar stability thereby indicating the benefit of combining the generation and activation of biochar into a single step. However, it is noted that further investigation should be completed to improve the reliability and understand where the limit of the increased stability extends.

Bibliography

Ahmad, M, Rajapaksha, AU, Lim, JE, Zhang, M, Bolan, N, Mohan, D, Vithanage, M, Lee, SS and Ok, YS (2014) "Biochar as a sorbent for contaminant management in soil and water: A review" *Chemosphere*, *99*, 19–33 ISSN: 18791298 DOI: 10.1016/j.chemosphere.2013.10.071 URL: http://dx.doi.org/10.1016/j.chemosphere.2013.10.071.

Ahmed, A, Abu Bakar, MS, Sukri, RS, Hussain, M, Farooq, A, Moogi, S and Park, YK (2020) "Sawdust pyrolysis from the furniture industry in an auger pyrolysis reactor system for biochar and bio-oil production" *Energy Conversion and Management*, *226*, (October): 113502 ISSN: 01968904 DOI: 10.1016/j.enconman.2020.113502 URL: https://doi.org/10.1016/j.enconman.2020.113502.

Ahmed, MB, Zhou, JL, Ngo, HH and Guo, W (2016) "Insight into biochar properties and its cost analysis" *Biomass and Bioenergy*, *84*, 76–86 ISSN: 18732909 DOI: 10.1016/j.biombioe.2015.11.002 URL: http://dx.doi.org/10.1016/j.biombioe.2015.11.002.

Al Arni, S (2018) "Comparison of slow and fast pyrolysis for converting biomass into fuel" *Renewable Energy*, *124*, 197–201 ISSN: 18790682 DOI: 10.1016/j.renene.2017.04.060 URL: https://doi.org/10.1016/j.renene.2017.04.060.

Anca-Couce, A, Tsekos, C, Retschitzegger, S, Zimbardi, F, Funke, A, Banks, S, Kraia, T, Marques, P, Scharler, R, Jong, W de and Kienzl, N (2020) "Biomass pyrolysis TGA assessment with an international round robin" *Fuel*, *276*, ISSN: 00162361 DOI: 10.1016/j.fuel.2020.118002.

ASTM (2022) "Standard Specifications for Diesel Oils" *ASTM D975*,

Babler, MU, Phounglamcheik, A, Amovic, M, Ljunggren, R and Engvall, K (Dec. 2017) "Modeling and pilot plant runs of slow biomass pyrolysis in a rotary kiln" *Applied Energy*, *207*, 123–133 ISSN: 03062619 DOI: 10.1016/j.apenergy.2017.06.034.

Bartoli, M, Giorcelli, M, Jagdale, P, Rovere, M and Tagliaferro, A (2020) "A review of non-soil biochar applications" *Materials*, *13*, (2): 1–35 ISSN: 19961944 DOI: 10.3390/ma13020261.

Beesley, L, Moreno-Jiménez, E, Gomez-Eyles, JL, Harris, E, Robinson, B and Sizmur, T (2011) "A review of biochars' potential role in the remediation, revegetation and restoration of contaminated soils" *Environmental Pollution*, *159*, (12): 3269–3282 ISSN: 02697491 DOI: 10.1016/j.envpol.2011.07.023 URL: http://dx.doi.org/10.1016/j.envpol.2011.07.023.

Benanti, E, Freda, C, Lorefice, V, Braccio, G and Sharma, VK (2011) "Simulation of olive pits pyrolysis in a rotary kiln plant" *Thermal Science*, *15*, (1): 145–158 ISSN: 03549836 DOI: 10.2298/TSCI090901073B.

Bieniek, A, Jerzak, W and Magdziarz, A (2021) "Experimental studies of intermediate pyrolysis of woody and agricultural biomass in a fixed bed reactor" in: vol. 323 DOI: 10.1051/e3sconf/202132300003.

Binder, JB and Raines, RT (2010) "Fermentable sugars by chemical hydrolysis of biomass" *Proceedings of the National Academy of Sciences of the United States of America*, *107*, (10) ISSN: 00278424 DOI: 10.1073/pnas.0912073107.

Blanco-Canqui, H (2019) "Biochar and Water Quality" *Journal of Environmental Quality*, *48*, (1): 2–15 ISSN: 0047-2425 DOI: 10.2134/jeq2018.06.0248.

Boateng, AA and Barr, PV (1996) "A thermal model for the rotary kiln including heat transfer within the bed" *International Journal of Heat and Mass Transfer*, *39*, (10): 2131–2143 ISSN: 00179310 DOI: 10.1016/0017-9310(95)00272-3.

Brassard, P, Godbout, S and Raghavan, V (2017) "Pyrolysis in auger reactors for biochar and bio-oil production: A review" *Biosystems Engineering*, *161*, 80–92 ISSN: 15375110 DOI: 10.1016/j.biosystemseng.2017.06.020.

Brassard, P, Godbout, S, Raghavan, V, Palacios, JH, Grenier, M and Zegan, D (2017) "The production of engineered biochars in a vertical auger pyrolysis reactor for carbon sequestration" *Energies*, *10*, (3): 1–15 ISSN: 19961073 DOI: 10.3390/en10030288.

Cai, J, He, Y, Yu, X, Banks, SW, Yang, Y, Zhang, X, Yu, Y, Liu, R and Bridgwater, AV (2017) "Review of physicochemical properties and analytical characterization of lignocel-

lulosic biomass" *Renewable and Sustainable Energy Reviews*, *76*, (October 2016): 309–322 ISSN: 18790690 DOI: 10.1016/j.rser.2017.03.072.

Campuzano, F, Brown, RC and Martínez, JD (2019) "Auger reactors for pyrolysis of biomass and wastes" *Renewable and Sustainable Energy Reviews*, *102*, (April 2018): 372–409 ISSN: 18790690 DOI: 10.1016/j.rser.2018.12.014 URL: https://doi.org/10.1016/j.rser.2018.12.014.

Cengel, YA and Ghajar, AJ (2015) *Heat and Mass Transfer*, McGraw Hill Education, New York.

Clough, T, Condron, L, Kammann, C and Müller, C (2013) "A Review of Biochar and Soil Nitrogen Dynamics" *Agronomy*, *3*, (2): 275–293 ISSN: 2073-4395 DOI: 10.3390/agronomy3020275.

Conto, DD, Silvestre, WP, Baldasso, C and Godinho, M (Oct. 2016) "Performance of rotary kiln reactor for the elephant grass pyrolysis" *Bioresource Technology*, *218*, 153–160 ISSN: 18732976 DOI: 10.1016/j.biortech.2016.06.082.

de Beer, ZW (2018) *Effective Thermal Conductivity Measurement of Phlogopite and Gypsum-coal powdered beds* tech. rep. Hatfield,Pretoria: University of Pretoria.

Dhyani, V and Bhaskar, T (2018) "A comprehensive review on the pyrolysis of lignocellulosic biomass" *Renewable Energy*, *129*, 695–716 ISSN: 18790682 DOI: 10.1016/j.renene.2017.04.035 URL: https://doi.org/10.1016/j.renene.2017.04.035.

Downie, A, Munroe, P, Cowie, A, Van Zwieten, L and Lau, DM (2012) "Biochar as a Geoengineering Climate Solution: Hazard Identification and Risk Management" *Critical Reviews in Environmental Science and Technology*, *42*, (3): 225–250 ISSN: 15476537 DOI: 10.1080/10643389.2010.507980.

Ekebafe, MO, Ekebafe, LO and Ugbesia, SO (2015) "Biochar composts and composites" *Science Progress*, *98*, (2): 169–176 ISSN: 00368504 DOI: 10.3184/003685015X14301544319061.

Enaime, G, Baçaoui, A, Yaacoubi, A and Lübken, M (2020) "Biochar for wastewater treatment-conversion technologies and applications" *Applied Sciences (Switzerland)*, *10*, (10) ISSN: 20763417 DOI: 10.3390/app10103492.

Fan, F, Yang, Z, Li, H, Shi, Z and Kan, H (2018) "Preparation and properties of hydrochars from macadamia nut shell via hydrothermal carbonization" *Royal Society Open Science*, *5*, (10) ISSN: 20545703 DOI: 10.1098/rsos.181126.

Al-Farraji, A, Marsh, R and Steer, J (2017) "A Comparison of the Pyrolysis of Olive Kernel Biomass in Fluidised and Fixed Bed Conditions" *Waste and Biomass Valorization*, *8*, (4): 1273–1284 ISSN: 1877265X DOI: 10.1007/s12649-016-9670-6.

Felix, CB, Chen, WH, Ubando, AT, Park, YK, Lin, KYA, Nguyen, TB and Dong, CD (2022) "A Comprehensive Review of Thermogravimetric Analysis (Tga) in Lignocellulosic and Algal Biomass Gasification" *SSRN Electronic Journal*, DOI: 10.2139/ssrn.4042456.

Filiberto, DM and Gaunt, JL (2013) "Practicality of biochar additions to enhance soil and crop productivity" *Agriculture (Switzerland)*, *3*, (4): 715–725 ISSN: 20770472 DOI: 10.3390/agriculture3040715.

Funke, A, Grandl, R, Ernst, M and Dahmen, N (2018) "Modelling and improvement of heat transfer coefficient in auger type reactors for fast pyrolysis application" *Chemical Engineering and Processing - Process Intensification*, *130*, (May): 67–75 ISSN: 02552701 DOI: 10.1016/j.cep.2018.05.023 URL: https://doi.org/10.1016/j.cep.2018.05.023.

Ghorbannezhad, P and Abbasi, M (2021) "Optimization of Pyrolysis Temperature and Particle Size on the Phenols and Hemicellulose Fast Pyrolysis Products in a Tandem Micro-Pyrolyzer" *8*, (3): 68–74.

Glaser, B, Haumaier, L, Guggenberger, G and Zech, W (Feb. 2001) "The 'Terra Preta' phenomenon: A model for sustainable agriculture in the humid tropics" *Die Naturwissenschaften*, *88*, 37–41 DOI: 10.1007/s001140000193.

Guajardo, N and Schrebler, RA (2024) *Upstream and Downstream Bioprocessing in Enzyme Technology* DOI: 10.3390/pharmaceutics16010038.

Heidari, A, Stahl, R, Younesi, H, Rashidi, A, Troeger, N and Ghoreyshi, AA (2014) "Effect of process conditions on product yield and composition of fast pyrolysis of Eucalyptus grandis in fluidized bed reactor" *Journal of Industrial and Engineering Chemistry*, *20*, (4): 2594–2602 ISSN: 22345957 DOI: 10.1016/j.jiec.2013.10.046 URL: http://dx.doi.org/10.1016/j.jiec.2013.10.046.

Hosokai, S, Matsuoka, K, Kuramoto, K and Suzuki, Y (2016) "Modification of Dulong's formula to estimate heating value of gas, liquid and solid fuels" *Fuel Processing Technology*, *152*, 399–405 ISSN: 03783820 DOI: 10.1016/j.fuproc.2016.06.040 URL: http://dx.doi.org/10.1016/j.fuproc.2016.06.040.

Hu, E, Tian, Y, Yang, Y, Dai, C, Li, M, Li, C and Shao, S (Jan. 2022) "Pyrolysis behaviors of corn stover in new two-stage rotary kiln with baffle" *Journal of Analytical and Applied Pyrolysis*, *161*, ISSN: 01652370 DOI: 10.1016/j.jaap.2021.105398.

Hu, Q, Jung, J, Chen, D, Leong, K, Song, S, Li, F, Mohan, BC, Yao, Z, Prabhakar, AK, Lin, XH, Lim, EY, Zhang, L, Souradeep, G, Ok, YS, Kua, HW, Li, SF, Tan, HT, Dai, Y, Tong, YW, Peng, Y, Joseph, S and Wang, CH (2021) "Biochar industry to circular economy" *Science of the Total Environment*, *757*, 143820 ISSN: 18791026 DOI: 10.1016/j.scitotenv.2020.143820 URL: https://doi.org/10.1016/j.scitotenv.2020.143820.

Hu, X and Gholizadeh, M (2019) "Biomass pyrolysis: A review of the process development and challenges from initial researches up to the commercialisation stage" *Journal of Energy Chemistry*, *39*, (x): 109–143 ISSN: 20954956 DOI: 10.1016/j.jechem.2019.01.024 URL: https://doi.org/10.1016/j.jechem.2019.01.024.

Igbokwe, VC, Ezugworie, FN, Onwosi, CO, Aliyu, GO and Obi, CJ (2022) "Biochemical biorefinery: A low-cost and non-waste concept for promoting sustainable circular bioeconomy" *Journal of Environmental Management*, *305*, ISSN: 10958630 DOI: 10.1016/j.jenvman.2021.114333.

Ippolito, JA, Cui, L, Kammann, C, Wrage-Mönnig, N, Estavillo, JM, Fuertes-Mendizabal, T, Cayuela, ML, Sigua, G, Novak, J, Spokas, K and Borchard, N (2020) "Feedstock choice, pyrolysis temperature and type influence biochar characteristics: a comprehensive meta-data analysis review" *Biochar*, *2*, (4): 421–438 ISSN: 2524-7972 DOI: 10.1007/s42773-020-00067-x URL: https://doi.org/10.1007/s42773-020-00067-x.

Jeffery, S, Verheijen, FG, Velde, M van der and Bastos, AC (2011) "A quantitative review of the effects of biochar application to soils on crop productivity using meta-analysis" *Agriculture, Ecosystems and Environment*, *144*, (1): 175–187 ISSN: 01678809 DOI: 10.1016/j.agee.2011.08.015 URL: http://dx.doi.org/10.1016/j.agee.2011.08.015.

Joubert, JE, Carrier, M, Dahmen, N, Stahl, R and Knoetze, JH (2015) "Inherent process variations between fast pyrolysis technologies: A case study on Eucalyptus grandis" *Fuel*

Processing Technology, *131*, 389–395 ISSN: 03783820 DOI: 10.1016/j.fuproc.2014.12.012 URL: http://dx.doi.org/10.1016/j.fuproc.2014.12.012.

Kazemi Shariat Panahi, H, Dehhaghi, M, Ok, YS, Nizami, AS, Khoshnevisan, B, Mussatto, SI, Aghbashlo, M, Tabatabaei, M and Lam, SS (2020) "A comprehensive review of engineered biochar: Production, characteristics, and environmental applications" *Journal of Cleaner Production*, *270*, 122462 ISSN: 09596526 DOI: 10.1016/j.jclepro.2020.122462 URL: https://doi.org/10.1016/j.jclepro.2020.122462.

Lehmann, J, Rillig, MC, Thies, J, Masiello, CA, Hockaday, WC and Crowley, D (2011) "Biochar effects on soil biota - A review" *Soil Biology and Biochemistry*, *43*, (9) ISSN: 00380717 DOI: 10.1016/j.soilbio.2011.04.022.

Lestrange, MD (2019) *Mathematical Modelling for Thermal Energy Storage in both a Packed Bed and a Square Structured System* tech. rep. Hatfield,Pretoria: University of Pretoria.

Li, H, Dong, X, Silva, EB da, Oliveira, LM de, Chen, Y and Ma, LQ (July 2017) *Mechanisms of metal sorption by biochars: Biochar characteristics and modifications* DOI: 10.1016/j.chemosphere.2017.03.072.

Li, S, Harris, S, Anandhi, A and Chen, G (2019) "Predicting biochar properties and functions based on feedstock and pyrolysis temperature: A review and data syntheses" *Journal of Cleaner Production*, *215*, 890–902 ISSN: 09596526 DOI: 10.1016/j.jclepro.2019.01.106 URL: https://doi.org/10.1016/j.jclepro.2019.01.106.

Mante, O, Agblevor, F, Oyama, S and McClung, R (Feb. 2012) "The influence of recycling non-condensable gases in the fractional catalytic pyrolysis of biomass" *Bioresource technology*, *111*, 482–90 DOI: 10.1016/j.biortech.2012.02.015.

Merckel, R, Labuschagne, F and Heydenrych, M (Feb. 2019) "Oxygen consumption as the definitive factor in predicting heat of combustion" *Applied Energy*, *235*, 1041–1047 ISSN: 0306-2619 DOI: 10.1016/J.APENERGY.2018.10.111.

Mitchell, DA, Berovic, M and Krieger, N (2002) "Overview of solid state bioprocessing" *Biotechnology Annual Review*, *8*, ISSN: 13872656 DOI: 10.1016/S1387-2656(02)08009-2.

Mohan, D, Pittman, CU and Steele, PH (2006) "Pyrolysis of wood/biomass for bio-oil: A critical review" *Energy and Fuels*, *20*, (3): 848–889 ISSN: 08870624 DOI: 10.1021/ef0502397.

El-Naggar, A, Lee, SS, Rinklebe, J, Farooq, M, Song, H, Sarmah, AK, Zimmerman, AR, Ahmad, M, Shaheen, SM and Ok, YS (2019) "Biochar application to low fertility soils: A review of current status, and future prospects" *Geoderma*, *337*, (September 2018): 536–554 ISSN: 00167061 DOI: 10.1016/j.geoderma.2018.09.034 URL: https://doi.org/10.1016/j.geoderma.2018.09.034.

NASA (2024) *The Carbon Cycle* URL: https://earthobservatory.nasa.gov/features/CarbonCycle.

Oasmaa, A, Solantausta, Y, Arpiainen, V, Kuoppala, E and Sipilä, K (2010) "Fast pyrolysis bio-oils from wood and agricultural residues" *Energy and Fuels*, *24*, (2): 1380–1388 ISSN: 08870624 DOI: 10.1021/ef901107f.

Oram, NJ, Van de Voorde, TF, Ouwehand, GJ, Bezemer, TM, Mommer, L, Jeffery, S and Groenigen, JWV (2014) "Soil amendment with biochar increases the competitive ability of legumes via increased potassium availability" *Agriculture, Ecosystems and Environment*, *191*, 92–98 ISSN: 01678809 DOI: 10.1016/j.agee.2014.03.031 URL: http://dx.doi.org/10.1016/j.agee.2014.03.031.

Palamanit, A, Khongphakdi, P, Tirawanichakul, Y and Phusunti, N (2019) "Investigation of yields and qualities of pyrolysis products obtained from oil palm biomass using an agitated bed pyrolysis reactor" *Biofuel Research Journal*, *6*, (4): 1065–1079 ISSN: 22928782 DOI: 10.18331/BRJ2019.6.4.3.

Panwar, NL, Pawar, A and Salvi, BL (2019) "Comprehensive review on production and utilization of biochar" *SN Applied Sciences*, *1*, (2): 1–19 ISSN: 25233971 DOI: 10.1007/s42452-019-0172-6 URL: https://doi.org/10.1007/s42452-019-0172-6.

Phounglamcheik, A, Babler, MU, Donaj, P, Amovic, M, Ljunggren, R and Engvall, K (2017) "Pyrolysis of Wood in a Rotary Kiln Pyrolyzer: Modeling and Pilot Plant Trials" in: vol. 105 Elsevier Ltd: pp. 908–913 DOI: 10.1016/j.egypro.2017.03.413.

Pichler, M, Haddadi, B, Jordan, C, Norouzi, H and Harasek, M (Dec. 2021) "Dataset for the simulated biomass pyrolysis in rotary kilns with varying particle residence time distributions" *Data in Brief*, *39*, ISSN: 23523409 DOI: 10.1016/j.dib.2021.107603.

Piersa, P, Unyay, H, Szufa, S, Lewandowska, W, Modrzewski, R, Ślżak, R and Ledakowicz, S (2022) "Review An Extensive Review and Comparison of Modern Biomass Torrefaction Reactors vs. Biomass Pyrolysis—Part 1" *Energies*, *15*, (6) ISSN: 19961073 DOI: 10.3390/en15062227.

Pimenta, AS, Vital, BR, Bayona, JM and Alzaga, R (1998) "Characterisation of polycyclic aromatic hydrocarbons in liquid products from pyrolysis of Eucalyptus grandis by supercritical fluid extraction and GC/MS determination" *Fuel*, *77*, (11): 1133–1139 ISSN: 00162361 DOI: 10.1016/S0016-2361(98)00031-3.

Proch, F, Bauerbach, K and Grammenoudis, P (July 2021) "Development of an upscalable rotary kiln design for the pyrolysis of waste tyres" *Chemical Engineering Science*, *238*, ISSN: 00092509 DOI: 10.1016/j.ces.2021.116573.

Prussi, M, Yugo, M, Prada, LD, Padella, M and Edwards, R (2020) *JEC Well-to-Tank report v5* tech. rep.: p. 248 DOI: 10.2760/959137.

Roberts, P, Hunt, C, Arroyo-Kalin, M, Evans, D and Boivin, N (2017) "The deep human prehistory of global tropical forests and its relevance for modern conservation" *Nature Plants*, *3*, (August) ISSN: 20550278 DOI: 10.1038/nplants.2017.93.

Roggero, CM, Tumiatti, V, Scova, A, De Leo, C, Binello, A and Cravotto, G (2011) "Characterization of oils from haloclean pyrolysis of biomasses" *Energy Sources, Part A: Recovery, Utilization and Environmental Effects*, *33*, (5): 467–476 ISSN: 15567036 DOI: 10.1080/15567030903096980.

Sakhiya, AK, Anand, A and Kaushal, P (2020) *Production, activation, and applications of biochar in recent times*, vol. 2 3 Springer Singapore: pp. 253–285 ISBN: 0123456789 DOI: 10.1007/s42773-020-00047-1 URL: https://doi.org/10.1007/s42773-020-00047-1.

Saldarriaga, JF, Aguado, R, Pablos, A, Amutio, M, Olazar, M and Bilbao, J (Jan. 2015) "Fast characterization of biomass fuels by thermogravimetric analysis (TGA)" *Fuel*, *140*, 744–751 ISSN: 00162361 DOI: 10.1016/j.fuel.2014.10.024 URL: https://linkinghub.elsevier.com/retrieve/pii/S0016236114010199.

Sánchez-Reinoso, A, Ávila-Pedraza, E and Restrepo-Díaz, H (2020) "Use of biochar in agriculture — Uso de biocarbón en la agricultura" *Acta Biologica Colombiana*, *25*, (2): 327–338.

Shoaib, AM, El-Adly, RA, Hassanean, MH, Youssry, A and Bhran, AA (Dec. 2018) "Developing a free-fall reactor for rice straw fast pyrolysis to produce bio-products" *Egyptian Journal of Petroleum*, *27*, (4): 1305–1311 ISSN: 20902468 DOI: 10.1016/j.ejpe.2018.08.002.

Singh, J and Singh, C (2020) *J S Singh, C Singh - Biochar Applications in Agriculture and Environment Management (2020, Springer International Publishingspringer) – libgen.li.pdf*.

Sohi, SP, Krull, E, Lopez-Capel, E and Bol, R (2010) "A review of biochar and its use and function in soil" *Advances in Agronomy*, *105*, (1): 47–82 ISSN: 00652113 DOI: 10.1016/S0065-2113(10)05002-9.

Suliman, W, Harsh, JB, Abu-Lail, NI, Fortuna, AM, Dallmeyer, I and Garcia-Perez, M (Jan. 2016) "Influence of feedstock source and pyrolysis temperature on biochar bulk and surface properties" *Biomass and Bioenergy*, *84*, 37–48 ISSN: 18732909 DOI: 10.1016/j.biombioe.2015.11.010.

Swart, SD (2012) "Design , Modelling and Construction of a Scalable Dual Fluidised Bed Reactor for the Pyrolysis of Biomass" (January).

Tan, RR (2019) "Data challenges in optimizing biochar-based carbon sequestration" *Renewable and Sustainable Energy Reviews*, *104*, (November 2018): 174–177 ISSN: 18790690 DOI: 10.1016/j.rser.2019.01.032 URL: https://doi.org/10.1016/j.rser.2019.01.032.

Tinwala, F, Mohanty, P, Parmar, S, Patel, A and Pant, KK (2015) "Intermediate pyrolysis of agro-industrial biomasses in bench-scale pyrolyser: Product yields and its characterization" *Bioresource Technology*, *188*, ISSN: 18732976 DOI: 10.1016/j.biortech.2015.02.006.

Tomczyk, A, Sokołowska, Z and Boguta, P (2020) "Biochar physicochemical properties: pyrolysis temperature and feedstock kind effects" *Reviews in Environmental Science and Biotechnology*, *19*, (1) ISSN: 15729826 DOI: 10.1007/s11157-020-09523-3.

Wang, J and Wang, S (2019) "Preparation, modification and environmental application of biochar: A review" *Journal of Cleaner Production*, *227*, 1002–1022 ISSN: 09596526 DOI: 10.1016/j.jclepro.2019.04.282 URL: https://doi.org/10.1016/j.jclepro.2019.04.282.

Wang, Y, Yang, S, Bao, G and Wang, H (2018) *Pyrolysis of macadamia nut shell and peel to evaluate their bioenergy potential: Physicochemical characteristics, kinetics analysis, thermodynamics parameters and reaction mechanism* tech. rep. Kunming University of Science and Technology URL: https://ssrn.com/abstract=4400998.

Welty, JR, Wicks, CE, Wilson, RE and Rorrer, GL (2008) *Fundamentals of Momentum, Heat, and Mass Transfer*, John Wiley & sons, Inc, New Jersey.

Williams, CL, Karlsson, MC, Emerson, RM, Smith, WA and Bhattacharjee, T (2022) "Green biomass processing to lower slurry viscosity and reduce biofuel cost" *Biomass and Bioenergy*, *165*, ISSN: 18732909 DOI: 10.1016/j.biombioe.2022.106566.

Woolf, D, Amonette, JE, Street-Perrott, FA, Lehmann, J and Joseph, S (2010) "Sustainable biochar to mitigate global climate change" *Nature Communications*, *1*, (5): 1–9 ISSN: 20411723 DOI: 10.1038/ncomms1053 URL: http://dx.doi.org/10.1038/ncomms1053.

Wright, MM, Satrio, JA, Brown, RC, Daugaard, DE and Hsu, DD (2010) "Techno-economic analysis of biomass fast pyrolysis to transportation fuels. Technical Report NREL/TP-6A20-46586" *Nrel*, *89*, (November): 463–469 URL: https://doi.org/10.1016/j.fuel.2010.07.029.

Wu, H, Chen, R, Du, H, Zhang, J, Shi, L, Qin, Y, Yue, L and Wang, J (2019) "Synthesis of activated carbon from peanut shell as dye adsorbents for wastewater treatment" *Adsorption Science and Technology*, *37*, (1-2) ISSN: 20484038 DOI: 10.1177/0263617418807856.

Xiang, W, Zhang, X, Chen, J, Zou, W, He, F, Hu, X, Tsang, DC, Ok, YS and Gao, B (2020) "Biochar technology in wastewater treatment: A critical review" *Chemosphere*, *252*, ISSN: 18791298 DOI: 10.1016/j.chemosphere.2020.126539.

Xie, T, Reddy, KR, Wang, C, Yargicoglu, E and Spokas, K (2015) "Characteristics and applications of biochar for environmental remediation: A review" *Critical Reviews in Environmental Science and Technology*, *45*, (9): 939–969 ISSN: 15476537 DOI: 10.1080/10643389.2014.924180.

Xie, Y, Wang, L, Li, H, Westholm, LJ, Carvalho, L, Thorin, E, Yu, Z, Yu, X and Skreiberg, Ø (2022) "A critical review on production, modification and utilization of biochar" *Journal of Analytical and Applied Pyrolysis*, *161*, (March 2021) ISSN: 01652370 DOI: 10.1016/j.jaap.2021.105405.

Yaashikaa, PR, Kumar, PS, Varjani, S and Saravanan, A (2020) "A critical review on the biochar production techniques, characterization, stability and applications for circular bioeconomy" *Biotechnology Reports*, *28*, ISSN: 2215017X DOI: 10.1016/j.btre.2020.e00570.

Yang, X, Zhang, S, Ju, M and Liu, L (2019) "Preparation and modification of biochar materials and their application in soil remediation" *Applied Sciences (Switzerland)*, *9*, (7) ISSN: 20763417 DOI: 10.3390/app9071365.

Zhang, C, Liu, L, Zhao, M, Rong, H and Xu, Y (2018) "The environmental characteristics and applications of biochar" *Environmental Science and Pollution Research*, *25*, (22): 21525–21534 ISSN: 16147499 DOI: 10.1007/s11356-018-2521-1.

Zheng, W (2010) "Using Biochar as a Soil Amendment for Sustainable Agriculture" *... the Sustainable Agriculture ...* *7276*, (December) URL: http://www.ideals.illinois.edu/handle/2142/25503.

Zhou, Y, Berruti, F, Greenhalf, C, Tian, X and Henry, HA (2017) "Increased retention of soil nitrogen over winter by biochar application: Implications of biochar pyrolysis temperature for plant nitrogen availability" *Agriculture, Ecosystems and Environment*, *236*, 61–68 ISSN: 01678809 DOI: 10.1016/j.agee.2016.11.011 URL: http://dx.doi.org/10.1016/j.agee.2016.11.011.